University of Alabama at Birmingham

UAB Digital Commons

All ETDs from UAB

UAB Theses & Dissertations

2010

Chronic Alcohol Consumption Promotes Opening of the Mitochondrial Permeability Transition Pore and Increases Mitochondrial Injury in Liver

Adrienne Lester King
University of Alabama at Birmingham

Follow this and additional works at: https://digitalcommons.library.uab.edu/etd-collection

CHRONIC ALCOHOL CONSUMPTION PROMOTES OPENING OF THE
MITOCHONDRIAL PERMEABILITY TRANSITION PORE AND INCREASES
MITOCHONDRIAL INJURY IN LIVER

by

ADRIENNE LESTER KING

SHANNON M. BAILEY, COMMITTEE CHAIR
SCOTT W. BALLINGER
VICTOR M. DARLEY-USMAR
DALE A. DICKINSON
AIMEE L. LANDAR
MATHIEU J. LESORT

A DISSERTATION

Submitted to the graduate faculty of The University of Alabama at Birmingham,
in partial fulfillment of the requirements for the degree of
Doctor of Philosophy

BIRMINGHAM, ALABAMA

2010

CHRONIC ALCOHOL CONSUMPTION PROMOTES OPENING OF THE
MITOCHONDRIAL PERMEABILITY TRANSITION PORE AND INCREASES
MITOCHONDRIAL INJURY IN LIVER

ADRIENNE LESTER KING

ENVIRONMENTAL HEALTH SCEINCES

ABSTRACT

Alcoholic liver disease is a serious public health concern. In particular, the
mitochondrion is a specific target of ethanol toxicity and much of the damage can
be related to unregulated Ca^{2+} homeostasis and oxidative stress which are key
players in the induction of the mitochondrial permeability transition pore (MPTP)
within the organelle. The mechanism behind the induction of the MPTP remains
elusive. Therefore, this body of work will provide insight on what effects chronic
alcohol consumption has on mitochondrial dysfunction with an emphasis on the
MPTP. **Chapter 2: Assessment of mitochondrial dysfunction arising from
treatment with hepatotoxicants** provides a description of several biochemical
assays used to assess mitochondrial function when exposed to toxicants such as
ethanol. **Chapter 3**: **Chronic ethanol consumption enhances sensitivity to
Ca^2+-mediated opening of the mitochondrial permeability transition pore
and increases cyclophilin D in liver** presents data which test the hypothesis
that chronic alcohol consumption causes mitochondrial dysfunction leading to
increased sensitivity to the induction of the MPTP and impairment of Ca^{2+}
retention capacity. The most significant findings were isolated liver mitochondria
from ethanol-fed rats had decreased Ca^{2+} retention capacity, increased
sensitivity to Ca^{2+}-mediated induction of the MPTP, and increased levels of

Cyclophilin D. **Chapter 4: Cyclophilin D gene ablation is not protective against mitochondrial dysfunction in alcoholic liver disease** extends and expands on the results presented in Chapter 3. This chapter further investigated the role of Cyp D in alcohol-induced mitochondrial injury using a Cyp D null mouse model. In this study we observed steatosis in livers of both wild-type and Cyp D$^{-/-}$ mice fed the ethanol-containing diet. State 4 respiration (ADP-independent) was increased in liver mitochondria isolated from both ethanol-fed wild-type and Cyp D$^{-/-}$ mice. Lastly, liver mitochondria from ethanol-fed Cyp D$^{-/-}$ were more sensitive than control-fed Cyp D$^{-/-}$ to Ca^{2+}-mediated MPTP induction. These findings suggest that Cyp D gene ablation is not protective against alcohol induced mitochondrial dysfunction. Together this information provides a more comprehensive understanding of the molecular events that contribute to chronic ethanol-induced mitochondrial dysfunction and damage. An understanding of which we propose will better guide future therapeutic approaches for alcoholic liver disease.

Key words: alcohol, liver, mitochondria, calcium, MPTP

DEDICATION

I dedicate this work in memory to my late father, Dr. William Loy Lester. Dad you were my first cheerleader in this process and I know that you are so proud!!!

ACKNOWLEDGMENTS

First, I would like to thank my God for giving me the physical and mental strength to finish this body of work. I know it is through His grace and mercy that I have been able to accomplish this goal. The prayers were many and they truly were a comfort in a time of need. Amen.

I would like to thank my mentor, Dr. Shannon M. Bailey. Through her expertise, she has taught me to think scientifically. She gave of her time and support to help me develop into the researcher that I am today. Also, I would like to thank the members of my committee: Dr. Ballinger, Dr. Dickinson, Dr. Lesort, Dr. Landar, and Dr. Darley-Usmar. All of your guidance was much appreciated.

The members of the Bailey laboratory past and present were very instrumental in helping me throughout this process. I would especially like to thank Telisha and Whitney. You both were right there when I needed a hand. Most importantly both of you were always there to listen to me.

Lastly, I would like to thank my family. Thank you to my brother-in law, Maurice for getting those scientific articles that I needed to help me write my papers and this dissertation. I couldn't have done it without them. I would like to thank my in-laws for feeding my husband just about every Sunday when I had to get back on the road to Birmingham. My mother and my sister have been my rock. Mom, words can not express my gratitude to you over the last 5 years.

There were days when I didn't know if I was going to make it and you were right there for me. Some days it was just the call that I needed from you to let me know that everything was going to be alright. To my sister and my friend, Cindy I don't know where to start. Having a sister as close as we are is indescribable. From the talks on the phone over posters, abstracts, and statistics you were right there.

Lastly, to my beloved husband Kimani. Thank you for letting me go and pursue my goals and dreams. Thank you for letting me be a weekend wife for the last past 5 years. Thank you for allowing us to sacrifice through this together. For this, I love you and words can not express my thanks to you.

TABLE OF CONTENTS

LIST OF TABLES

LIST OF FIGURES

CHRONIC ETHANOL CONSUMPTION ENHANCES SENSITIVITY
TO CA^{2+}-MEDIATED OPENING OF THE MITOCHONDRIAL
PERMEABILITY TRANSITION PORE AND INCREASES
CYCLOPHILIN D IN LIVER

CYCLOPHILIN D GENE ABLATION IS NOT PROTECTIVE
AGAINST MITOCHONDRIAL DYSFUNCTION IN
ALCOHOL LIVER DISEASE

CONCLUSIONS AND FUTURE WORK

CHAPTER 1

INTRODUCTION

Background and significance

Alcoholic liver disease (ALD) is a major cause of death and disability

worldwide. Prolonged, heavy consumption of alcohol is the third leading cause

of preventable death in the United States (US) (102) with alcoholic liver disease

continuing to be a significant cause of morbidity and mortality. It is estimated that

approximately 12,000 deaths occur each year from alcohol-related chronic liver

disease and cirrhosis in the US (97). Alcohol-induced liver damage is

characterized by a spectrum of liver abnormalities and metabolic impairments.

Multiple cell types in the liver (e.g., hepatocytes, Kupffer cells, and hepatic

stellate cells) have disrupted metabolic processes from chronic exposure to

alcohol. Hepatocytes, the most abundant and metabolically active cell in the

liver, are the primary site for alcohol metabolism in the body (115). Chronic

exposure to ethanol damages mitochondria, increases the generation of reactive

oxygen and nitrogen species (ROS/RNS), decreases glutathione (GSH) content,

and initiates lipid peroxidation in hepatocytes (36, 46, 133, 136). Ethanol

increases gut permeability thus facilitating the leakage of endotoxin from the gut

into the hepatic portal circulation. Once activated by endotoxin, Kupffer cells, the

resident macrophages of the liver, produce a variety of soluble bio-active factors. These factors include cytokines, chemokines, ROS, and RNS all of which provide physiologically diverse and pivotal paracrine effects on other liver cell types, which, can ultimately contribute to the pathobiology of alcoholic liver injury (41, 78, 129). For example, the hepatic stellate cells are normally quiescent in liver with their main function being storage of vitamin A (123). Stellate cells, once activated by substances released from injured hepatocytes and/or activated Kupffer cells, transdifferentiate into myofibroblast-like cells that produce excessive amounts of extracelluar matrix (ECM), which causes fibrosis (123).

Chronic ethanol consumption leads to oxidative stress and damage through increased ROS production and impairment in numerous protective antioxidant defense mechanisms. Oxidative stress has been identified as a key component in initiating and possibly sustaining the pathogenic pathways responsible for the progression from the earliest stage of alcoholic liver disease, i.e. fatty liver stage (i.e. steatosis), to the more chronic and severe stages; alcoholic hepatitis and cirrhosis (36, 120). It has been shown that the metabolism of ethanol modifies the cellular redox state of the liver by increasing the $NADH/NAD^+$ ratio (11). As a consequence of increased NADH and decreased NAD^+ there is an inhibition in beta-oxidation leading to the accumulation of triglyceride and other fatty acids in hepatocytes. This results in the condition known as steatosis. Moreover, this increase in reducing equivalents can lead to increased production and accumulation of lactic acid, which is another metabolite known to induce hepatic stellate cell activation and

2

fibrogenesis (47). Chronic ethanol-related disturbances in mitochondrial structure and function may also be responsible for increased ROS production by mitochondria (14). Therefore, mitochondria may be an important contributor to oxidative stress and damage observed in liver following exposure to ethanol. The following sections will review key aspects of ethanol-induced liver injury with specific emphasis on how chronic ethanol consumption alters: (1) mitochondrial function and bioenergetics; (2) mitochondrial production of ROS; (3) induction of the mitochondrial permeability transition pore (MPTP), and (4) mitochondrial Ca^{2+} handling.

Ethanol-related liver injury

The early stage of alcoholic liver disease is primarily characterized by the accumulation of fat in hepatocytes. This condition is known as fatty liver or steatosis. Various mechanisms have been proposed as to how chronic alcohol consumption leads to fat accumulation in hepatocytes. Excess fat could result from all, some, or a combination of the following:

1. Increased fatty acid synthesis in hepatocytes

2. Decreased fatty acid oxidation (i.e., decreased mitochondrial beta-oxidation

3. Increased transport of fatty acids from peripheral organs (e.g., adipose) to the liver

4. Decreased export of fatty acids and/or triglyceride from the hepatocyte.

3

The importance of fat accumulation in the disease process is that fat may sensitize the liver to other toxic agents and/or metabolic disturbances leading to further injury (115). If heavy alcohol consumption continues, steatosis may progresses to steatohepatitis. Histological features of alcoholic hepatitis include neutrophilic infiltration, varying degrees of fibrosis, hepatocyte necrosis, and the presence of Mallory bodies (115). About 10–35% of alcoholics have changes in liver histology consistent with alcoholic hepatitis (1). In addition, severe alcoholic hepatitis is a rare clinical syndrome that presents with fever, jaundice, and hepatic encephalopathy and has a poor prognosis. The short-term mortality rate of patients with severe alcoholic hepatitis is approximately 50% (1). The end stage of alcoholic liver disease is cirrhosis and is defined as an irreversible remodeling of the liver with fibrosis. This occurs due to excessive accumulation of ECM scar mass from activated hepatic stellate cells (123). The risk of developing cirrhosis is increased in patients with alcoholic hepatitis (1). The probability of developing cirrhosis in patients with alcoholic hepatitis is approximately 10–20% per year, and approximately 70% of the patients with alcoholic hepatitis will ultimately develop cirrhosis with continued alcohol consumption (1).

The development of alcohol-induced liver disease is a complex process that involves many stages and is influenced by a number of factors, which include: gender and age, as well as molecular factors such as oxidative stress, immune response, and energy metabolism defects (15, 29, 104, 132). For instance, the enzymes involved in the metabolism of alcohol are less active in

4

women, which predispose women to damaging or toxic effects of alcohol for longer periods of time (55). In addition, acetaldehyde, the oxidation product of ethanol (discussed in detail below) can promote oxidative stress, as well as initiate immune responses via protein adduct formation (29, 132, 133). Lastly, it is well established that ethanol consumption and metabolism causes decreases in cellular ATP levels and impairs mitochondrial function (14, 126). Despite intense research, identification of factors that lead to the onset and progression of alcoholic liver disease remains equivocal.

Ethanol metabolism

The primary enzyme responsible for ethanol metabolism in liver is alcohol dehydrogenase, which oxidizes ethanol to acetaldehyde, a highly reactive and toxic molecule. NADH is formed as a by-product of this reaction (Figure 1A). Due to its reactivity, acetaldehyde is known to interact with proteins and form unstable adducts (133). The formation of these aldehyde-protein adducts is believed to be a key event in the development of alcohol-induced liver injury (133). It has been shown that acetaldehyde binds to proteins, which results in structural and functional alterations in proteins and decreases anti-oxidative defenses by binding glutathione (GSH) (120, 133). In the liver, acetaldehyde has been shown to form adducts with DNA resulting in point mutations and chromosomal aberrations (109). Acetaldehyde is oxidized by hepatic aldehyde dehydrogenase 2 (ALDH2) to acetate in the mitochondrion (Figure 1C). This reaction also results in the production of NADH.   Aldehyde dehydrogenase is a

A. $CH_3CH_2OH + NAD^+$ $\xrightarrow{\text{alcohol dehydrogenase}}$ $CH_3CHO + NADH + H^+$

ethanol   acetaldehyde

B. $CH_3CH_2OH + NADPH + H^+ + O_2$ $\xrightarrow{\text{CYP 450}}$ $CH_3CHO + NADP^+2H_2O$

ethanol   acetaldehyde

C. $CH_3CHO + NAD^+$ $\xrightarrow{\text{aldehyde dehydrogenase}}$ $CH_3COO^- + NADH + H^+$

acetaldehyde   acetate
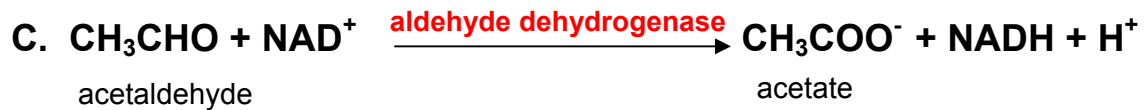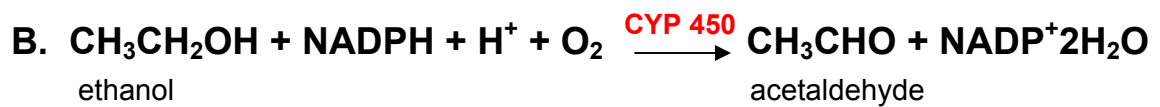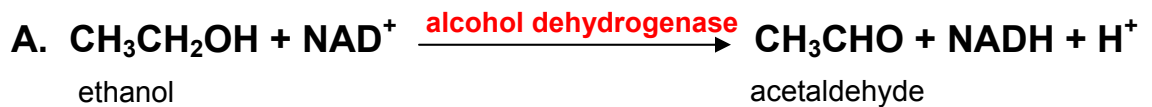
Figure 1: The metabolism of ethanol. (A) Alcohol dehydrogenase metabolizes ethanol to acetaldehyde. (B) The microsomal system contributes to ethanol metabolism via the cytochrome P450 system, which produces acetaldehyde. (C) Aldehyde deydrogenase metabolizes acetaldehyde to acetate.

key detoxifying enzyme that keeps acetaldehyde levels in the micromolar range even when blood levels of ethanol may be in millimolar range. The microsomal ethanol oxidizing system (MEOS) also participates in ethanol metabolism via catalysis by the cytochrome P450 (CYP450) isoenzymes (Figure 1B). The enzymes in this family vary in their capacity to oxidize ethanol with CYP450 2E1 having the greatest capacity to oxidize ethanol to acetaldehyde. Importantly, CYP450 2E1 is inducible by chronic ethanol exposure and therefore contributes more to ethanol metabolism in the chronic alcohol consumer (35). Metabolism of alcohol via CYP450 2E1 also results in the production of acetaldehyde which is a known higly toxic compound that contributes to the toxic effects of alcohol (33, 104, 133).

As a result of the oxidation of ethanol by alcohol dehydrogenase and subsequent oxidation of acetaldehyde, there is a significant increase in the ratio of NADH/ NAD$^+$. The shift in the NADH/NAD$^+$ ratio is observed in the cytoplasm as well as in the mitochondrion (11). The increased levels of NADH can be readily re-oxidized by the mitochondrial electron transport chain. As a consequence of increased NADH, mitochondrial ROS production could be stimulated due to increased flux of reducing equivalents into the electron transport chain. It is believed that this mechanism may be responsible for ethanol-dependent mitochondrial ROS production and will be discussed in detail in the following section.

Ethanol-related alterations to hepatic mitochondrial function

In normal hepatocytes, mitochondria synthesize the majority of cellular ATP via the oxidative phosphorylation system. The mitochondrial oxidative phosphorylation system is comprised of 5 enzyme complexes (Figure 2). Complex I (NADH-ubiquinone reductase) is the largest of the complexes and is composed of 45 subunits. Of the 45 subunits, 7 are products of the mitochondrial genome. Complex I catalyzes the transfer of electrons from NADH to ubiquinone. Complex II (succinate-ubiquinone reductase) is composed of 4 nuclear encoded proteins and transfers electrons from succinate to ubiquinone. Complex III (ubiquinone-cytochrome *c* reductase) is composed of 11 subunits, one of which (cytochrome b) is mitochondrial encoded. Complex III transfers electrons from reduced ubiquinone (i.e., ubiquinol) to cytochrome *c.* Complex IV (cytochrome *c* oxidase) is composed of 13 subunits, three of which are mitochondrial encoded. Complex IV belongs to the heme-copper oxygen reductase super-family whose members catalyze the complete reduction of dioxygen to water. Complex V is the mitochondrial ATP synthase. Electron transport and oxidative phosphorylation are coupled by an electrochemical gradient that is generated across the inner mitochondrial membrane. The efflux of protons from the matrix to the intermembrane space compartment through Complexes I, III, and IV create an electrochemical gradient across the inner mitochondrial membrane. The energy stored in this electrochemical gradient is
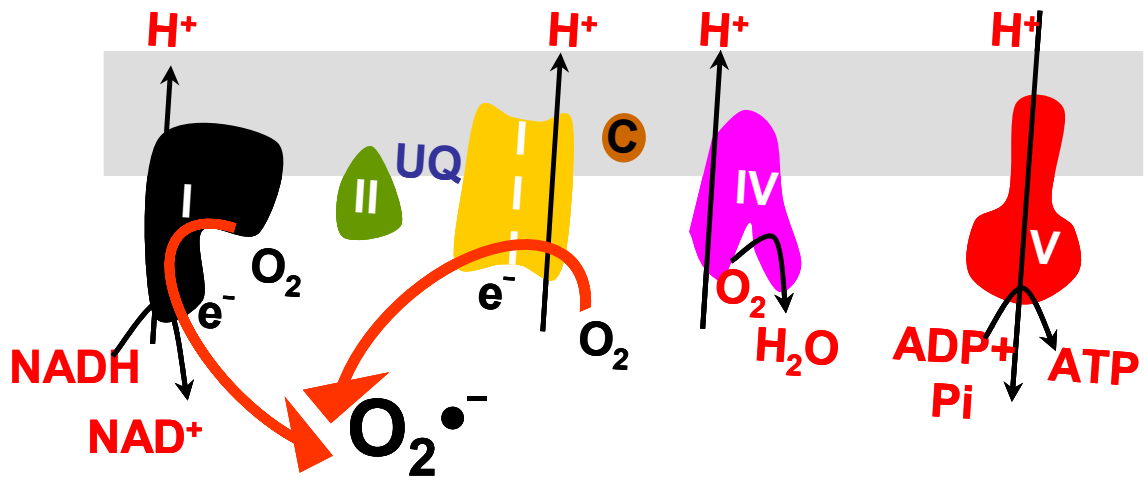
Figure 2. Components of the oxidative phosphorylation system. The electron transport chain consists of: Complex I (NADH-ubiquinone reductase), Complex II (succinate-ubiquinone reductase) Complex III (ubiquinone cytochrome c reductase) Complex IV (cytochrome c oxidase), and Complex V (ATP synthase). Protons are pumped from the matix by Complexes I, III, and IV into the intermembrane space. The sites for reactive oxygen species production are primarily Complexes I and III.

used by Complex V, the ATP synthase, to generate ATP from ADP and inorganic phosphate (P_i). It is known that all the complexes of the electron transport chain except Complex II are impaired by chronic alcohol consumption (44).

One of the earliest manifestations of hepatocyte injury by alcohol is morphologic abnormalities to the mitochondrion. Mitochondria often appear enlarged and swollen with disrupted and missing cristea (83). In addition, there are often functional abnormalities that occur in the mitochondrion following chronic alcohol exposure. Early studies by Cunningham and colleagues reported that chronic ethanol consumption depresses mitochondrial protein synthesis, which is due to a decrease in the number of competent ribosomes in hepatic mitochondria (39). This decrease in ribosome content adversely affects the synthesis of the 13 proteins that are encoded by the mitochondrial DNA (mtDNA) (28, 39). These proteins include subunits of Complexes I, III, IV, and V. Moreover, electron transport and proton translocation through Complex I are impaired due to decreased content of iron-sulfur centers of Complex I in mitochondria from ethanol-fed animals (127). Cytochrome *b* in Complex III is also decreased in animals fed chronic alcohol, as well as the activity and heme content of cytochrome *c* oxidase (128). Finally, the function of ATP synthase is decreased in liver mitochondria from ethanol-fed animals due to a decrease in the concentration of two subunits of the membrane-spanning, F_o, portion of the enzyme complex (23, 103). Therefore, as discussed chronic alcohol consumption results in generalized depression in hepatic mitochondrial energy metabolism (39, 44, 125, 128). These alterations in several of the Complexes of

the electron transport chain result in a decreased rate and efficiency of ATP synthesis via the oxidative phosphorylation system. These events can lead to the production of oxidative stress that has long been associated with alcoholic liver disease.

Ethanol-associated increases in oxidative stress

Oxidative stress has been implicated as a major factor in the development of alcoholic liver disease (2, 36). Oxidative stress is characterized by an imbalance between reactive species production and removal, as well as a decrease in antioxidant defense mechanisms. The ability of acute and chronic alcohol consumption to increase ROS production has been demonstrated in a variety of systems including in vitro cell culture systems, in vivo experimental animal models, and human studies (1, 9, 14, 80, 105). However, despite the increased understanding of alcohol metabolism and toxicity the mechanisms by which ethanol induces oxidative stress and causes cell injury remain elusive. There are several pathways that are implicated as having a key role in ethanol induced oxidative damage and include: Kupffer cell activation (50, 129); ethanol mobilization of iron (135); ethanol induced hypoxia (9); decrease in the antioxidant enzyme glutathione peroxidase-1 (13); production of the reactive product acetaldehyde (2, 33, 75, 136); and other damage to mitochondria (14, 15, 30, 31, 38). Many of these pathways are not exclusive of one another and collectively these pathways can contribute to alcoholic liver disease.

There have been several studies done both *in vivo* and *in vitro* that show ethanol-induced oxidative stress plays a role in cell injury. Using the intragastric feeding model developed by Drs. French and Tsukamoto (131) it was shown that alcohol induced liver injury was associated with enhanced lipid peroxidation, formation of the1-hydroxyethyl radical, and formation of lipid radicals (132). Also, in the intragastric model the addition of iron enhanced lipid peroxidiation (130). Iron promotes oxidative stress by catalyzing the conversion of superoxide ($O_2^{\bullet-}$) or hydrogen peroxide (H_2O_2) to the powerful oxidant hydroxyl radical ($\bullet OH$). In addition, several *in vitro* studies haven shown that ethanol can produce oxidative stress. Studies with isolated hepatocytes from control and ethanol fed rats indicted that alcohol metabolism results in increased production of ROS (11). Alcohol and acetaldehyde metabolism increases NADH concentrations in the cytosol and mitochondria, respectively. It is proposed that alcohol-dependent damage to complexes I and III and increased NADH concentrations, leads to increased ($O_2^{\bullet-}$) production in mitochondria from ethanol-exposed animals (12). Interestingly, it has also been shown that chronic ethanol exposure increases CYP2E1 in the mitochondrion, contributing to increased production of ($O_2^{\bullet-}$) in mitochondria (35). These findings support the hypothesis that oxidative stress from increased reactive species may be a critical pathogenic event for alcohol-dependent mitochondrial dysfunction. Importantly chronic ethanol-mediated oxidative stress may enhance the vulnerability of mitochondria to undergo induction of the mitochondrial permeability transition pore (MPTP), leading to cell death.

The mitochondrial permeability transition pore (MPTP)

Chronic ethanol exposure is known to be associated with a range of intracellular stresses, which are detrimental to mitochondrial function (98). These include oxidative stress, decreased mitochondrial respiratory chain components, degradation of mitochondrial DNA, depletion of mitochondrial GSH, and acetaldehyde adduct formation (2, 10, 74), all conditions which are capable of predisposing the mitochondrion to induction of the MPTP (8, 20, 26, 100, 116). The mitochondrial inner membrane can undergo a generalized increase in solutes (the mitochondrial permeability transition), which results in loss of membrane potential, swelling of the inner mitochondrial membrane, rupture of the outer membrane, and eventually cell death. The MPTP is a non-specific pore with a diameter of 2.3 nm, which allows passage of small molecular weight solutes with a molecular cut-off up to 1.5 kDa through the mitochondrial inner membrane (68). While there continues to be considerable debate about what specific protein components comprise the pore, a better picture of pore components and the conditions that are needed to induce the MPTP are emerging. It has been proposed that the MPTP is made up of the voltage dependent anion channel (VDAC: outer membrane), the adenine nucleotide translocase (ANT: inner membrane), cyclophilin D (Cyp D: matrix) and other molecules (Figure 3) (60, 68, 139).

Voltage Dependent Anion Channel (VDAC). The most abundant protein located in the outer membrane is VDAC (also known as porin), a 31 kDa protein. VDAC

functions as gatekeeper for the entry and exit of mitochondrial metabolites; thereby it controls cross-talk between mitochondria and the rest of the cell. Thus, in addition to regulating the metabolic and energetic functions of mitochondria, VDAC appears to be a convergence point for a variety of cell survival and cell death signals mediated by its association with various ligands and proteins. The VDAC family consists of 3 gene products (VDAC1, 2, and 3) that are similar in structure and function (118). The VDAC protein makes a pore in the mitochondrial outer membrane that allows low molecular weight solutes to pass and gain access to the inner membrane transport systems (7, 42). In the open state the VDAC channel is permeable to solutes up to 5 kDa (16). There has been much debate as to whether VDAC is a necessary component of the MPTP. Recently, genetic approaches have been used to determine whether VDAC is truly a component of the MPTP. Bernardi and colleagues (87) demonstrated that mitochondria from VDAC1$^{-/-}$ mice still exhibit a normal cyclosporin A-sensitive MPT response. Similarly, Ca^{2+}-induced MPT was unaffected in either VDAC1$^{-/-}$ or VDAC3$^{-/-}$ mitochondria (18). Taken together, these studies provide strong evidence suggesting that VDAC may be dispensable for MPT and it is not an essential component of the MPTP.

Adenine Nucleotide Translocase (ANT). The ANT is an anti-porter that mediates the exchange of ATP and ADP across the inner mitochondrial membrane. The ANT proteins belong to a large family of 6 transmembrane inner mitochondrial

14
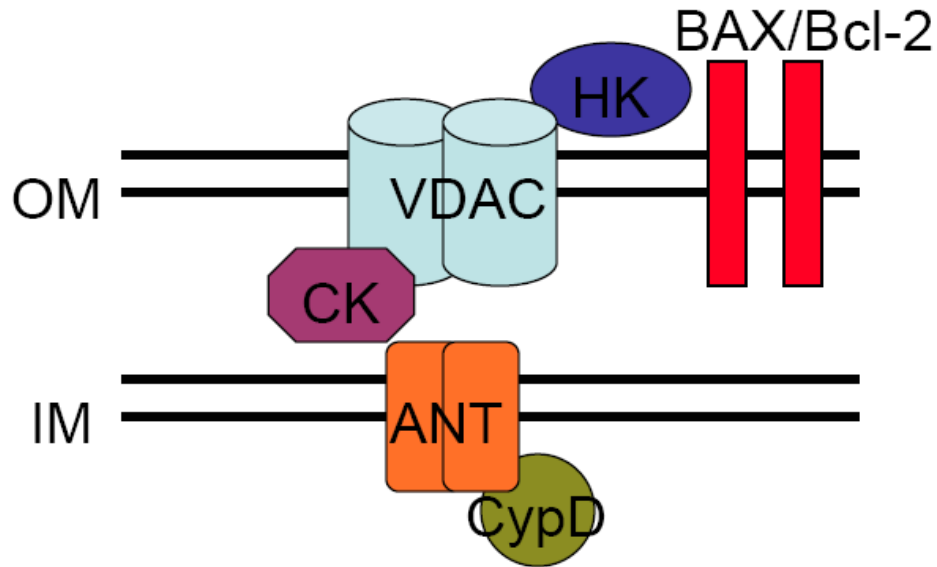
Figure 3. The components of the mitochondrial permeability transition pore. The MPTP is thought to be composed of 3 main components: voltage dependent anion channel (VDAC), adenine nucleotide translocator (ANT), and cyclophilin D (Cyp D). VDAC is the most abundant protein located on the outer membrane. ANT is the most abundant protein located on the inner mitochondrial membrane. CypD is a matrix protein that serves as a chaperone. There are also additional accessory proteins such as Hexokinase (HK), Creatine Kinase and the pro- and anti-apoptotic proteins (BAX and Bcl-2).

membrane carriers (32). There are 3 isoforms of ANT: ANT1 is predominantly in cardiac and skeletal muscle (122), ANT2 is predominantly in liver (122), and ANT3 has been described in humans but appears to be lacking in rodents (34). The ANT operates as a gated pore that alternates between two conformations in which the ADP/ATP binding site is either on the matrix side of the inner membrane (m-state) or on the cytoplasmic side (c-state) (7, 16, 42). Ligands, such as bongkrekate, that bind to the (m-state) can inhibit the pore, whereas, carboxyatractylate, that binds to the (c-state) can activate the pore (7, 42). There has been considerable debate as to whether the ANT is an essential component of the MPT. Crompton et al. (43) found that reconstitution of an ANT-CypD complex in liposomes yielded a MPT-like pore. In addition, McStay et al. (100) reported that oxidizing agents can cross-link two thiol groups on the ANT and that this involves ADP and cyclophilin-D (Cyp D) binding enhancing opening the MPTP. However, Wallace and colleagues showed that mitochondria isolated from ANT1/2 double null mice still exhibit a normal cylosporin A-sensitive MPT response (86). These recent findings using genetically modified animals indicate that ANT may act as a peripheral regulatory protein that confers sensitivity of the pore to adenine nucleotides, ANT ligands, and Ca^{2+} rather than being a channel-forming unit of the pore as originally proposed.

Cyclophilin D (Cyp D). The third proposed component of the MPTP, Cyp D, belongs to the cyclophilin family. Cyclophilins are ubiquitous proteins that have *cis-trans* peptidyl-prolyl isomerase activity, which catalyze the rotation of proline

16

peptide bonds inducing a conformational change in the target protein (52).

Cyclophilins are approximately 109 amino acids long and belong to a diverse set

of proteins termed molecular chaperones (52). Molecular chaperones are

functionally responsible for correct folding, assembly, and transport of newly

synthesized proteins in the cell (3). In addition, due to the enzymatic properties

of chaperones they are accountable for the acceleration of the rate limiting steps

of protein folding (3). There have been several cyclophilins identified. The most

abundant is cyclophilin A, which is an 18 kDa protein originally identified as the

cytosolic binding protein for cyclosporin A and subsequently shown to be a

peptidyl-prolyl *cis-trans* isomerase (53). Cyclophilin A reduces the aggregation of

incompletely folded carbonic anhydrase (54), catalyzes the isomerization of a

peptidyl-prolyl bond in the Ca^{2+} regulating hormone calcitonin (79), and increases

the rate of folding of ribonuclease T1 (119). Cyclophilin B is a 21 kD protein that

contains a NH_2 terminal ER specific sequence (114). Cyclophilin B co-localizes

with the Ca^{2+} binding protein calreticulin in the ER, suggesting that it could a play

a role in mediating Ca^{2+} signaling (6). Cyclophilin C (23 kDa) is also an ER

protein which associates with a 77 kDa protein involved in signaling and cellular

processes (56). Cyclophilin 40 has dual localization in the cytoplasm and the

nucleus (81, 82). Cyclophilin 40 regulates Hsp90 ATPase activity during

receptor-Hsp90 assembly (76). Lastly, Cyclophilin D (Cyp D) is a soluble protein

located in the mitochondrial matrix and its' pathological role in the MPTP is

widely accepted (21). Cyclosporin A has long been identified as an inhibitor of

cyclophilin isomerase activity (24, 70). Use of cyclosporin A, as an inhibitor of

the MPTP, has been influential in understanding the molecular mechanism of the MPTP in both normal biology and pathophysiology. Cyclosporin A acts by binding to cyclophilins and inhibiting the *cis-trans* peptidyl-prolyl isomerase activity. It has been found that Cyp D can bind to cyclosporin A and delay opening of the MPTP (3, 57, 58, 94).

In 1998, Halestrap and colleagues provided strong evidence for the role of Cyp D and the ANT in the MPTP using a glutathione S-transferase (GST)/Cyp D fusion protein which bound the ANT (72). Furthermore, Compton et al. (43) created a GST-Cyp D fusion protein, which bound ANT and VDAC. This gave rise to the concept that Cyp D associates with ANT and VDAC and forms the VDAC/ANT/Cyp D complex; the MPTP. In addition, it was shown that increased Ca^{2+} and redox stress activated Cyp D via its peptidyl-prolyl activity and converted this complex into the MPTP (67, 69-71).

Genetic studies done recently helped to support the concept that Cyp D is an important regulatory component of the MPTP. Basso and colleagues generated mice devoid of Cyp D to study the properties of the MPTP (19). Several groups have shown that mitochondria from Cyp D[-/-] mice are resistant to the MPTP in an identical manner to that of mitochondria from wild-type mice treated with cyclosporin A (17, 48). For example, Du et al. (48) showed that Cyp D deficient cortical mitochondria were resistant to Ca^{2+} induced swelling and permeability transition. These data presented on the interactions between the components of the MPTP have a major implication for our understanding of how

ethanol may regulate the MPTP and the mechanism behind the regulation of the MPTP.

Ethanol and the mitochondrial permeability transition pore (MPTP)

Previous studies support the concept that chronic ethanol-mediated mitochondrial dysfunction may involve enhanced sensitivity to the MPTP. For example, Pastorino et al. (110) showed that mitochondria isolated from livers of rats fed ethanol for 6 weeks were more sensitive to induction of the MPTP than liver mitochondria isolated from iso-calorically matched controls. However, the mechanisms responsible for this increased sensitivity were not identified. It has been reported that acute ethanol treatment promoted apoptosis in primary hepatocytes cultures *in vitro* by increased mitochondrial ROS formation, depolarization, and cytochrome *c* release, which are all characteristics of the pore opening (11, 117). When treated with ethanol, HepG2 cells over-expressing CYP2E1 exhibit increased cell death, which is preceded by mitochondrial depolarization and prevented by cyclosporin A suggesting the involvement of the MPTP (35). However, the mechanisms responsible for the regulation and the increased MPTP sensitivity in liver mitochondria from ethanol-fed animals compared to control animals are not known and remain undefined.

Mitochondria permeability transition pore (MPTP) and cell death protein interactions

There is now considerable evidence that ethanol exposure also disturbs the balance of pro- and anti-apoptotic factors that participate in the induction of the MPTP (74). The mitochondrial pathway for apoptosis is dependent on the B-cell CLL/Lymphoma 2 (Bcl-2) family of proteins. The Bcl-2 family is divided into three groups based on the presence of homology domains. The anti-apoptotic proteins (e.g., Bcl-2, Bcl-w, Bcl-x_L) contain BH domains 1- 4 and are generally integrated within the outer mitochondrial membrane (37). The pro-apoptotic members are divided into 2 classes: the effector molecules and the BH3- only proteins. The effector molecules (e.g., Bak and Bax) contain BH1-3 domains and can permeabilize the outer mitochondrial membrane by creating a proteolipid pore that may be responsible for cyctochrome *c* release from mitochondria(85). The BH3-only proteins (e.g., Bid, Bim, Bad, Bik, bNIP3, and PUMA) function in distinct cellular stress pathways (37). The combined signaling within the Bcl-2 family of proteins dictates the fate of the affected cell. What continues to be controversial in the field is how interactions among the proteins of the Bcl-2 family can trigger induction of the MPTP and which ones are key signals required for cell death.

Pro-apoptotic proteins, including Bax, are responsible for the permeabilization of the mitochondrial outer membrane, whereas anti-apoptotic proteins, including Bcl-2 and Bcl-x_L preserve mitochondrial integrity and prevent release of cytochrome *c* (5). The pro-apoptotic protein Bax is a cytosolic protein

that translocates to the mitochondrion during apoptosis (5). After activation, Bax

inserts into the outer mitochondrial membrane and forms larger oligomeric

structures that are proposed to potentiate the MPTP (5, 101). In contrast to Bax,

the Bcl-2 family proteins, Bcl-2 and Bcl-x_L, inhibit cell death, depending upon the

intracellular location of these proteins. In summary, the possible disruption in the

balance between pro- and anti-apoptotic pathways eventually leads to

permeabilization of mitochondrial membranes and release of pro-apoptotic

proteins from mitochondria, ultimately leading to cell death.

Calcium, oxidative stress, and the mitochondrion

Dysregulation of mitochondrial Ca^{2+} homeostasis is now recognized to

play a key role in several pathologies including liver disease (93). It known that

mitochondria can sequester large amounts of Ca^{2+} and that Ca^{2+} is a key trigger

of the induction of the MPTP (64, 77, 108, 124). In addition, it has been reported

that oxidants cause a rapid increase in Ca^{2+} concentration in the cytoplasm of

diverse cell types (51).

Calcium concentrations in the mitochondrion are dependent on those in

the cytoplasm which, in turn, depend on Ca^{2+} flux through channels of the

endoplasmic reticulum (ER) and the plasma membrane (51). The cytoplasmic

Ca^{2+} concentration is approximately 0.1 µM compared to an extracelluar Ca^{2+}

concentration of approximately 1 mM and about 5 mM in the ER (22).

Mitochondria can take up Ca^{2+} through a uniporter, which represents a gated,

highly selective ion channel (59, 61, 63). A uniporter is a mechanism which

facilitates passive transport of Ca^{2+} down its electrochemical gradient without coupling Ca^{2+} transport to the transport of another ion (64). The uniporter displays second order kinetics with separate activation and transport sites (59, 65). In addition, it has been determined that the uniporter is hardly saturable by Ca^{2+} due to its half-activation constant, $K_{0.5}$ of 19 mM Ca^{2+} (59). In addition, it has been shown that the uniporter can be blocked by ruthenium red (61, 65).

Ca^{2+} can be released from mitochondria through two separate Ca^{2+} efflux mechanisms: sodium (Na^+)-dependent and Na^+-independent mechanisms (25, 61, 62). These two efflux pathways are found in different tissues types, have different types of kinetics, and different inhibitors. The Na^+-dependent efflux mechanism is dominant in heart, brain, skeletal muscle, adrenal cortex, and many other tissues. The kinetics of the Na^+-dependent efflux mechanism have been found to be first order Ca^{2+} dependence (63). This efflux pathway is inhibited by a wide range of inhibitors such as tetraphenyl phosphonium and very high levels of ruthenium red (113). The Na^+-independent efflux mechanism is dominant in kidney, lung, and liver (65). The kinetics of the Na^+-independent efflux mechanism have been found to be second order Ca^{2+} dependence (63). This efflux pathway is inhibited by CN^-, low levels of FCCP, and very high levels of ruthenium red (113). Both efflux pathways are more limited (i.e., saturable) than the influx path due to slower reaction kinetics (45). These transport systems, influx and efflux, help maintain proper mitochondrial Ca^{2+} and cytosolic Ca^{2+} levels which are needed for cell viability.

It is known that mitochondria have the ability to sequester large amounts of Ca^{2+} in response to increases in cytosolic Ca^{2+} levels (49, 66). As stated previously, oxidants cause an increase in cytoplasmic Ca^{2+} concentration. Recently, Yan et al. (137) using isolated hepatocytes found that chronic alcohol consumption increased intracellular Ca^{2+} levels compared to control animals. However, the effect that chronic alcohol has on isolated mitochondrial Ca^{2+} uptake and accumulation has not been investigated and still remains unknown.

Summary

It is known that the oxidative metabolism of ethanol generates many cytotoxic effects in the liver. In particular, the mitochondrion is a specific target of ethanol toxicity and much of the damage can be related to oxidative stress, which can cause damage to mitochondria and induction of the MPTP within the organelle. It has also been reported that oxidants can cause a rapid increase in Ca^{2+} concentration in the cytoplasm and mitochondrial accumulation of Ca^{2+} is a key trigger for the induction of the MPTP. Induction of the MPTP can have devastating affects on cellular metabolism and signaling, which can lead to cell death.

Therefore, this dissertation will discuss the following: Chapter 2 will provide detailed listings and descriptions of several biochemical assays used to assess mitochondrial function when exposed to toxicants such as ethanol. Chapter 3 will provide a more comprehensive understanding of the molecular changes contributing to the induction of the MPTP specifically looking at what

effect chronic alcohol consumption has on Cyp D levels and Ca^{2+} handling using some of the methods described in Chapter 2. Finally, Chapter 4 will extend and expand on the results presented in Chapter 3. This chapter will further investigate the role of Cyp D in ethanol-induced mitochondrial injury using a Cyp D null mouse model. Together this information provides a more comprehensive understanding of the molecular changes that contribute to chronic ethanol-induced mitochondrial dysfunction and damage. This new information will help to guide the development of future therapeutic approaches to treat alcohol liver disease.

CHAPTER 2

ASSESSMENT OF MITOCHONDRIAL DYSFUNCTION ARISING FROM
TREATMENT WITH HEPATOTOXICANTS

by

ADRIENNE L. KING AND SHANNON M. BAILEY

Department of Environmental Health Sciences and Center for Free Radical
Biology, University of Alabama at Birmingham

ABSTRACT

Mitochondrial dysfunction from toxicants is recognized as a causative factor in the development of numerous liver diseases including steatohepatitis, cirrhosis, and cancer. Toxicant-mediated damage to mitochondria result in depressed ATP production, inability to maintain proper cellular calcium homeostasis, and increased reactive oxygen species production. These disruptions contribute to hepatocellular death and lead to liver pathology. Herein, we describe a series of basic and advanced methodologies that can be incorporated into research projects aimed to understand the role of mitochondrial dysfunction in toxicant-induced hepatotoxicity. Protocols are provided for isolation of liver mitochondria, assessment of respiratory function, measurement of mitochondrial calcium uptake, and reactive oxygen species production, as well as characterization of the mitochondrial protein thiol proteome using 2D gel electrophoresis. Data obtained from these methods can be integrated into a logical and mechanistic framework to advance understanding of the role of mitochondrial dysfunction in the pathogenesis of toxicant-induced liver diseases.

INTRODUCTION

Studies demonstrate that mitochondrial dysfunction is a key causative factor in liver disease. Indeed, defects in mitochondrial energy metabolism, disrupted calcium handling, and increased reactive oxygen/nitrogen species production are observed in many metabolic disorders and diseases induced by toxicants. Mitochondria have emerged as a main research focus through work defining new functions of this key organelle in normal cellular physiology and pathophysiology. Specifically, studies show a critical role of mitochondrial reactive oxygen/nitrogen species production in regulating cellular signaling pathways involved in cell survival and death. Given this, along with advances made in proteomics technologies, mitochondria are recognized as top candidates for proteomics analysis. However, assessment of mitochondrial function and it's proteome following toxicant exposure are not trivial undertakings.

In this unit, a technique used to isolate mitochondria from liver tissue (Support Protocol) is presented along with methods needed to assess mitochondria functionality. The methods described include measurement of mitochondrial respiration (Basic Protocol 2), calcium accumulation (Basic Protocol 3), and reactive oxygen species production (Basic Protocol 4). A presentation of proteomics approaches (Basic Protocol 1), is also included to provide researchers the basic tools needed to identify alterations in the mitochondrial proteome that contribute to toxicant-mediated diseases. Specifically, methods are presented that demonstrate how thiol labeling reagents in combination with electrophoresis and western blotting can be used to detect

27

oxidant-mediated alterations in mitochondrial protein thiols. A few select pieces

of data are presented highlighting the power of proteomics to identify

mitochondrial targets that contribute to mitochondrial dysfunction and

hepatotoxicity in response to specific toxicant exposures and metabolic stressors

such as alcohol and environmental tobacco smoke.

BASIC PROTOCOL 1 - **Mitochondrial Protein Thiol Assessment with**

Proteomics

The ability to detect and possibly identify mitochondrial proteins susceptible to

oxidative modifications will facilitate understanding of the molecular mechanisms

that contribute to oxidative damage and mitochondrial dysfunction from

hepatotoxicant exposures. The key posttranslational modification to

mitochondrial proteins to be discussed herein is protein thiol modification. To

monitor changes in the mitochondrial thiol proteome, we will present an

established method that uses a "thiol-tagging" approach in combination with 1D

and 2D gel electrophoresis techniques. In this method, unmodified thiols (e.g.,

P-SH) are "tagged" with a thiol labeling reagent (biotinylated iodoacetamide,

BIAM) that can be visualized by western blotting. In contrast, protein thiol groups

that have been oxidized (e.g., $P-SO_xH$) or modified (e.g., P-SSG) can not be

labeled by the "thiol-tag" and therefore are identified by a decrease in the

intensity of the labeling reagent on western blots.

NOTE: Most standard 1D SDS-PAGE, 2D IEF/SDS-PAGE, western blotting

protocols, reagents, and instruments can be used for assessment of protein thiol

alterations with BIAM labeling as presented in the previous section. In light of this, details regarding standard SDS-PAGE gel electrophoresis will not be presented; however, specific instructions for 2D IEF/SDS-PAGE are outlined below as this technique is not a routine method for most laboratories. Details for the detection of BIAM-labeled mitochondrial proteins by western blotting are provided.

Materials

Freshly isolated liver mitochondria (see Support Protocol)

Bio-Rad protein assay kit (Bio-Rad, cat. no. 500-0006)

Ice

10 M Tris buffer (pH 8.5) containing 1% (w/v) Triton X-100

Protease inhibitor cocktail (Sigma, cat. no. P8340)

Biotin-conjugated iodoacetamide (BIAM; Invitrogen, cat. no. B1591)

Dimethylformamide

2-mercaptoethanol

Rehydration buffer for IEF gel strips (see recipe)

Dithiothreitol (DTT) stock solution (1 M DTT dissolved in water; stored at −20ºC in 50-µl aliquots)

Ampholines Electrophoresis Reagent (e.g., Sigma, cat. no. A5174, pH between 3 and 10) or equivalent carrier ampholines or ampholytes

Tributylphosphine (Bio-Rad, cat. no. 163-201)

Equilibration buffer (see recipe) Agarose solution: ultrapure,

low-melting-temperature agarose solution (1.0% w/v agarose in 1X SDS-PAGE running buffer)

1X SDS-PAGE buffer (see recipe)

1.5 mm acrylamide resolving gel gel plates

Molecular weight markers

Coomassie blue or SYPRO Ruby

Transfer buffer (see recipe)

Blocking buffer: 1% (w/v) BSA in 1X TBS-T (filter-sterilize into bottles and store at 4ºC) 10X TBS-T stock solution for washing blots (see recipe)

Streptavidin horseradish peroxidase conjugate (GE Healthcare, cat. no. RPN1231V)

SuperSignal west pico chemiluminescent substrate (Pierce, cat. no. 34080)

50%, 50 mM NH_4HCO_3/50% acetonitrile solution

Promega Gold trypsin

0.1% (v/v) formic acid

α-cyano-4-hydroxycinnamic acid matrix

1.5-mL microcentrifuge tubes

Ice buckets

Standard laboratory vortex

Aluminum foil

Two-dimensional IEF gel electrophoresis equipment including:

IEF gel electrophoresis apparatus (e.g., Invitrogen ZOOM IPG runner, cat. no. ZM0001)

Invitrogen ZOOM strips (cat. no. ZM0011, pH 3-10)

ZOOM IPG Runner Cassettes (Invitrogen, cat. no. ZM0003)

ZOOM Dual Power Supply (Invitrogen, cat. no. ZP10002)

Forceps

15-mL conical tubes

Rotating shaker

Two-dimensional SDS-PAGE apparatus

Transfer membrane: nitrocellulose or PVDF

Electroblotting apparatus

X-ray film or imaging instrument (e.g., Bio-Rad Fluor-S Imager or ChemiDoc XRS) compatible with chemiluminescent detection methods

PD-Quest Image Analysis software (Bio-Rad Laboratories)

Savant SpeedVac

C18 ZipTips (Millipore)

MALDI-TOF target plates

Voyager De-Pro mass spectrometer

Voyager Explorer software

Additional reagents and equipment for isolating liver mitochondria (Support Protocol)

Carry out BIAM labeling of mitochondrial protein thiol

1. Prepare freshly isolated liver mitochondria from the livers of control and toxicant treated rats as described in the Support Protocol.

2. Determine the protein concentration of the liver mitochondria suspension using the Bio-Rad protein assay kit.

3. *Prepare 1 mg mitochondrial protein pellets:* Pipet a volume of mitochondrial suspension equal to 1 mg protein into a 1.5-m microcentrifuge tube. Keep samples on. Prepare mitochondrial protein pellets by centrifuging mitochondrial suspensions at 13,500 *x g* at 4°C for 10 min.

4. After centrifugation, remove and discard supernatant keeping mitochondrial pellets on ice at all times. Prepare a sufficient number of 1-mg mitochondrial samples tubes for desired gel electrophoresis and western blotting studies.

5. Gently re-suspend each 1-mg mitochondrial pellet in 100 µL of 10 mM Tris buffer (pH 8.5) containing 1% w/v Triton X-100 and 2 µL of protease inhibitor cocktail.

    Re-suspension is done with gentle up-and-down pipetting of sample until mitochondrial pellet is "dissolved" in buffer leaving a brown translucent extract in the tubes. Place samples on ice.

6. Prepare a 50 µM BIAM stock solution by dissolving BIAM in dimethylformamide.

For example, dissolve 2.3 mg BIAM into 1.0 mL of

dimethylformamide. Note that it will take approximately 5-10 min of

vigorous vortexing to get BIAM into solution. BIAM solution can be

prepared before experiments and stored in freezer as small

aliquots. It is not recommended that BIAM used for labeling

reactions undergo multiple freeze-thaw cycles. Use new BIAM

aliquot for labeling reactions.

7. Add 1.0 µL of BIAM into each 100 µL of mitochondrial extract and vortex the tubes for 30 sec. Wrap sample tubes in aluminum foil and incubate at room temperature for 15 min.

8. Terminate the labeling reaction by adding 1 µL of 2 M 2-mercaptoethanol stock solution to each sample tube. Vortex the tube for 30 secs.

9. Determine the protein concentration of samples of the samples using the Bio-Rad protein assay kit.

BIAM-labeled samples can be stored up to 6-12 months at -80°C

until gel electrophoresis and immunblotting experiments.

Run the one-dimensional IEF gel strips for two-dimensional gels

10. Thaw the BIAM-labeled mitochondria extracts and keep on ice.

Typically, the protein concentration used for 2D IEF/SDS-PAGE

gels with the Invitrogen ZOOM system is 50-200 µg per gel strip.

This concentration helps to achieve optimal resolution of proteins

and maximal BIAM label signal on immunnoblots. It is important to

note that protein concentration of stored samples should be re-measured as concentration may change from storage. An optimal protein concentration for sample is between 5 to10 µg/µL as this will ensure minimal dilution of chemicals in the IEF rehydration buffer. Please refer to manufacturer's manual for specific details on setup and use for two-dimensional gel proteomics.

11. Remove the needed number of rehydration buffer and DTT tubes from freezer and thaw to room temperature.

    Do not store thawed reagents on ice as urea and DTT will precipitate. Do not re-freeze left over DTT. Use a new aliquot for each experimental day.

12. Add 10 µL ampholines, 10 µL 200 mM tributylphosphine, 40 µL 1M DTT to 1.0 mL of rehydration buffer. Mix well and keep at room temperature.

13. Prepare the sample solution for rehydration.

    An example of conditions are given below for rehydration of IEF gel strips with buffer and a protein sample that has a protein concentration equal to10 µg protein/µL.

14. Incubate the protein samples in rehydration buffer (see table 1 for example) for at least 30 min at room temperature before loading samples onto IEF gel strips. Vortex samples every 5 to 10 min during this extraction incubation step.

Rehydrate the one-dimensional IEF gel strips for two-dimensional gels

15. Following the detailed procedures provided for the Invitrogen ZOOM system (or comparable system), slowly load the entire 160 µL of BIAM-labeled mitochondrial sample into an empty strip lane in the ZOOM IPG Runner Cassette.

    Note that the sample loads along the length of the gel lane by capillary action. Pipette the sample slowly to minimize bubble formation in the gel lane slot. Bubbles will result in uneven rehydration of IEF gel strip when strips are inserted in the slots.

Table 1. Quantities for Rehydration of IEF Gel Strips

Desired protein amount	Volume of sample	Volume of rehydration
50 µg	5 µL	155 µL
100 µg	10 µL	150 µL
200 µg	20 µL	140 µL

16. After loading all samples into the Invitrogen ZOOM cassette gel lanes, remove the IEF gel strips from freezer, keeping strips on ice. Carefully remove each IEF gel strip from the plastic backing; hold gel strip from the marked negative end (-) with a clean forceps.

    It is important here to make sure that the plastic backing is removed from IEF gel strips. Sometimes the plastic backing does not peel

off. If plastic backing is not removed, the IEF gel strip will not be rehydrated by the sample.

17. Gently slide the IEF gel strip (gel side up) into the ZOOM cassette lane until the strip reaches the positive end (+) of the cassette.

18. After all strips are inserted into the cassette, seal the ends and allow gel strips to rehydrate with sample overnight (16 hr) at room temperature.

Perform IEF

19. After rehydration is complete (16 hr), assemble the ZOOM runner according to the instruction manual directions.

20. Perform IEF using the following conditions: 175 V for 20 min, ramp to 2000 V for 45 min, hold at 2000 V for 30 min, ramp down to 500 V for 30 min, and then hold at 500 V for 2 hr.

> *As the IEF proceeds, the bromophenol blue dye front will migrate from the top of the IEF gel strip and a green/blue/yellow band will appear at the positive end of the strip after IEF is completed.*

21. After IEF, remove cassettes from ZOOM runner, seal, and freeze up to 1 day to 2 wk at -80ºC until two-dimensional SDS-PAGE is performed.

Assemble two-dimensional SDS-PAGE gels

22. Remove previously run IEF gel strips from the freezer and allow the strips to thaw for several minutes at room temperature before the equilibration step.

23. Prepare 1 ml of equilibration buffer per IEF gel strip: remove needed equilibration buffer tubes and DTT aliquots from freezer and thaw; add 50 μl DTT to each 1-mL aliquot of equilibration buffer

24. Remove the IEF gel strips from the ZOOM cassette by carefully pealing off the plastic covering and using forceps place each IEF gel strip into a separate 15-mL conical tube, gel side up, and then cover each strip with 1 mL of equilibration buffer. Gently rock the strips on a rotating shaker for 15 min at room temperature.

25. During equilibration, prepare the warm agarose solution (1.0% w/v agarose in 1X SDS-PAGE running buffer).

    Prepare the agarose solution fresh on the day of each experiment. This solution is used to seal the IEF gel strips into place above the SDS-PAGE acrylamide gel.

26. After equilibration, remove the gel strips from the tubes, cut the small plastic end from the negative side, rinse strips in standard 1X SDS-PAGE running buffer, and slide the IEF gel strips between the 1.5 mm acrylamide gels plates

27. Gently pipet the warm agarose solution over the gel strip to seal the strip on top of the acrylamide resolving gel. Do not introduce bubbles into the space between the bottom of the gel strip and the top of the resolving gel, as this will prevent transfer of proteins from strip.

28. Slide a "tooth" from a 1.5-mm gel comb between plates at the negative end of the gel.

> *This serves to form a well that can be used for adding molecular weight markers*

29. Allow the agarose to set up for 15 to 30 min before beginning electrophoresis.

30. Once the agarose has hardened, remove the gel comb tooth and load 5 µL molecular weight markers into the homemade well

31. Assemble the gel apparatus per manufacturer's instructions (e.g., Bio Rad).

Run the two-dimensional gels

32. Fill both the inner and outer buffer chambers with standard 1X SDS-PAGE running buffer.

33. Perform electrophoresis for 1 to 2 hr at 100 V (room temperature) or until the dye front reaches the bottom edge of the gel.

34. After two-dimensional gel electrophoresis is completed, stain gels for total protein (Coomassie blue or SYPRO Ruby) and/or subject to immunoblotting to detect abundance of BIAM-labeled protein thiols.

Transfer proteins

35. After conventional one- or two-dimensional SDS-PAGE gel electrophoresis, remove the gel from between the glass plates, and discard the acrylamide stacking gel (one dimensional gel) or agarose sealant gel (two-dimensional gel).

36. Discard the IEF gel strip, and incubate the acrylamide resolving gel (soaked) in transfer buffer for 15 min at room temperature.

37. Transfer to either nitrocellulose or PVDF membranes for immunoblotting.

    Our laboratory typically uses nitrocellulose membranes for this application. Again, most commercially available wet immunoblotting units can be used with the protocol described herein.

Perform immunoblotting

38. After transfer, incubate the membrane in 100 ml blocking buffer. Incubate overnight Incubate overnight at 4ºC on a rotating shaker platform.

    Note that the concentration of BSA can be increased to 3% or 5% (w/v), if additional membrane blocking is required for specific tissue samples.

39. After blocking, remove the membranes from the blocking buffer and subjected to multiple washes in 50 mL 1X TBS-T.

40. After washes, incubate membranes in a 1:100,000 dilution of the streptavidin horseradish peroxidase conjugate for 1 hr at room temperature to visualize BIAM-labeled mitochondrial proteins.

41. Again, subject membrane to multiple 50 mL 4 X 15 minute washes in 1X TBS-T before reaction with chemiluminescent reagents.

Detect antibody binding

42. Incubate washed membranes with 10 mL SuperSignal West Pico Chemiluminescent substrate for 1 to 2 min at room temperature and follow with the visualization of the BIAM-labeled proteins by either film exposures or through use of chemiluminescent imaging device.

> *Representative results for both standard 1D and 2D SDS-PAGE gel electrophoresis experiments using BIAM-labeled mitochondrial proteins are shown in Figures 1 and 2, respectively. Details regarding experiments are included in figure legends.*

Analyze two-dimensional gel and immunoblot

43. Scan stained gels using an imager, e.g. Bio-Rad Fluor-S imager or ChemiDoc XRS (Bio-Rad Laboratories).

44. Then analyze for differences in protein density using PD-Quest Image Analysis software.

45. For image analysis of 2D gels, individual protein spots on each gel are identified by the software program. While the computer program identifies individual protein spots on each gel, it is critical that these IDs are manually verified to generate a match-set of gels for control (untreated) and treatment group gels.

46. Compare the protein across all gels and select a reference gel.

> *The reference gel serves as the master gel image. The master gel typically contains the highest abundance of detected protein spots.*

47. Using a built-in algorithm, perform automatic matching of protein spots in each gel to the corresponding protein spots in the master gel by manual verification to correct for any proteins that may have been incorrectly matched to proteins in the master gel.

48. To correct for any inter-gel protein loading differences, normalize the density data for all protein spots in each gel to the total density in valid protein spots for that particular gel.

49. Transfer normalized protein spot densities into an Excel spreadsheet and calculate the mean densities for statistical analyses.

50. Analyze BIAM-labeled mitochondrial proteins visualized using a Bio-Rad Chemi-Doc imager for differences in protein thiol intensity using the same approaches described for gel analysis.

51. Normalize protein thiol blot intensities to total protein by dividing protein thiol blots densities by protein gel densities.

52. Similarly, normalize the thiol intensity of individual proteins to density of its corresponding protein.

53. Perform statistical analysis on both protein and protein thiol blot densities essentially as described in (Venkatraman et al. 2004; Andringa et al. 2008).
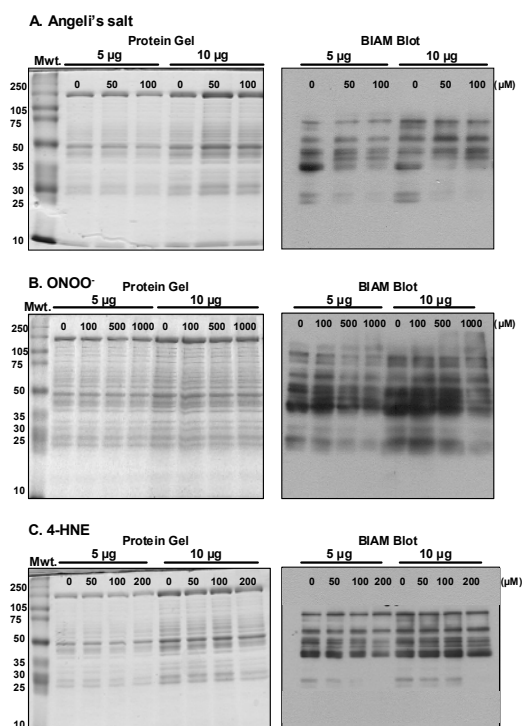
Figure 1. Treatment with Angeli's salt, peroxynitrite, and 4-hydroxynonenal increase protein thiol modifications in liver mitochondria. In this figure representative experiments are presented, which show modification of mitochondrial protein thiols by reactive nitrogen and lipid species using the BIAM labeling technique in combination with 1D SDS-PAGE and western blotting. Freshly isolated rat liver mitochondria (1.0 mg protein/mL) were incubated with increasing concentrations of the nitroxyl donor Angeli's salt (AS, panel A, 0-100 µM), peroxynitrite (ONOO⁻, panel B, 0-1000 µM), or 4-hydroxynonenal (4HNE, panel C, 0-200 µM) for 15 min at 37°C. After incubations, sample tubes were placed on ice and immediately centrifuged at 10,000xg for 10 min at 4°C. After centrifugation, the supernatant was discarded and mitochondrial pellets were subjected to the BIAM-labeling protocol included in Basic Protocol, step 1. The BIAM-labeled mitochondrial samples (5 or 10 µg protein) were then separated on 1D SDS-PAGE gels (10% acrylamide) using standard gel electrophoresis techniques. The extent of labeling was determined by western blotting using streptavidin-HRP (Basic Protocol, step 4). Note that the left-side panel show gels with blots on the right-side of panels. It is important to note that these treatments, especially at high concentrations, did not result in protein degradation or loss of protein in samples. More importantly, however is the loss or decrease in the BIAM signal in mitochondrial treated with AS and ONOO⁻, with less of a decrease observed in the 4HNE group. These basic experiments demonstrate that protein thiol groups have been oxidized or modified as a consequence of these treatments. These changes in thiols are detected using western blotting where decreased labeling with BIAM is shown by decreased streptavidin-HRP immunoreactivity (i.e., signal) on the blot.

A. Control Diet, Filtered Air

B. Ethanol Diet, Filtered Air

C. Control Diet, ETS

D. Ethanol Diet, ETS

pI 3 → 10

Mwt. (kDa)
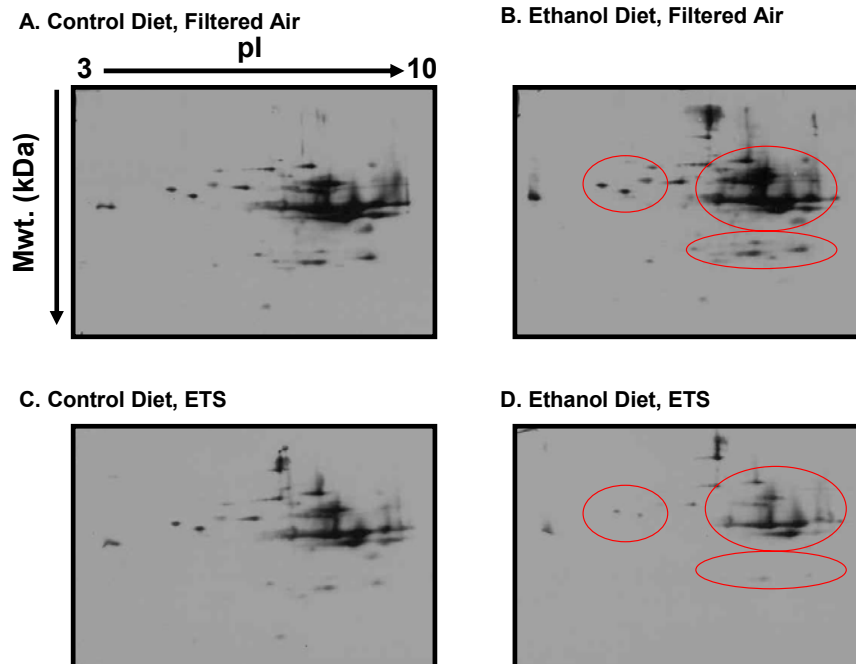
Figure 2. Modification of the mitochondrial thiol proteome by chronic alcohol consumption and environmental tobacco smoke. In this figure representative 2D western blots are shown for BIAM-labeled mitochondrial proteins. For this experiment, mice were exposed to a control or an ethanol (29% total daily calories) containing diet and either filtered air or low-level environmental tobacco smoke (ETS, 10 mg/m^3 total suspended particulate) for 4 weeks (Bailey et al. 2009). After exposures, mitochondria were isolated from livers of mice and incubated with the thiol labeling reagent BIAM (50 µM) per Basic Protocol, step 1. The samples were then subjected to 2D gel electrophoresis and BIAM labeling was determined by western blotting with streptavidin-HRP (Basic Protocol, steps 2-4). A decrease in BIAM-labeling signal indicates oxidation and/or modification of cysteine residues in proteins. Based on this, a preliminary assessment of the mitochondrial thiol proteome shows that co-exposure to ethanol and ETS results in a significant decrease in thiol labeling of multiple mitochondrial proteins (panel D, red circled area) as compared to control groups (panels A and C) and the ethanol alone group (panel B, red circled area). It is important to note analysis of the gels showed equal loading of protein and no major loss in protein content in the ethanol + ETS group. Therefore, the decreased signal is due to a loss in protein thiols in response to modification/oxidation of thiols and simply a change in protein content (gels not shown).

Identify proteins with matrix-assisted laser desorption ionization time-of-flight (MALDI-TOF) mass spectrometry

54. Excise protein spots of interest (i.e., those altered in abundance and/or via thiol modification) from the gels.

55. Subject the protein gel plugs to processing via standard methods in a mass spectrometry core laboratory.

    See http://www.uab.edu/proteomics and Bailey et al. (2008) and Andringa et al. (2009) for helpful information.

56. Typically, destain samples by three 30-minwashes in a 50%, 50 mM NH_4HCO_3/50% acetonitrile solution followed by a 16-hr incubation at 37ºC with 12.5 ng/µl Promega Gold trypsin to digest proteins.

57. Extract the resulting peptide solution by two 30-min washes with a 50/50 solution of 5% formic acid and acetonitrile.

58. Collect supernatants and dry using a Savant SpeedVac.

59. Resuspend the dried peptide samples in 0.1% (v/v) formic acid and desalt on C18 ZipTips.

60. Dilute 1:10 with a saturated solution of α-cyano-4-hydroxycinnamic acid matrix before applying to MALDI-TOF target plates.

61. After plating, dry samples before analysis with a Voyager De-Pro mass spectrometer in the positive mode.

62. Analyze spectra are using Voyager Explorer software and identify peptide masses by mass spectrometry masses submitted to the MASCOT database (see *http://www.matrixscience.com*) for protein identification.

63. Classify proteins identified from gels using the Universal Protein Resource Web site (*http://www.uniprot.org*) maintained by UniProt Consortium.

ISOLATION OF LIVER MITOCHONDRIA

To ensure the success of proteomic studies (Basic Protocol 1) and functional measurements (Basic Protocols 2 to 4) described within this unit, it is essential that proper methods are used for the isolation of liver mitochondria with high respiratory capacity. We have included a method in this Support Protocol section, which should ensure preparation of highly functional, tightly coupled liver mitochondria.

NOTE: All protocols using live animals must first be reviewed and approved by an Institutional Animal Care and Use Committee (IACUC) and must follow officially approved procedures for the care and use of laboratory animals.

Reagents and materials for mitochondrial isolation

Isolation buffer (see recipe)

Rat, e.g., Sprague-Dawley, 200-250 g body weight will have on average an 8-10 g liver

Protease inhibitors (see recipe)

Bio-Rad protein assay kit (Bio-Rad, product # 500-0006)

100 -and 50 mL beakers

Tweezers

Scissors

50-mL glass homogenizer with serrated-bottom Teflon pestle

Motor-driven homogenizer/mixer (Fisher Dyna-Mix product # 14-498-45A)

or comparable drill press

Appropriate-size centrifuge tubes (e.g., Sorvall centrifuge tube 50 mL size

product # 03146)

Standard laboratory centrifuge

Glass rods

Smooth-bottom Teflon pestle to fit same 50 mL glass homogenizer

15 mL glass homogenizer

Smooth-bottom Teflon pestle to fit same 15 mL glass homogenizer

10 mL graduated cylinder

Standard spectrophotometric cuvettes for protein determination

UV-visible spectrophotometer

Additional reagents and equipment for euthanasia (Donovan and Brown,

2006)

Prepare the isolation buffer

1. Prepare a sufficient amount of isolation buffer for mitochondrial isolation.

    For example, 500 mL of isolation buffer needed for 1 rat liver.

2. Add protease inhibitors to 500 mL of buffer: 50 µL of PMSF (final conc. 4

    µg/mL), 100 µL of leupeptin and 100 µL of aprotinin (final conc. 2 µg/mL)

    and 500 µL of pepstatin (final conc. 1 µg/mL).

For preparation of liver mitochondria from 2 rat livers double the amount of isolation buffer and the amount of all protease inhibitors.

3. Pour small amount of isolation buffer in one 250 mL beaker and 10 mL of isolation buffer per gram of liver into another 250 mL beaker. Place buffer on ice.

    It is important that buffer remain ice-cold throughout the isolation procedure.

Isolate the liver

4. Weigh the rat.

5. Following approved euthanasia protocol (Donovan and Brown, 2006) quickly remove liver and place it into the beaker containing the small amount of buffer to rinse liver of blood.

6. Use tweezers to remove the liver from the beaker and weigh liver making sure to dab off excess buffer.

7. Place liver into the beaker containing the larger volume of buffer (10 mL/g liver) use scissors chop the liver into small pieces.

Homogenize the liver

8. Pour ¼ of the liver into a 50 mL glass homogenizer and add a small amount of additional buffer, e.g., 10 to15 mL. Using the serrated pestle, homogenize the liver with the motor-driven homogenizer instrument.

Bring the homogenizer up gently making sure to homogenize most of the liver.

> *This usually takes 3 to 5 passes. It is very important not to over homogenize the liver tissue at this step. If homogenization is too harsh and rigorous, mitochondria will be of poor quality and uncoupled. This step needs to be optimized per each laboratory and laboratory personnel. It is also important that the commercially purchased pestles are modified such that the "fit" between pestle and glass homogenizer is loosened. This is easily accomplished by taking pestle and glass homogenizer to a research machine shop. A "looser" fit is needed than that originally manufactured. A tight fit results in "overworked" liver tissue and poor mitochondria preparation.*

Fractionate the homogenate

9. Once homogenization is complete, pour the homogenized liver into 50 mL centrifuge tube.

10. Repeat step 7, until all liver is homogenized pouring each aliquot into a centrifuge tube on ice.

> *Typically, the entire liver can be homogenized in 4 rounds and divided among 4, 50 mL centrifuge tubes. Rinse pestle with water between each homogenization step.*

11. Balance centrifuge tubes and centrifuge 10 min at 560 *x g*, 4ºC.

This separates the pelleted nuclear fraction and cellular debris from supernatant fraction containing mitochondria.

12. Pour supernatant from nuclear pellet and save in a 100 mL beaker on ice.

    This fraction containing mitochondria is referred to as post-nuclear fraction.

13. Using a small volume of isolation buffer, gently break up the nuclear pellet with glass rods and then re-suspend in the centrifuge tube using the smooth pestle.

    It is important that commercially purchased smooth pestles are also modified so that they fit loosely into the centrifuge tubes. Again, this is easily accomplished by taking pestles and tubes to a research machine shop, as described above in step 7.

14. Repeat centrifugation of washed nuclear fraction 10 min at 560 *x g,* at 4°C.

15. Add supernatant from nuclear wash step to the beaker containing the saved post-nuclear fraction from step 12.

    The nuclear pellet can be saved for investigation or discarded.

Isolate mitochondria

16. Pour the post-nuclear fraction containing mitochondria into four clean 50 mL centrifuge tubes and centrifuge 10 min at 8500 *x g,* 4°C to obtain the crude mitochondrial pellet and post-mitochondrial supernatant.

17. Pour post-mitochondrial supernatant from mitochondrial pellets into a clean 250 mL beaker.

The post-mitochondrial supernatant can be saved for preparation of cytosolic and microsomal fraction or discarded. If post-mitochondrial supernatant is to be saved it is recommended that protease inhibitors (Sigma product # P8340) are added at a concentration of 20 µL/mL.

Wash mitochondria

18. Add a small amount of isolation buffer to each of the four dry mitochondrial pellets, 5 to 10 mL, and carefully scrape the mitochondrial pellet from the bottom of each of the four centrifuge tubes using clean glass rods.

19. Gently resuspend the mitochondrial pellets by using a smooth-bottomed pestle that loosely fits into the centrifuge tube.

    Again, see comments above in step 7 and 13 regarding modification of pestles to loosen the fit between homogenizer and centrifuge tubes.

20. Once all mitochondrial pellets are resuspended, add 40 to 45 mL of additional isolation to buffer to each of the four centrifuge tubes.

21. Centrifuge the washed mitochondria 10 min at 8500 $x\,g$, 4ºC to obtain a second round of mitochondrial pellets.

22. After centrifugation pour off supernatant and repeat wash described in step 18. However, at this step combine the small volume of mitochondria from 2 centrifuge tubes to 1 centrifuge tube, and then gently resuspend as in step 18.

Thus, at this step you will have two centrifuge tubes of re-suspended, washed mitochondria as compared to four tubes. For mitochondrial preparations used for measurement of calcium accumulation, resuspend the pellet in 30 mL of isolation buffer without EDTA.

23. Centrifuge the washed mitochondria 10 min at 8500 x g, 4ºC to obtain a third round of mitochondrial pellets.

24. After centrifugation, pour off supernatant and repeat wash as in step 16 and 18. However, at this step combine the small volume of mitochondria from the two remaining centrifuge tubes into 1 tube, and then gently re-suspend as in step 18.

Thus, at this step you will have one centrifuge tube of re-suspended, washed mitochondria as compared to two tubes.

25. Centrifuge the washed mitochondria 10 min at 8500 x g, 4ºC to obtain the final mitochondrial pellet.

Prepare mitochondrial samples

26. After centrifugation pour off supernatant and add a small amount of buffer to final mitochondrial pellet.

Typically, one should add 5 mL per 10 g of original liver weight, which will result in approximately a 30 mg/mL mitochondrial protein concentration. It is important that mitochondria are resuspended in small volume of buffer resulting in a concentrated mitochondrial

suspension, e.g., 30 to 50 mg/mL. Mitochondria maintain

functionality if they are stored under concentrated conditions.

27. For final resuspension gently scrape the mitochondrial pellet from the bottom of the centrifuge using a glass rod and gently resuspend as before using smooth pestle.

28. To ensure full homogenization, transfer the mitochondrial suspension to a 15 mL glass homogenizer and homogenize by hand using a smooth-bottom pestle.

> *This last homogenization step helps to ensure that all mitochondria*
>
> *are resuspended and will not fall out of solution when mitochondria*
>
> *are stored on ice for assays and experiments.*

29. Transfer the final mitochondrial suspension to a 10 mL graduated cylinder and record the volume. Keep mitochondria on ice at all times.

> *At this point, mitochondria are now ready for use in assays and*
>
> *experiments. It is important to note, that mitochondria do have a*
>
> *limited "shelf-life". Experiments with isolated mitochondria should*
>
> *be completed within 2 to 4 hr following isolation.*

30. Perform a protein assay immediately to determine the concentration of isolated mitochondria.

31. Measure mitochondrial respiration rates and extent of coupling at this time to assess quality and functionality of mitochondria (see Basic Protocol 2).

Measurement of Mitochondrial Respiration

Liver mitochondria isolated by the method described in the Support Protocol section should always be tested for respiratory capacity and coupling before performing proteomic and functional assays. Indeed, only coupled mitochondria with high respiratory capacity should be used in experiments. Mitochondrial respiratory function should also be measured to determine whether toxicant exposure damages mitochondria. This can be determined by measuring mitochondrial state 3 and 4 respiration rates and the respiratory control ratio. For example, comparison of respiratory rates (state 3 and 4) between control and experimental groups (e.g., toxicant exposures) can be a very powerful test to help determine whether toxicant exposure causes a mitochondrial defect, which could be important in disease pathogenesis.

Materials

S16 electrode cleaning kit (Hansatech Instruments) containing:

No.1 course electrode disc polish

No.2 fine electrode disc polish

50% saturated KCl electrolyte solution (Fisher)

Air-saturated H_2O

Sodium hydrosulfate

HEPES respiration buffer (see recipe) Glutamate-Malate solution (see recipe) Freshly isolated liver mitochondria (see Support Protocol)

ADP for respiration measurements: 0.027 M ADP in 0.067 M NaPO4

buffer, pH

6.8 (see recipe for NaPO4 buffer)

70% (w/v) ethanol

Succinate (1 M solution, pH 7.2 with 10 N KOH and store at 4∘C)

Rotenone (1 mM in 95% ethanol)

Circulating water bath

S1 oxygen electrode disc (Hansatech, cat. no. S1)

Pasteur pipets, glass

Scissors

Cigarette paper www.rizla.com

Teflon membrane (Hansatech, cat. no. S4)

Forceps

Small and large O-rings (Hansatech, cat. no. S5)

O-ring membrane applicator (Hansatech, cat. no. A2)

Liquid-phase electrode chamber (Hansatech, cat. no. DW1)

Oxygraph controlling unit with Oxygraph software (Hansatech, cat. no.

OXYG1)

Small stir bar

Spatulas

25-µl syringe (Hamilton, cat. no. 80230) with extended length needle

(Hamilton, special order 22S 3.6-in. point style 2)

Prepare the oxygen electrode instrument

1. Turn the circulating water bath on with temperature set at 30°C.

2. The oxygen electrode disc should be cleaned before each use. The anode
    should be cleaned with the No.1 course electrode disc polish and the
    cathode should be cleaned with No.2 fine electrode disc polish. The
    electrode should be rinsed thoroughly with ddH$_2$O before assembly.

    > *Please note that these directions are also included with the*
    >
    > *manufacturer's instructions. Users are strongly encouraged to refer*
    >
    > *to these materials for set-up, operation, and maintenance.*

3. Using a glass Pasteur pipette, place a drop of the KCL electrolyte solution
    on the top of the cathode with placement of 3 more drops equally spaced
    on the anode.

4. Cut a 1.5 cm x 1.5cm piece of cigarette paper.

5. Cut a 2.5 cm X 2.5 cm of Teflon membrane.

6. Place the cigarette paper over cathode using forceps.

7. Place the Teflon membrane over the cigarette paper using forceps.

8. Once the paper and membrane are properly in place with no wrinkles,
    place the small o-ring on the o-ring/membrane applicator, apply the
    applicator instrument on top of the cathode and push down.

    > *This will seal the paper and membrane to the electrode disc.*
    >
    > *Remove and replace with fresh paper and membrane if wrinkles or*
    >
    > *bubbles are present.*

9. Next, place the larger outer o-ring into its slot on the anode and place the electrode disc onto the bottom of the chamber per manufacturer's instructions.

Assemble the Oxygraph

10. Carefully screw electrode disc into the DWI chamber.

11. Place DWI chamber on top of the Oxygraph controlling unit and connect tubes from the circulating water bath to the chamber.

12. Attach electrode wire cable to electrode disc electrical connection.

13. Plug Oxygraph into the wall socket.

14. Turn the power on (gray button in front).

    Green light will illuminate.

15. Fill inner chamber with ddH$_2$O and place small stir bar into the inner chamber.

16. To engage the Oxygraph software, turn on computer and select Oxygraph plus software. Click the blue button on tool bar to start stirrer; the stir bar will begin to stir. Make sure stir bar is properly setting and stirring on top of the electrode.

Calibrate the Oxygraph electrode

17. Place a 50 mL conical tube containing air saturated H$_2$O (vigorously shaken ddH$_2$O) in 30ºC water bath.

18. Remove water out of the inner chamber using glass Pasteur pipette and replace with 1840 µL of fresh air saturated H_2O.

19. Allow H_2O to stir for about a minute making sure that the stir bar stirs in the center of the chamber.

20. On the Oxygraph plus software select "CALIBRATE" then "Liquid Phase" and set temperature at 30ºC and continue to follow steps for calibration provided by the manufacturer.

21. Allow the oxygen concentration trace to stabilize and establish zero oxygen in chamber and select "OK".

22. Using a spatula, add a small amount (i.e. enough to fit on end of spatula) of sodium hydrosulfate into the chamber and then cap the chamber.

23. Allow the oxygen concentration trace to stabilize at zero and follow steps on the software to complete calibration.

24. Once the calibration process is complete remove the sodium hydrosulfate containing H_2O from the chamber and rinse thoroughly four to five times with 2 mL fresh ddH_2O.

> *The oxygen electrode is now ready for respiration measurements. Please make sure that when not in use the inner chamber is filled with fresh ddH_2O to prevent membrane from drying out.*

Measure mitochondrial respiration using glutamate/malate as oxidizable substrate (Complex I-linked respiration)

25. Add 1.74 mL of HEPES respiation buffer to the inner chamber.

26. Add 20 µL of glutamate/malate stock solution to the inner chamber.

27. Add 80 µL of isolated mitochondria from a suspension of ~ 30 mg mitochondria protein/mL.

28. Insert the cap into the inner chamber.

29. Under the hardware option on the Oxygraph software click "Start Recording".

30. After establishing a low baseline rate of respiration (state 2 respiration: respiration in the presence of substrate and before addition of ADP), add 9 µL of ADP (0.027 M) through the injection port using a Hamilton syringe.

    Addition of ADP stimulates state 3 respiration. The high rate of state 3 respiration continues until all added ADP is depleted and converted to ATP.

31. Let oxygen concentration trace continue until state 4 respiration has been reached. Continue to measure state 4 respiration (respiration in the absence of ADP) for 5 min.

32. After respiration measurement is completed, rinse chamber thoroughly with ddH$_2$O and repeat with 2 to 3 additional measurements per mitochondrial sample.

    It is important to note that respiration with glutamate/malate should be performed before succinate-mediated respiration studies as the rotenone will contaminate the Teflon membrane. The presence of rotenone in the membrane will inhibit complex I mediated respiration with glutamate/malate.

33. Also, rinse chamber three times, each time 2 mL 70% ethanol before performing succinate-mediated measurements.

Measure mitochondrial respiration using succinate as oxidizable substrate (Complex II-linked respiration)

34. Add 1.79 mL of HEPES respiation buffer to the inner chamber.

35. Add 26 µL of succinate to the inner chamber.

36. Add 20 µL of isolated mitochondria from a suspension of approximately 30 mg mitochondria protein/mL.

37. Add 3.67 µL of rotenone.

38. Insert the cap into the inner chamber.

39. Once all reagents are added select "Start recording". After establishing a low baseline rate of respiration (state 2 respiration: respiration in the presence of substrate and before addition of ADP), add 9 µL of ADP (0.027 M) through the injection port using a Hamilton syringe.

    Addition of ADP stimulates state 3 respiration. The high rate of state 3 respiration continues until all added ADP is depleted and converted to ATP.

40. Let oxygen concentration trace continue until state 4 respiration has been reached. Continue to measure state 4 respiration (respiration in the absence of ADP) for 5 min.

41. After respiration measurement is complete, rinse the chamber thoroughly with ddH$_2$O and repeat with two to three additional measurements per mitochondrial sample.

42. After all respiration measurements for each mitochondrial sample are completed, rinse and disassemble the Oxygraph electrode instrumentation.

> *Please make sure to store the electrode in a jar containing dessicant. This will help to extend the life of the electrode disc.*

Calculate respiratory rates and respiratory control ratio

43. See Figure 3 for an example of a typical measurement of mitochondrial respiration using glutamate/malate as oxidizable substrate.

44. Calculate the state 3 (ADP-dependent) and state 4 (ADP-independent) respiration rates using oxygen consumption data obtained from the Oxygraph software output.

> *A brief description of this process and calculation is included in following segments. Please note that detailed instructions are included by the manufacturer for these manipulations of the software as well.*

45. After each individual respiration measurement is completed, using the Oxygraph software click "Rate" and a cursor will appear on the oxygen trace. Obtain the state 3 rate by measuring the change in oxygen

concentration over time after the ADP is added and before the ADP is depleted.

This is the faster rate of respiration (see Figure 3).

46. Obtain the state 4 rate by measuring the slower change in oxygen concentration over time.

This is the lower rate of respiration that occurs after state 3 respiration is completed (see Figure 3).

47. Use these changes in oxygen concentration for both state 3 and 4 are then used to obtain the oxygen consumption rate (OCR) or respiration rate by using the following calculation:

    a. oxygraph rate obtained is divided by 1000 to give (μmol/mL/min)

    b. number obtained in (a) is multiplied by 2 to obtain (μg O atom/mL/min)

    c. protein assay should be performed: the protein concentration of mitochondrial suspension is then multiplied by 80 and then divided by 1000 to give (mg protein in 80 μL mitochondria) for glutamate/malate; however, for succinate-driven respiration the protein concentration should be multiplied by 20 and then divided by 1000 to give (mg protein in 20 μL mitochondria)

    d. number obtained in (c) is then divided by 1.84 to give mg protein per mL in chamber

    e. divide the number obtained in (b) by the number obtained in (d) to give OCR (μg O atom/min/mg protein).

48. To obtain the respiratory control ratio (RCR), the state 3 rate (ADP-dependent) is divided by the state 4 rate (ADP-independent).

> *The higher the RCR the higher quality of mitochondria whereas a low number (e.g., < 3) indicates poor quality mitochondria. Typically, liver mitochondria from a normal healthy rat or mouse will have RCR in the range of 6-10. Diseased mitochondria will be lower.*

Mitochondrial Calcium Accumulation Measurement

Studies show that a key predictor of mitochondrial dysfunction from toxicant exposures is the inability of mitochondria to sequester calcium. Moreover, the inability to accumulate calcium is critical in the initiation of apoptotic and necrotic cell death. Towards this end, a number of fluorescence-based molecules and assays have been developed to monitor and quantify toxicant-mediated alterations in mitochondrial calcium accumulation. Here, we describe the use of Calcium green 5N (CaG5N) to monitor calcium accumulation in mitochondria isolated from liver using the method described in Support Protocol.

Materials

Bio-Rad protein assay kit (Bio-Rad, cat. no. 500-0006)

HEPES Respiration buffer without EDTA (see recipe)

Succinate (1 M solution, pH 7.2 with 10 N KOH and store at 4ºC)
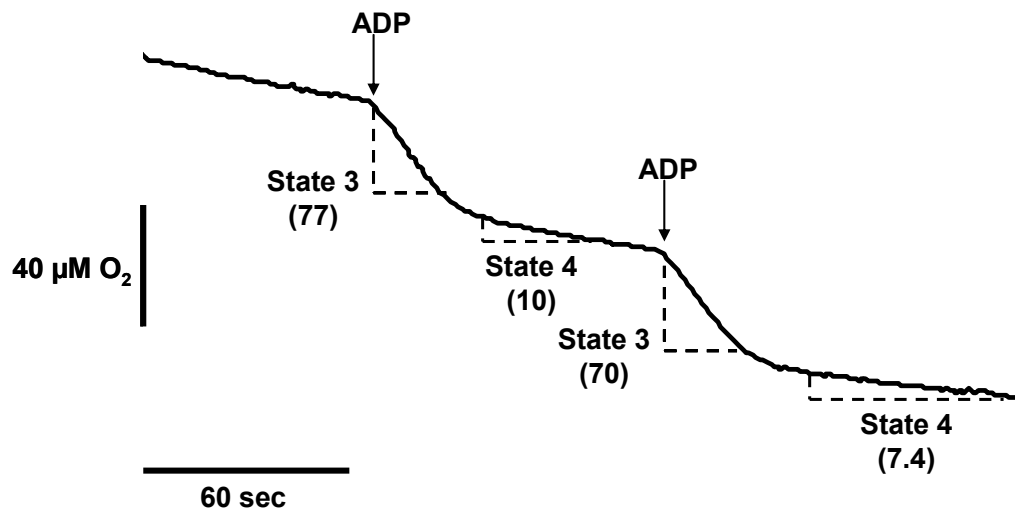
Figure 3. Liver mitochondria respiration. This figure illustrates a representative experiment showing liver mitochondria consuming oxygen in the presence of the Complex I-linked oxidizable substrates glutamate/malate. ADP is added at the arrows to stimulate state 3 respiration, i.e., ADP-dependent respiration. When the ADP is depleted (i.e., converted to ATP) mitochondria revert back to a slower rate of oxygen consumption; state 4 respiration; i.e., ADP-independent respiration. The change in oxygen concentration over time for state 3 and state 4 respiration (dashed line sections) are shown on the trace (numbers in parentheses). These numbers are used to calculate the respiration rates and the respiratory control ratio as described in Basic Protocol 2.

Rotenone (1 mM in 95% ethanol)

0.027 M ADP in 0.067 M NaPO$_4$ buffer, pH 6.8 (see recipe for NaPO$_4$

buffer)

Oligomycin: 1 mg/m in ethanol (Sigma, cat. no. O4876)

Calcium green 5N dye (CaG5N; see recipe) 10 mM calcium chloride

dihydrate

1 mM Cyclosporin A (Alexis Biochemical, cat. no. L15684) in ethanol

(store in the freezer)

Perkin Elmer LS 55 Fluorescence spectrometer or comparable instrument

Re-circulating water bath

4.5-ml four-sided clear cuvettes

Additional reagents and equipment for isolating liver mitochondria

(Support Protocol)

Prepare mitochondria and equipment

1. Isolate liver mitochondria as described in Support Protocol except at step

   22 (Support Protocol) resuspend mitochondria in isolation buffer without

   EDTA. See isolation buffer under materials. Continue with isolation

   procedure of mitochondria as described in Support Protocol.

2. After isolation of mitochondria, perform a protein assay on isolated

   mitochondria to determine concentration of final mitochondrial suspension.

3. Turn on spectrofluorometer and re-circulating water bath set at 37°C.

4. Select parameters on spectrofluorometer so that you can monitor fluorescence changes in CaG5N over time (i.e. time drive or kinetics based program).

> *For the LS 55, select "Time Drive" on FL WinLab software to monitor changes over time.*

5. Set excitation and emission wavelengths to 506 nm and 532 nm, respectively. Set slit widths are set at 2.5 with time set for 2000 seconds.

Prepare the reaction

6. To cuvette a 4.5 mL clear cuvette, add:

> 2 mL of respiration buffer without EDTA,
>
> 16 µL of 1M succinate (8 mM final)
>
> 2 µL of 1 mM rotenone (1 µM final)
>
> 14.8 µL of 0.027 M ADP (0.2 mM final)
>
> 2 µL of 1 mg/mL oligomycin (2 µg/mL final)
>
> 0.2 mg/mL isolated mitochondria protein.
>
> Mix the contents in the cuvette.

Perform calcium accumulation assay

7. Add 2 µL CaG5N Dye to cuvette, mix well, and place the cuvette in thermostatically controlled cuvette chamber.

8. Establish base-line fluorescence reading for 2 to 3 min before initiating calcium additions.

9. Add sequential 50 nmol calcium additions to cuvette to monitor calcium accumulation. Continue to add calcium additions to cuvette until the induction of mitochondrial permeability transition (MPT).

10. *Optional.* Add cyclosporin A (2 μL) can be added to cuvette to inhibit the MPT, i.e., increase calcium accumulation before induction of the MPT. For this, add cyclosporin A to cuvette right after mitochondria protein. Proceed with assay as described.

> *The final concentration of cyclosporin A in the assay is 1μM.*
>
> *See figure 4 for an example of a typical experimental readout and induction of the MPT in mitochondria incubated in the absence and presence of cyclosporin A.*

Calculate mitochondrial calcium accumulation

11. Sum the additions of calcium that were added to the cuvette to induce the MPT pore and report total nmol calcium per mg protein.

> *For example, five additions at 20 nmol before MPT pore is induced would be equal to 100 nmol of calcium. This number is then divided by the amount of protein in the cuvette (0.2 mg) for a total of 500 nmol calcium/mg protein.*
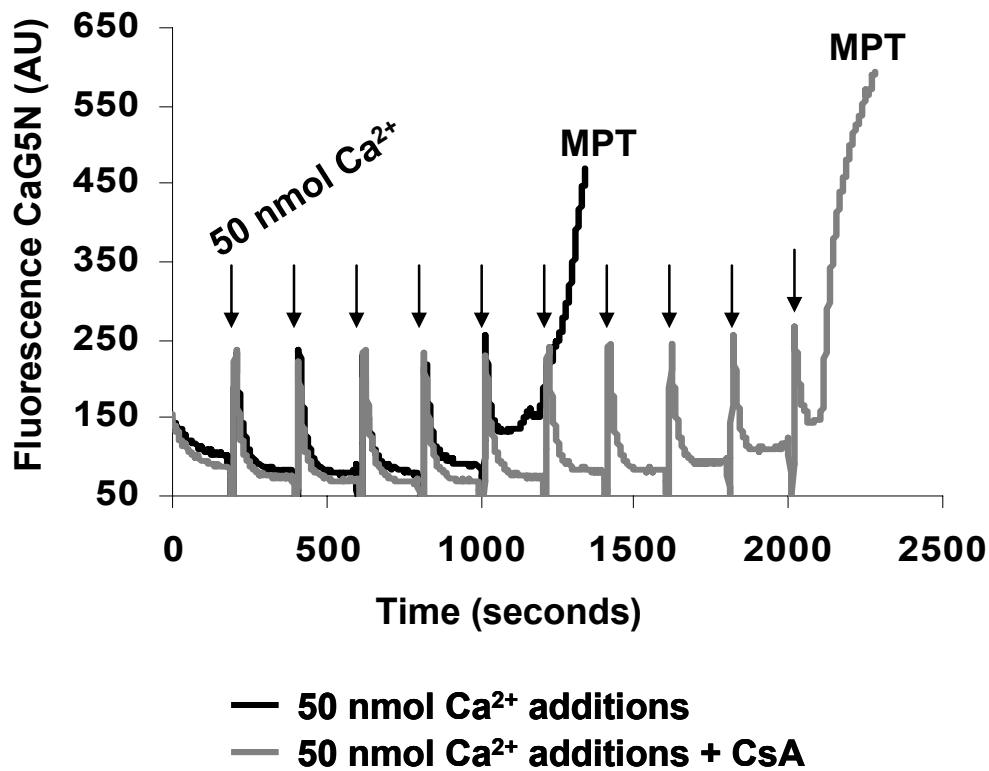
Figure 4. Liver mitochondria calcium accumulation and MPT induction. This figure shows a representative experiment of mitochondrial calcium accumulation using the fluorescent dye calcium green 5N (CaG5N) that monitors extra-mitochondrial calcium. As shown in the figure, with each 50 nmol calcium addition (arrows) there is a brief increase in fluorescence signal followed by a rapid decrease in the signal as calcium is taken up and accumulated into mitochondria. Note that mitochondria have a finite ability to accumulate calcium. When this "calcium threshold" level is reached there is a rapid release of calcium, which is indicated by the rapid rise in fluorescence (black line). This rapid release of calcium into the extra-mitochondrial space is related to formation of the mitochondrial permeability transition (MPT) pore. Note that when mitochondria are pretreated with cyclosporin A (CsA), an inhibitor of the MPT pore, mitochondria are able to accumulate twice as much calcium before the induction of the MPT pore, i.e., rapid increase in fluorescence signal (gray line).

Mitochondrial Reactive Oxygen Species (ROS) Measurement

It is proposed that many toxic agents exert cell injury via increased mitochondrial reactive oxygen species (ROS) production. This increased production of mitochondrial ROS leads to enhanced formation of secondary reactive species contributing to posttranslational modifications of mitochondrial proteins (see Basic Protocol) and activation/inactivation of oxidant sensitive pathways. Like calcium measurements, a number of fluorescent and chemiluminescent probes have been developed which detect, quantify, and potentially identify ROS. Our laboratory has used the fluorescent probe, 2',7'-dichlorodihydrofluorescein diacetate (H$_2$DCFDA) to assess mitochondrial and hepatocyte ROS production from toxicant exposures. The protocol described below can easily be adapted to measure mitochondrial ROS production from tissues other than liver, as well.

Materials

Freshly isolated liver mitochondrial suspension (see Support Protocol)

Bio-Rad protein assay kit (Bio-Rad, cat. no. 500-0006)

HEPES respiration buffer (see recipe)

1 M succinate solution (see recipe)

Antimycin A: 10 mM solution in DMSO (make fresh for each experiment)

Carbonylcyanide-p-trifluoromethoxyphenylhydrazone (FCCP): 1 mM solution in ethanol (store up to 1 year at 4ºC)

21% O$_2$/74% N$_2$/5% CO$_2$ gas mixture

50-mL Erlenmeyer flasks

Rubber stoppers

Shaking water bath set at 37°C

PerkinElmer LS 55 Fluorescence spectrometer or comparable instrument

1. Keep prepared mitochondrial suspension (Support Protocol) on ice.

2. Determine the protein concentration of mitochondrial suspension.

3. Suspend mitochondria (0.5 mg/mL = 1.5 mg total protein) in 3.0 mL of
   HEPES respiration buffer containing 2 μM H_2DCFDA in the presence and
   absence of substrates (e.g., succinate), mitochondrial respiratory inhibitors
   (e.g., antimycin), and/or uncouplers for 0 to 60 min to measure ROS
   production.

   For these studies, add succinate to 50 mL flasks at a final

   concentration of 0.2 mM; add antimycin at a final concentration of

   15 μM; and add FCCP at a final concentration of 5 μM.

   Glutamate/malate can be substituted for succinate to serve as the

   oxidizable substrate. Note that equal volumes of the vehicle used

   for antimycin (DMSO) should be added to 50 mL flasks not

   exposed to antimycin treatment.

   Inclusion of antimycin can be used as positive control, as it is a

   known stimulator of mitochondrial ROS generation from complex III,

   whereas FCCP addition can be used as a negative control because

   dissipation of the membrane potential inhibits ROS production.

   See Figure 5 for an example of ROS production in mitochondria

   incubated with antimycin +/- FCCP. Note that ROS production from

> *mitochondria is membrane potential dependent, thus, coupled*
>
> *mitochondria are required for all ROS assays.*

4. Seal the flasks with rubber stoppers and continuously aerate with 21% O_2/74% N_2/5% CO_2 throughout the incubation period.

   > *The O_2 tension can be altered to study mitochondrial ROS*
   >
   > *production under lower, more physiological relevant O_2 tensions.*

5. Perform incubations at 37ºC in shaking water bath.

6. During incubation, tune the fluorescence spectrometer with excitation and emission wavelengths set to 488 and 525 nm, respectively. As the fluorescence emission of the product DCF is strong, typically keep slit widths at low settings.

   > *Optimize these settings for your laboratory instrumentation.*

7. After incubations, determine the concentration of DCF generated in mitochondria by reading the fluorescence of the mitochondrial suspensions.

The fluorescence values can be reported as arbitrary fluorescence units. However, the concentration of DCF generated can be determined from standard curves using known concentrations of DCF added to mitochondria (0.5 mg/mL), which are reported as pmol DCF/mg mitochondrial protein (Bailey and Cunningham 1998; Young et al. 2002).
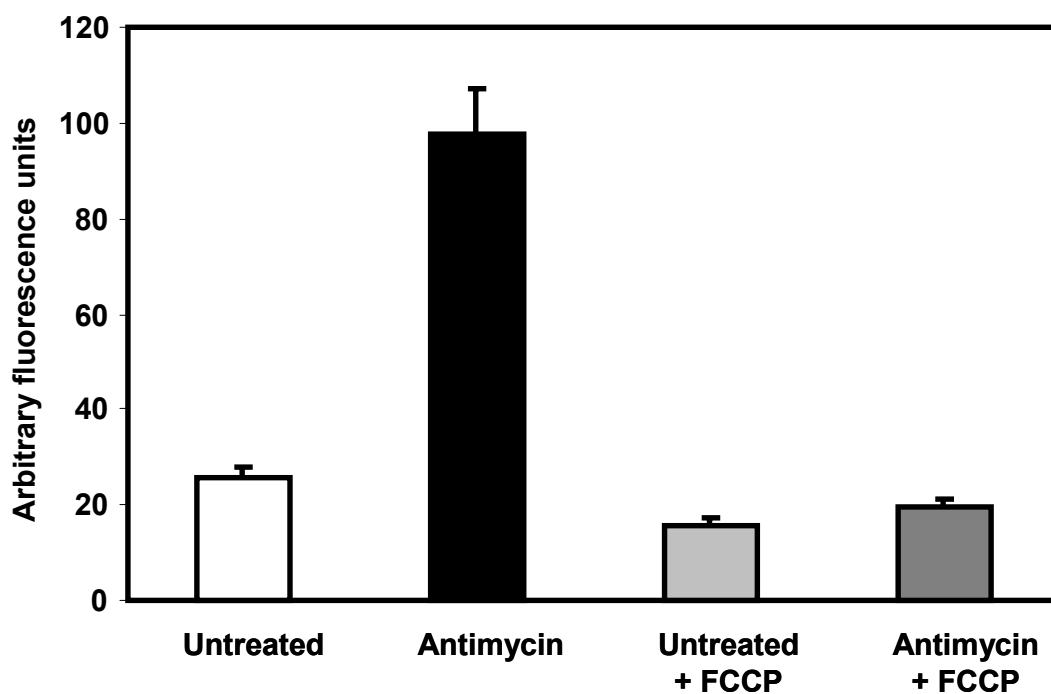
Figure 5. Liver mitochondrial reactive oxygen species production – effect of antimycin and FCCP. Freshly isolated liver mitochondria were suspended at a concentration of 0.5 mg/mL and incubated with 2 µM H_2DCFDA for 60 min in the presence of 0.2 mM succinate. Identical flasks were set-up in the presence of antimycin with and without FCCP. The flasks containing the mitochondrial suspension are sealed and aerated with 21% O_2 throughout the incubation. After 60 min, the mitochondrial suspensions are transferred to fluorometric cuvettes and the excitation/emission of DCF was read at 488/525 nm, respectively. Note that antimycin, a respiratory inhibitor of Complex III, stimulates ROS production whereas dissipation of the mitochondrial membrane potential with FCCP attenuates ROS production in mitochondria incubated with and without antimycin.

REGENTS AND SOLUTIONS

*Use Milli-Q-purified water or equivalent in all recipes and protocol steps. For common stock solutions, see **APPENDIX 2A**; for suppliers, see **SUPPLIERS APPENDIX**.*

Calcium green 5N dye

Prepare a 420 µM stock solution of calcium green 5N dye (CaG5N, Invitrogen, cat. no. C3737) in sterile ddH2O. Store up to 6 months at 20ºC

For experiments, dilute to 200 µM concentration (24 µl of dye + 26 µl of sterile ddH2O).

This dye is light sensitive.

Equilibration buffer

6 M urea

2% (w/v) SDS

0.375 M Tris base

20% (v/v) glycerol

0.002% (w/v) bromphenol blue

Adjust to pH 8.8 with HCl

Divide into 2-mL aliquots

Store up to 1 year at −20ºC

Before using this buffer, warm to 37ºC to redissolve the urea back into buffer solution

Glutamate-malate solution

0.4575 M glutamate

0.4575 M malate

Adjust to pH 7.2 using KOH

Store up to 1 year at 4ºC

HEPES respiration buffer

130 mM KCl

2 mM KH_2PO_4

3 mM HEPES

2 mM $MgCl_2$

1 mM EGTA

Adjust to pH 7.2 using KOH or HCl

Store up to 6 months at 4ºC

Isolation buffer

0.25 M sucrose

5 mM Tris·Cl, pH 7.4 (*APPENDIX 2A*)

1 mM EDTA

Store up to 6 months at 4ºC

NaPO₄ buffer

0.067 M monobasic, NaH₂PO₄:

6.7 mL of 0.5 M stock, bring to 50 mL final volume with ddH$_2$O

0.067 M dibasic, Na$_2$HPO$_4$

6.7 mL of 0.5 M stock, bring to 50 mL final volume with ddH$_2$O

Take 25 ml of monobasic and 25 mL of dibasic Na$_2$HPO$_4$, mix, and measure the pH; bring to final pH of 6.8 with a little more monobasic, if needed.

Protease inhibitors

PMSF (Sigma)

40 mg/mL in methanol

Prepare fresh

Leupeptin (Sigma)

10 mg/mL in ddH2O

Store up to 6 months at –20ºC

Pepstatin (Sigma)

1mg/mL in methanol

Store up to 6 months at –20ºC

Aprotinin (Sigma)

10 mg/ml in 10 mM HEPES, pH 8.0

Store up to 6 months at –20ºC in 100-μL aliquots

Do not freeze/thaw

Rehydration buffer

7 M urea

2 M thiourea

2% (w/v) CHAPS

0.5% (w/v) N-dodecyl-β-D-maltoside

0.002% (w/v) bromphenol blue

Store up to 1 year at –20ºC

SDS-PAGE buffer, 1X

10X stock solution

30 g Tris base

144 g glycine

100 mL of 10% (w/v) SDS

Adjust the final volume 1 liter

Stock solution can be stored up to 6 months at 4ºC

Dilute stock solution from 10X to 1X with ddH$_2$O when running the 2D

SDS-PAGE gel step

Succinate, 1 M

Stock solution:

1M Succiante, 16.2 g into 100 mL final volume

Adjust pH to 7.2 with KOH

Store up to 1 year at 4ºC

This stock solution is diluted 1 to 10 with ddH$_2$O to obtain a 0.1 M working stock solution for experiments.

TBS-T, 10X

10X stock wash buffer:

0.2 M Tris·Cl, pH 7.4 (*APPENDIX 2A*)

9% (w/v) NaCl

Add 5 mL of Tween-20 to 1 liter of the 10X stock wash buffer and stir for 1 hr to ensure that the detergent is fully dissolved

1X TBS-T wash buffer

Dilute 10X TBS-T, 10X to 1X with ddH$_2$O

Store up to 6 months at 4ºC

Transfer buffer

This recipe makes 6 liters of transfer buffer. Add 17.4 g of Tris base and 87 g of glycine to 3.8 liters of ddH$_2$O. The pH of this solution should be between 8 and 8.5. If not, re-make the solution from fresh chemicals. Do not adjust the pH with addition of acid or base. After making this preliminary buffer solution, take two 4-liter beakers and to each of these large beakers add 600 mL methanol, 500 mL ddH$_2$O, 1.9 liters buffer solution. Mix well and then combine the solutions from both beakers into a large carboy container for storage. Store at 4ºC. Transfer buffer can be re-used 6 times before discarding.

COMMENTARY

Background Information

While many of the causative factors of hepatotoxicity have been identified, the molecular mechanisms responsible for the development of liver disease following toxicant exposure remain poorly defined. A leading hypothesis for the pathogenesis of alcoholic, nonalcoholic (obesity/diabetes), and toxicant mediated liver disease is the "multi-hit" hypothesis. The "first-hit" typically involves the abnormal accumulation of fat in hepatocytes (i.e., steatosis) due to disrupted lipid metabolism and (adipo)cytokine networks followed by "second-hits", which may involve oxidative/nitrative stress resulting from increased mitochondrial production of reactive oxygen/nitrogen species (ROS and RNS) (Mantena et al. 2008). It is these so-called "second-hits" that initiate the inflammatory and fibrogenic responses leading to development of steatohepatitis and fibrosis/cirrhosis. Moreover, hepatocyte cell death following compromised mitochondrial bioenergetics and a dramatic drop in cellular ATP is critical to liver disease progression (Jou et al. 2008). Based on this, the mitochondrion is proposed to play an essential role in severe liver disease with mitochondrial damage, decreased ATP production, and excess ROS/RNS production accompanying and contributing to pathology (Bailey 2003).

Due to the preponderance of evidence linking mitochondrial damage and dysfunction to hepatotoxicity and liver pathology from multiple insults, diseases, and toxicants, a series of well-established methodologies are presented to help laboratories begin to explore the role of the mitochondrion in their investigations.

77

It should be pointed out that this is obviously not an all inclusive list as there are many, many different approaches and techniques not described in this article that can be applied to successfully study mitochondria in the context of hepatotoxicity. Indeed, this article is simply a starting point for novices.

One important starting point for most laboratories should be assessment of the respiratory capacity of isolated mitochondria using classic respirometry approaches as described in Alternate Protocol 1. While a somewhat "old-fashioned" method, taking a bioenergetic approach to understanding how mitochondrial function is altered is extremely powerful and can provide important insight in how toxicant exposure impacts mitochondrial function. For example, identifying a decrease in state 3 respiration (i.e., ADP-dependent) is important in that it suggests that toxicant exposure has caused a decrease in the rate at which mitochondria synthesize ATP via oxidative phosphorylation. This could be related to damage or changes in the activities of the respiratory complexes. Moreover, if state 4 respiration (i.e., ADP-independent) is increased by toxicant exposure this would indicate that mitochondria are unable to conserve the proton (H^+) gradient across the inner membrane that is generated as a consequence of electron transport. In this situation, mitochondria are less well coupled (i.e., uncoupled) with the efficiency of ATP synthesis negatively impacted. This is significant as this may increase susceptibility of hepatocytes to necrosis when increased ATP levels are needed acutely under oxidative, toxicant, or metabolic stress situations.

Clearly, demonstrating altered respiration function carries significant weight when linking mitochondrial defects to disease pathogenesis. If there is no overt alteration in respiratory function it may be more difficult to support the role of mitochondria in the disease process. If respiration changes are observed, the next step in characterizing changes in mitochondrial function would be to assess the activities of each of the respiratory complexes using complex specific spectrophotometric (Darley-Usmar et al. 1987) and/or in-gel activity assays (Wittig et al. 2007). This is an important next step as a defect in overall respiratory capacity may be due to a lesion in only one of the respiratory complexes. Moreover, characterizing respiratory function is critical as electron transport underpins the ability of mitochondria to accumulate calcium and produce ROS as both these processes are dependent on the presence of a high mitochondrial membrane potential (i.e., $\Delta\Psi$).

Disturbances in the function of the respiratory chain are also likely to be associated with increased ROS production and oxidative damage to the liver. During electron transfer, electrons can "leak" from Complexes I and III and be passed one at a time to molecular oxygen to form low amounts of superoxide anion ($O_2^{\bullet-}$), which subsequently is converted to hydrogen peroxide (H_2O_2) via action of manganese superoxide dismutase (MnSOD). Possible mechanisms for increased mitochondrial ROS include molecular alterations in Complexes I and III that essentially block or inhibit the transfer of electrons along the respiratory chain. These overly reduced complexes then transfer electrons to oxygen to increase ROS, which can initiate a cycle of more lipid peroxidation,

posttranslational protein modification, mitochondrial damage, and further ROS production.

Mitochondria are also important regulators of cellular calcium homeostasis by taking up calcium via a uniporter protein located in the inner membrane and releasing calcium under normal conditions via the Na^+/Ca^{2+} antiporter. Mitochondrial calcium capacity is however limited and when exceeded, calcium release rapidly occurs through induction of the MPT pore. Formation of the MPT pore allows passage of small molecules (<1500 Da) into and out of mitochondria resulting in mitochondrial depolarization, swelling, and outer membrane rupture, which might contribute to the release of cytochrome *c* and other pro-apoptotic proteins from mitochondria. It is proposed that a critical factor enhancing the sensitivity of mitochondria following toxicant exposures to apoptotic and necrotic stimuli like ROS/RNS may be a change in mitochondrial responsiveness to calcium and ability to accumulate calcium (Lemasters et al. 2002). Therefore, assessing the ability of mitochondria to sequester calcium and determining the "calcium threshold" before undergoing the MPT may be important parameters to measure especially when one is interested in ascertaining whether a toxicant enhances susceptibility to apoptotic or necrotic cell death.

One mechanism by which oxidative/nitrative stress leads to mitochondria damage and increased susceptibility to MPT is likely to involve posttranslational modification of mitochondrial proteins. Oxidative modifications to mitochondrial proteins may impair their activities leading to deficits in key mitochondrial metabolic pathways. A number of irreversible, as well as reversible,

modifications to cysteine residues are known to occur upon interaction of the free sulfhydryl group (P-SH) with various ROS/RNS and reactive lipids (Cooper et al. 2002). Each of these thiol modifications has the potential of eliciting unique biological responses that could disrupt mitochondrial function in response to toxicant exposures. For example, studies show that ROS promote formation of the MPT pore presumably through the oxidation of critical thiols in the adenine nucleotide translocator; one of three proteins involved in pore formation (McStay et al. 2002). Moreover, a new aspect of mitochondrial function is the role it plays in signal transduction, especially those cellular signaling pathways that regulate how the cell responds to oxidative and metabolic stress (Gutierrez et al. 2006). This suggests that mitochondrial dysfunction may disrupt critical cellular signaling pathways and contribute to the pathophysiology of liver disease from alcohol, drugs, and other environmental toxicants. Therefore, the ability to detect, identify, and functionally characterize mitochondrial proteins that may be susceptible to oxidative modification is critical to understanding the molecular mechanisms that contribute to oxidant damage and mitochondrial dysfunction from toxicant exposures. The key posttranslational modification discussed in this article is protein thiol modification. Because alterations in the redox state of protein thiols regulate mitochondrial functions such as respiration and oxidant production, identification of those proteins with altered thiol groups will increase our understanding of hepatotoxic mechanisms.

In conclusion, while the presence of these posttranslational modifications in proteins predicts that the structure and/or function of a protein may be altered,

the key finding for researchers is still whether there is a change in protein activity. Therefore, functional assays should be performed, if available, for those proteins identified as containing posttranslational modifications. It is only when a direct link between a functional change and posttranslational modification is demonstrated that the posttranslational modification can be stringently tied to mitochondrial toxicity and disease.

Critical Parameters and Troubleshooting

There are several critical experimental parameters and steps that must be adhered to ensure successful outcomes when working with mitochondria. First, it is important that harvesting of liver tissue is done quickly and that liver is immediately placed in ice-cold isolation buffer. Indeed, it is essential for liver and mitochondria to be kept cold at all stages in the isolation process; therefore, it is highly recommended that homogenization and wash step are conducted in a cold room kept at 4ºC and that isolation buffer is ice-cold as well. If a cold room is not available, all reagents and mitochondrial suspensions must be kept on ice. Second, care should be taken to optimize homogenization and washing steps as too harsh of a treatment of liver and mitochondria will result in damaged mitochondria that are uncoupled and have poor respiratory capacity. For example, polytron-mediated homogenization is too "rough" for isolation of coupled functional mitochondria from soft liver tissue. If mitochondria have low RCR due to low state 3 or high state 4 respiration, steps need to be taken to optimize isolation procedure. Note that harsh treatment typically results in high

state 4 respiration, which is indicative of damaged inner membrane and leakage of H$^+$'s across the inner membrane, i.e., uncoupled mitochondria. Third, the sucrose-containing isolation buffer can be made ahead of time in large batches. However, if this is done, please make sure to autoclave buffers with storage at 4°C as bacteria and other microorganisms can grow in this sucrose-containing solution. Please discard all unused buffer remaining at the end of each mitochondrial preparation (i.e. do not save leftover buffer). Remember that protease inhibitors are added to isolation buffer on the day of experiment to prevent protein degradation. This is important for proteomic experiments. Fourth, it is important that glutamate/malate-dependent respiration be performed before succinate-dependent respiration as rotenone will "poison" the Teflon membrane of the oxygen electrode. Rotenone will leach back into solution in the chamber and thereby inhibit Complex I-mediated respiration with glutamate/malate. Also, remember to rinse the oxygen electrode chamber three times with 70% ethanol before performing succinate-mediated measurements. Fifth, after all experiments are done extra mitochondria should be saved for activity assays, western blots, proteomics, etc…For this, we typically save mitochondria as 1.0 mg pellets by centrifuging mitochondria 10 min at 13,500 $x\ g$, 4°C, removing supernatant, and placing the pellet in -80°C freezer.

Anticipated Results

Details regarding anticipated results and interpretation of data are included within the description of each Protocol. In addition, we have included a

representative example of data output (Figures 1-5) for each experimental protocol with specific details regarding methodology provided within the figure legends. As a supplement to this information, a brief synopsis of anticipated results will be briefly summarized here with some additional comments provided to help readers establish these methods in their laboratories.

To monitor changes in the mitochondrial protein thiol proteome, we have presented in this article a thiol-labeling or "tagging" approach that can be used in combination with 1D and 2D gel electrophoresis techniques. Specifically, we present the "BIAM approach" that was developed by Rhee and colleagues to identify protein cysteinyl groups susceptible to oxidative modification by H_2O_2 and other oxidizing species (Kim et al. 2000). BIAM reacts with and covalently labels reduced, unmodified cysteines but not cysteines that have been oxidized or modified by ROS/RNS or reactive lipids. As shown in Figure 1 and 2, these representative data from both *in vitro* and *in vivo* studies illustrate the power and feasibility of the BIAM technique to detect and possibly identify mitochondrial proteins containing oxidized thiols in response to toxicant exposures. Indeed, using this method in combination with 2D proteomics we found that the thiol content of HMG-CoA synthase, the key regulatory protein of ketogenesis, was significantly decreased following acetaminophen exposure and that this modification decreased enzyme activity (Andringa et al. 2008). Presented here (Figure 2) is data showing a significant loss in the liver mitochondrial protein thiol proteome in animals co-exposed to alcohol and environmental tobacco smoke. Importantly, the use of the biotin-tag for labeling thiols has the added advantage

that it can be used to quantify the degree of incorporation of the BIAM into a specific protein band or spot on 2D gels and used to calculate the amount of protein thiols lost due to oxidation or modification (Landar et al. 2006). It is also important to note that other types of amino acid modifications may also alter mitochondrial physiology such as carbonylation and nitration, as well as electrophilic lipid adduction, e.g. 4-hydroxynonenal (Radi 2004). One important thing to note about these experiments is that it is critical to always include a duplicate (i.e., companion) gel with each blot that can be stained for total protein. While this is important for analysis, the protein stained gel is also critical to show that toxicant treatment doesn't result in massive protein degradation and loss, which will hinder ones ability to properly interpret the results. It is also important to make sure that only those blots with signal intensities below signal saturation are used for analyses to ensure linearity of responses. This is especially significant when using super-sensitive enhanced chemiluminescence reagents to visualize proteins on blots. Therefore, it is recommended that imaging instruments are used that can detect saturation of signal intensities of protein bands or spots versus simple film developers.

With regards to mitochondrial preparations, one should expect a yield of ~ 20 to 30 mg of mitochondria protein per one gram of rat or mouse liver (Venkatraman et al. 2004). One rat liver weighing 10 to 15 g will provide sufficient mitochondrial protein to perform all assays described within this chapter whereas multiple mouse livers will need to be collected and pooled to get enough protein to perform functional assays described. Related to this, is that the

amount of total mitochondrial isolated per g liver should be recorded as differences in yields between control and experimental groups may provide insight into whether toxicant exposure has effects on mitochondrial biogenesis.

State 3 and 4 respiratory rates for rat liver mitochondria using glutamate/malate as the oxidizable substrate typically average 0.08 to 0.12 and 0.015 to 0.025 µg atom O/min/mg protein, respectively, whereas succinate-driven rates for state 3 and 4 respiration are slightly higher, and average 0.15 to 0.25 and 0.03 to 0.05 µg atom O/min/mg protein, respectively. Respiration rates in mice liver mitochondria are usually higher due to higher metabolic rate and increased respiratory complex protein per total mitochondrial protein. While there are multiple methods and fluorescent-based probes used for measuring cellular and mitochondrial calcium accumulation, we have found the CaG5N compound is easy to use and of low cost for most laboratories as standard spectrofluorometers or fluorescence-based plate readers are used compared to more expensive microscopy set-ups. As mentioned earlier and shown in Figure 4, CaG5N measures extra-mitochondrial calcium continuously. In experiments, nmol aliquots of calcium are added sequentially to energized mitochondria until MPT pore induction, which results in release of calcium (i.e., rapid rise in CaG5N fluorescence) at the end of the experimental run. Initial calcium aliquots lead to a transient rise in extra-mitochondrial calcium followed by a rapid return to baseline fluorescence as calcium is taken up by mitochondria (see arrows). Using this type of approach, one can determine the calcium threshold before MPT pore induction as one indicator of mitochondrial vulnerability to cell death. For

example, if MPT pore induction and rapid release of calcium is triggered by less calcium (i.e., fewer additions) in toxicant-exposed mitochondria compared to untreated control mitochondria this illustrates that the toxicant has increased the susceptibility of mitochondria to calcium "overload", which increases vulnerability to MPT and ultimately cell death. Investigations focused on toxicant-mediated changes in mitochondrial calcium handling can be extended to include an examination of changes in levels of the proteins speculated to comprise the MPT pore, as well as those implicated in mitochondrial outer membrane permeabilization.

The method described for measuring ROS production – "the DCF assay" – is a fairly simple and straightforward method to begin to look at ROS production in mitochondria and in cells. The level of sensitivity of this assay is high and can detect pmol to nmol levels of ROS per mg mitochondrial protein. H_2DCFDA is cell and mitochondrial permeable and after uptake it becomes "trapped" inside after cleavage of the esters groups by esterases (H_2DCF). In the presence of a variety of ROS/RNS it is then oxidized to a fluorescent product, DCF (Figure 5). However, there are multiple caveats to this method that must be considered. For example, H_2DCFDA is a relatively non-specific indicator of ROS as it can react with H_2O_2, peroxynitrite ($ONOO^-$), and lipid hydroperoxides (Dikalov et al. 2007). In addition, oxidation of H_2DCF and DCF can occur in the presence of peroxidases and iron (Tampo et al. 2003). Based on this and other concerns, care should be taken when using this fluorescent-based probe for ROS production with more specific methods used to follow-up on preliminary studies

87

implicating mitochondrial ROS. Please refer to (Tarpey and Fridovich 2001; Dikalov et al. 2007) for additional insight regarding the utility of the DCF assay and other measurements of ROS.

Time considerations

It is important to reiterate that mitochondria once isolated from cells and tissues have a limited "shelf-life". Most mitochondrial preparations only remain viable, i.e., maintain high respiratory capacity, for 2-3 hr; therefore, it is important that all assays and experiments are completed within this timeframe to ensure accurate and reliable data collection. To maximize data collection during this limited time frame, it is recommended that a "team" approach is taken for experiments with each laboratory member trained to perform 1-2 assays versus having one person trying to performing all measurements. This "team" approach is essential for maximizing data collection from long-term animal studies or other types of studies that are expensive and time-consuming to set-up.

Also, note that calcium accumulation experiments are also time-consuming with each run taking up to 15-30 min depending on calcium concentration used. For example, use of lower amounts of calcium per addition (10 or 20 nmol) will take a longer time to induce the MPT than higher amounts of calcium per addition (50 or 100 nmol). Moreover, experiments done in the presence of cyclosporin A (inhibitor or MPT) will also prolong MPT induction. Based on these considerations, it is critical that time is taken to plan experiments accordingly so that calcium accumulation studies can begin as soon as the

protein concentration of the final mitochondrial suspension is determined.

Careful planning will help to ensure maximal data collection before mitochondria

lose functionality. When mitochondria lose functionality, they become much

more sensitive to calcium and will undergo MPT with fewer calcium additions.

These same time constraints also hold true for mitochondrial ROS

measurements and respiration measurements. Again, all functional

measurements must begin as soon after the isolation procedure is completed to

ensure best quality and reproducible results.

Literature Cited

Andringa, K., King, A. and Bailey, S. 2009. Blue native-gel electrophoresis proteomics. *Methods Mol Biol* 519: 241-58.

Andringa, K. K., Bajt, M. L., Jaeschke, H. and Bailey, S. M. 2008. Mitochondrial protein thiol modifications in acetaminophen hepatotoxicity: effect on HMG-CoA synthase. *Toxicol Lett* 177(3): 188-97.

Bailey, S. M. 2003. A review of the role of reactive oxygen and nitrogen species in alcohol-induced mitochondrial dysfunction. *Free Radical Research* 37: 585-596.

Bailey, S. M., Andringa, K. K., Landar, A. and Darley-Usmar, V. M. 2008. Proteomic approaches to identify and characterize alterations to the mitochondrial proteome in alcoholic liver disease. *Methods Mol Biol* 447: 369-80.

Bailey, S. M. and Cunningham, C. C. 1998. Acute and chronic ethanol increases reactive oxygen species generation and decreases viability in fresh, isolated rat hepatocytes. *Hepatology* 28: 1318-1326.

Bailey, S. M., Mantena, S. K., Millender-Swain, T., Cakir, Y., Jhala, N. C., Chhieng, D., Pinkerton, K. E. and Ballinger, S. W. 2009. Ethanol and tobacco smoke increase hepatic steatosis and hypoxia in the hypercholesterolemic apoE-/- mouse: implications for a "multi-hit" hypothesis of fatty liver disease. *Free Radic Biol Med* 46: 928-938.

Cooper, C. E., Patel, R. P., Brookes, P. S. and Darley-Usmar, V. M. 2002. Nanotransducers in cellular redox signaling: modification of thiols by reactive oxygen and nitrogen species. *Trends Biochem Sci* 27(10): 489-92.

Darley-Usmar, V. M., Capaldi, R. A., Takamiya, S., Millet, F., Wilson, M. T., Malatesta, F. and Sarti, P. (1987). Mitochondria: a practical approach. V. M. Darley-Usmar, D. Rickwood and M. T. Wilson. Oxford, IRL**:** 113-152.

Dikalov, S., Griendling, K. K. and Harrison, D. G. 2007. Measurement of reactive oxygen species in cardiovascular studies. *Hypertension* 49(4): 717-27.

Gutierrez, J., Ballinger, S. W., Darley-Usmar, V. M. and Landar, A. 2006. Free radicals, mitochondria, and oxidized lipids: the emerging role in signal transduction in vascular cells. *Circ Res* 99(9): 924-32.

Jou, J., Choi, S. S. and Diehl, A. M. 2008. Mechanisms of disease progression in nonalcoholic fatty liver disease. *Semin Liver Dis* 28(4): 370-9.

Kim, J. R., Yoon, H. W., Kwon, K. S., Lee, S. R. and Rhee, S. G. 2000. Identification of proteins containing cysteine residues that are sensitive to oxidation by hydrogen peroxide at neutral pH. *Anal Biochem* 283(2): 214-21.

Landar, A., Oh, J. Y., Giles, N. M., Isom, A., Kirk, M., Barnes, S. and Darley-Usmar, V. M. 2006. A sensitive method for the quantitative measurement of protein thiol modification in response to oxidative stress. *Free Radic Biol Med* 40(3): 459-68.

Lemasters, J. J., Qian, T., He, L., Kim, J. S., Elmore, S. P., Cascio, W. E. and Brenner, D. A. 2002. Role of mitochondrial inner membrane permeabilization in necrotic cell death, apoptosis, and autophagy. *Antioxid Redox Signal* 4(5): 769-81.

Mantena, S. K., King, A. L., Andringa, K. K., Eccleston, H. B. and Bailey, S. M. 2008. Mitochondrial dysfunction and oxidative stress in the pathogenesis of alcohol- and obesity-induced fatty liver diseases. *Free Radic Biol Med* 44(7): 1259-72.

McStay, G. P., Clarke, S. J. and Halestrap, A. P. 2002. Role of critical thiol groups on the matrix surface of the adenine nucleotide translocase in the mechanism of the mitochondrial permeability transition pore. *Biochem J* 367(Pt 2): 541-8.

Radi, R. 2004. Nitric oxide, oxidants, and protein tyrosine nitration. *Proc Natl Acad Sci U S A* 101(12): 4003-8.

Tampo, Y., Kotamraju, S., Chitambar, C. R., Kalivendi, S. V., Keszler, A., Joseph, J. and Kalyanaraman, B. 2003. Oxidative stress-induced iron signaling is responsible for peroxide-dependent oxidation of dichlorodihydrofluorescein in endothelial cells: role of transferrin receptor-dependent iron uptake in apoptosis. *Circ Res* 92(1): 56-63.

Tarpey, M. M. and Fridovich, I. 2001. Methods of detection of vascular reactive species: nitric oxide, superoxide, hydrogen peroxide, and peroxynitrite. *Circ Res* 89(3): 224-36.

Venkatraman, A., Landar, A., Davis, A. J., Ulasova, E., Page, G., Murphy, M. P., Darley-Usmar, V. and Bailey, S. M. 2004. Oxidative modification of hepatic mitochondria protein thiols: effect of chronic alcohol consumption. *Am J Physiol Gastrointest Liver Physiol* 286(4): G521-G527.

Wittig, I., Carrozzo, R., Santorelli, F. M. and Schagger, H. 2007. Functional assays in high-resolution clear native gels to quantify mitochondrial complexes in human biopsies and cell lines. *Electrophoresis* 28(21): 3811-20.

Young, T. A., Cunningham, C. C. and Bailey, S. M. 2002. Reactive oxygen species production by the mitochondrial respiratory chain in isolated rat hepatocytes and liver mitochondria: studies using myxothiazol. *Arch Biochem Biophys* 405(1): 65-72.

CHAPTER 3

CHRONIC ETHANOL CONSUMPTION ENHANCES SENSITIVITY TO CA^{2+} - MEDIATED OPENING OF THE MITOCHONDRIAL PERMEABILITY TRANSITION PORE AND INCREASES CYCLOPHILIN D IN LIVER

by

ADRIENNE L. KING[1], TELISHA M. SWAIN[1], DALE A. DICKINSON[1], MATHIEU J. LESORT[2], AND SHANNON M. BAILEY[1]

Departments of [1]Environmental Health Sciences and [2]Psychiatry and Behavioral Neurobiology, Center for Free Radical Biology, University of Alabama at Birmingham, Birmingham AL, 35294

Format adapted for dissertation

ABSTRACT

Chronic ethanol consumption increases mitochondrial oxidative stress and sensitivity to form the mitochondrial permeability transition pore (MPTP). The mechanism responsible for increased MPTP sensitivity in ethanol-exposed mitochondria and its relation to mitochondrial Ca^{2+} handling is unknown. Herein, we investigated whether increased sensitivity to MPTP induction in liver mitochondria from ethanol-fed rats compared to controls is related to an ethanol-dependent change in mitochondrial Ca^{2+} accumulation. Liver mitochondria were isolated from control and ethanol-fed rats and Ca^{2+}-mediated induction of the MPTP and mitochondrial Ca^{2+} retention capacity were measured. Levels of proposed MPTP proteins, as well as select pro- and anti-apoptotic proteins were measured along with gene expression. We observed increased steatosis and TUNEL-stained nuclei in liver of ethanol-fed rats compared to controls. Liver mitochondria from ethanol-fed rats had increased levels of pro-apoptotic Bax protein and reduced Ca^{2+} retention capacity than control mitochondria. We observed increased cyclophilin D (Cyp D) gene expression in liver and protein in mitochondria from ethanol-fed animals compared to controls, whereas there was no change in the adenine nucleotide translocase and voltage dependent anion channel. Together, these results suggest that enhanced sensitivity to Ca^{2+}-mediated MPTP induction may be due, in part, to higher Cyp D levels in liver

94

mitochondria from ethanol-fed rats. Therefore, therapeutic strategies aimed at normalizing Cyp D levels may be beneficial in preventing ethanol-dependent mitochondrial dysfunction and liver injury.

INTRODUCTION

Prolonged, heavy consumption of alcohol is the third leading cause of preventable death in the United States (US) with alcoholic liver disease specifically continuing to be a significant cause of morbidity and mortality. It is estimated that approximately 12,000 deaths occur each year from alcohol-related chronic liver disease and cirrhosis in the US (58). Chronic ethanol consumption causes liver disease by a complex interaction of multiple metabolic disturbances including oxidative and nitrative stress, redox imbalance (i.e., increased $NADH/NAD^+$), inflammation, and bioenergetic defects (59). Some of the earliest patho-physiological changes induced by chronic ethanol consumption in the liver occur at the level of the mitochondrion (26, 27). Studies show that the oxidative metabolism of alcohol is a key causative factor in liver injury through increased reactive oxygen and nitrogen species (ROS and RNS) production within the organelle (7, 9). Damage to mtDNA, mitochondrial protein synthesis inhibition, and enhanced susceptibility of hepatocytes to hypoxic and apoptotic stimuli implicate the mitochondrion in the pathobiology of alcoholic liver disease.

In addition to its role in cellular energy conservation, the mitochondrion has attracted much attention with regards to impacts on redox signaling pathways (44, 51) and as a regulator of cellular calcium (Ca^{2+}) homeostasis.

Specifically, mitochondria can control cytosolic Ca^{2+} levels by their ability to sequester and retain large amounts of Ca^{2+} (over 3 μmol Ca^{2+}/mg protein) via uptake of Ca^{2+} through the uniporter (37) and by regulated release of Ca^{2+} by either Na^+-dependent or Na^+-independent mechanisms (35, 68). Importantly, dysregulation of Ca^{2+} homeostasis is implicated in cell death mechanisms (71). Additionally, a link exists between ROS and mitochondrial Ca^{2+} (21, 46, 67) as increased ROS may cause Ca^{2+} overload in the cell (78) and increased Ca^{2+} can stimulate ROS production (20). Oxidants can disrupt Ca^{2+} transport systems leading to increased cytosolic and mitochondrial Ca^{2+} levels (21). While the exact mechanism for Ca^{2+}-induced mitochondrial ROS generation is not fully understood, Brookes et al. proposed that Ca^{2+} could enhance ROS production by stimulating the tricarboxylic acid cycle and oxidative phosphorylation thereby making mitochondria work "faster", which would increase O_2 consumption and presumably stimulate ROS production (20). Others propose that high mitochondrial Ca^{2+} triggers the mitochondrial permeability transition pore (MPTP), which may be followed by increased ROS production (50, 80). Together, these findings suggest that dysregulation of Ca^{2+} metabolism may contribute to oxidative injury to the mitochondrion.

Under conditions where there is increased ROS and mitochondrial Ca^{2+} storage capacity is exceeded, Ca^{2+} release from mitochondria occurs rapidly through the MPTP. This pore is a high conductance Ca^{2+}-activated channel that can be regulated by a wide variety of molecules (39, 80). MPTP formation leads to the free passage of molecules <1.5 kDa into and out of the mitochondrion.

These events can lead to mitochondrial swelling, the inability to maintain the mitochondrial membrane potential, decreased ATP production, and possible release of mitochondrial proteins involved in the initiation of apoptotic and/or necrotic cell death mechanisms. While many laboratories have studied the MPTP, the exact components of the pore and their functional roles remain elusive (39). One widely accepted paradigm suggests that the MPTP is composed of three main protein components: the voltage dependent anion channel (VDAC), the adenine nucleotide translocase (ANT), and cyclophilin D (Cyp D) (16, 41, 80). VDAC is located in the outer mitochondrial membrane and allows low molecular weight solutes to gain access to the inner membrane transport systems (13), whereas the ANT is located in the inner mitochondrial membrane and functions to import ADP into the matrix and export ATP to the cytosol (28). Cyp D is a mitochondrial matrix protein that has *cis-trans* peptidyl-prolyl isomerase activity, which allows it to behave like a chaperone protein (3, 32). Early experiments performed using *in vitro* systems provided some evidence to support the concept that oxidative stress may promote the translocation of Cyp D to the inner mitochondrial membrane where it participates in MPTP induction (12, 25). Previously, Pastorino and colleagues showed that mitochondria isolated from rats chronically fed ethanol had increased sensitivity to MPTP induction (65). The impact of chronic ethanol ingestion on the components that comprise and/or regulate the pore is not known.

Taken together, these results support the hypothesis that increased sensitivity for MPTP induction may contribute, in part, to chronic ethanol-

dependent mitochondrial dysfunction and liver injury. In the present study we tested this hypothesis by feeding male rats a control or ethanol-containing liquid diet for 5 wk and examined liver mitochondrial bioenergetics, mitochondrial Ca^{2+} retention capacity, and Ca^{2+}-mediated induction of the MPTP. These functional measurements were complemented by an assessment of ethanol-dependent changes in protein composition of the MPTP and select apoptotic proteins associated with mitochondria. Results from this study indicate that enhanced vulnerability to mitochondrial Ca^{2+} overload and increased Cyp D could predispose liver mitochondria to undergo MPTP formation and opening in response to chronic ethanol exposure.

MATERIALS AND METHODS

Materials. All chemicals were of the highest analytical grade and purchased from Sigma (St. Louis, MO) unless otherwise noted. Lieber-DeCarli control and ethanol liquid diets were purchased from Bio-Serv (Frenchtown, NJ). The pyruvate dehydrogenase antibody was a gift provided by Dr. Kirill Popov, Department of Biochemistry, University of Alabama at Birmingham.

Ethanol feeding protocol. Male Sprague-Dawley rats were individually housed and maintained under a 12 h light/dark cycle for the duration of the experiment. Animals were fed a standard rat chow diet for approximately 1 wk after procurement and weighed approximately 200 g at the start of the feeding protocol. Lieber-DeCarli control and ethanol-containing liquid diets were

formulated by Bio-Serv (Frenchtown, NJ). The nutritionally adequate ethanol diet

contains 36% of the total daily calories as ethanol, 35% as fat, 11% as

carbohydrate, and 18% as protein. The control diet is an identical formulation

with ethanol calories substituted by carbohydrate (i.e., dextrin maltose). Control

animals were pair-fed to their ethanol counterparts so that each pair was iso-

caloric. Animals were maintained on the feeding protocols for at least 31 days

before experiments. All animal protocols were approved by the institutional

animal care and use committee, and animals received humane care in

accordance with the National Institutes of Health (NIH) *Guide for the Care and

Use of Laboratory Animals* (NIH Publication No. 86-23).

Mitochondria isolation and respiration measurements.   Liver mitochondria

were isolated by differential centrifugation techniques (74). Oxygen consumption

of isolated liver mitochondria was monitored using a Clark-type oxygen electrode

(Hansatech Instruments, Amesbury, MA). Respiratory capacity was assessed by

measuring state 3 (i.e., ADP-dependent) and state 4 (i.e., ADP-independent)

respiration using succinate as the oxidizable substrate in the presence of

rotenone (1 μM) to inhibit complex I-mediated respiration. The respiratory control

ratio (RCR) was calculated as the ratio of state 3 and state 4 respiration rates

(i.e., state 3 divided by state 4 respiration).

Liver histology and biochemical measurements. Liver from control and

ethanol-fed rats was fixed in 10% formalin, sectioned, and stained with

hematoxylin-eosin for visualization of steatosis. Serum samples were assayed for alanine aminotransferase (ALT) activity and alcohol content using appropriate reagent sets from Pointe Scientific, Inc. (Canton, MI). Triglyceride levels were measured in serum and cytosolic liver fractions using an enzymatic-coupled assay that measures glycerol released from triglyceride (Pointe Scientific, Inc.).

Mitochondria Ca^{2+} retention capacity assessment. Mitochondrial Ca^{2+} retention capacity, (i.e., the threshold load of Ca^{2+} required to induce the MPTP) was measured using the cell impermeable fluorescent dye Calcium Green 5N (CaG5N, Invitrogen, Carlsbad, CA). Freshly isolated mitochondria were washed and re-suspended in 0.25 M sucrose buffer without EDTA. Experiments were performed using 0.2 mg/mL of isolated liver mitochondria incubated in respiration buffer (130 mM KCl, 2 mM KH$_2$PO$_4$, 3 mM HEPES, and 2 mM MgCl$_2$), 8 mM succinate, 1 µM rotenone, 0.2 mM ADP, 1 µg/mL oligomycin, and 0.2 µM CaG5N. The volume of the incubation mixture in the cuvette was 2.0 mL. Experiments were performed at 37°C in a Perkin Elmer LS 55 spectrofluorometer monitoring fluorescence with the excitation and emission wavelengths set at 506 and 532 nm, respectively. Single injections of Ca^{2+} (20 nmol) were added to the reaction mixture in the cuvette sequentially until induction of the MPTP. In select experimental runs, cyclosporin A (CsA, 1 µM) was used to demonstrate involvement of the MPTP, as CsA is an inhibitor of the MPTP (19). Inclusion of CsA allows for increased Ca^{2+} retention capacity before induction of the MPTP and subsequent release of Ca^{2+} from mitochondria (14).

Mitochondrial swelling assay. Mitochondria were re-suspended in Ca^{2+}-depletion buffer (1 mM EGTA, 10 mM NaCl and 5 mM succinate) and gently stirred at room temperature for 10 min followed by additionally stirring on ice for 5 min. Mitochondria were centrifuged for 10 min at 10,000xg at 4ºC. The mitochondrial protein pellet was then re-suspended in buffer containing 195 mM mannitol, 25 mM sucrose, and 40 mM HEPES, washed 2 times, and centrifuged for 10 min at 10,000xg at 4°C (53). The pellet was re-suspended in 2-3 mL of buffer and the protein concentration was determined by the Bradford protein assay (18). Isolated mitochondria (0.25 mg/mL) were incubated in a KCl-based buffer (150 mM KCl, 25 mM $NaHCO_3$, 1 mM $MgCl_2$, 1 mM KH_2PO_4, and 20 mM HEPES, pH 7.4) and were energized with the oxidizable substrate succinate (5 mM) in the presence of rotenone (10 µM). Ca^{2+} (200 nmol) was added to cuvettes and swelling was monitored by recording the decrease in absorbance for 20 min using a Beckman Coulter DU 640 Spectrophotometer at 540 nm and 30ºC. CsA (1 µM) was added to select samples prior to the addition of Ca^{2+} and swelling was monitored as described.

Western blotting. Immunoblots were performed by loading equal amounts of mitochondrial or cytosolic protein onto 10% or 12% SDS-PAGE gels. Note that the levels of mitochondrial proteins were measured from whole mitochondrial extracts. Levels of Cyp D were detected using a 1:10,000 dilution of antibody (Calbiochem, Gibbstown, NJ). Levels of ANT were detected using a 1:500

dilution of antibody (Santa Cruz, Santa Cruz, CA). Levels of VDAC were detected using 1:20,000 dilution of antibody (Calbiochem, Gibbstown, NJ). Levels of Bax and Bcl-2 were detected using 1:1,000 dilution of antibody (Cell Signaling, Beverly, MA). Levels of cytochrome *c* were detected using a 1:1,000 dilution of antibody (BD Pharmingen, San Diego, CA). After incubation of membranes with appropriate HRP-conjugated secondary antibodies (Sigma, St. Louis, MO) proteins were visualized using chemiluminescence. Membranes were then stripped and incubated with the appropriate loading control antibody. Levels of pyruvate dehydrogenase were detected using a 1:5,000 dilution as a loading control for mitochondrial protein. Levels of β-actin (Sigma, St. Louis, MO) were detected using a 1:5,000 dilution as a loading control for cytosolic proteins. Detection methods and the intensity of immunoreactive protein bands were quantified using Quantity One software (Bio-Rad Laboratories, Hercules, CA) as described in (10).

Terminal deoxynucleotidyl transferase dUTP nick end labeling (TUNEL).
Depariffinized and rehydrated liver sections from control and ethanol-fed rats were subjected to antigen retrieval in 0.1 M citrate buffer, pH 6.0. Tissues were blocked for 1 h at room temperature with 0.1 M Tris-HCl pH 7.5, containing 5% (w/v) BSA. Fifty microliters of the TUNEL reaction reagent (Roche, Indianapolis, IN) was added and liver sections were incubated for 60 min in the dark at 37°C in a humidified atmosphere. After sections were washed in phosphate-buffered saline (PBS), 50 µL of converter-alkaline phosphatase (AP) was added and liver

sections were incubated in a humidified dark chamber for 30 min at 37ºC.

Following this, sections were washed again in PBS and 100 µL of nitro-blue

tetrazolium chloride/5-bromo-4-chloro-3'-indolyphosphate p-toluidine salt

(NBT/BCIP) solution was added and incubated for 10 min at 25ºC in the dark.

Sections were then washed with PBS and mounted in PBS/glycerol and

visualized under light microscopy. For analysis by light microscopy, the number

of TUNEL-positive cells was counted per liver sample from 20 random high-

power fields (i.e., 40X magnification).

Gene Expression. Total RNA was isolated from liver tissue using TRIzol

(Invitrogen, Carlsbad, CA) following the manufacturer's directions. Reverse

transcription of 1 µg of total RNA was performed using RT^2 FirstStrand Kit

(SABiosciences, Frederick, MD). Real-Time PCR was performed using an

Applied Biosystems 7300 instrument with verified, gene-specific primers

purchased from SABiosciences (RT^2 qPCR SYBR Green-based primers).

Relative expression changes were determined by normalizing the relative

amount of gene-specific mRNA CT to the *Gapdh* (housekeeping gene) CT using

the comparative cycle threshold (ΔΔCT) method. The following rat specific RT^2

qPCR primer assays were used: *Vdac* (PPR50827A), *Ant* (PPR54853A), *Cyp D*

(PPR59729A), *Bax* (PPR06496A), *Bcl-2* (PPR06577A), *Cytochrome c*

(PPR42696A), and *Gapdh* (PPR06557A).

Statistical analysis. Data represent the mean ± S.E. for 6 pairs of animals per group. Significant differences between groups were obtained using the Student's paired *t*-test. For Real-Time PCR, significant differences between groups were obtained using the Wilcoxon Mann-Whitney non-parametric test. The level of statistical significance was set at $p<0.05$.

RESULTS

Animals and liver histology. For this study, rats were pair-fed a control or an ethanol-containing liquid diet for 5 wk; a diet and exposure protocol that is known to induce steatosis and mitochondrial dysfunction (10). There was no significant difference in body weight gain, liver weight gain, or the liver to body weight ratio between groups (Table 1). Consumption of ethanol increased serum triglyceride levels compared to control (Table 1); however, this difference was not statistically significant. In addition, there was a significant increase in liver triglyceride levels in the ethanol group compared to the control (Table 1). These data are in accordance with the increase in steatosis observed in livers of ethanol-fed animals compared to control-fed animals (Figure 1B). Controls showed no overt pathology or steatosis (Figure 1A). There was also a significant increase in serum ALT levels in the ethanol group compared to controls indicating mild hepatocellular injury (Table 1). These results demonstrate that this ethanol feeding regimen caused the early stage of alcoholic liver disease; steatosis.

Table 1. Effect of chronic ethanol consumption on various liver and serum measurements.

	Control	Ethanol
Body weight (g)	100.5 $\pm$ 9.3	95.3 $\pm$ 10.6
Liver weight (g)	10.8 $\pm$ 0.6	11.9 $\pm$ 0.8
Liver/body weight ratio (%)	3.1 $\pm$ 0.05	3.5 $\pm$ 0.15
Blood alcohol (mg/dL)	----	178 $\pm$ 35*
Serum ALT (IU/L)	43.2 $\pm$ 5.0	57.5 $\pm$ 3.0**
Serum triglycerides (mg/dL)	104.6 $\pm$ 12.5	162.1 $\pm$ 35
Liver triglycerides (mg/mg protein)	9.8 $\pm$ 1.8	41.1 $\pm$ 7.5*

*$p < 0.05$, **$p < 0.005$, compared to control
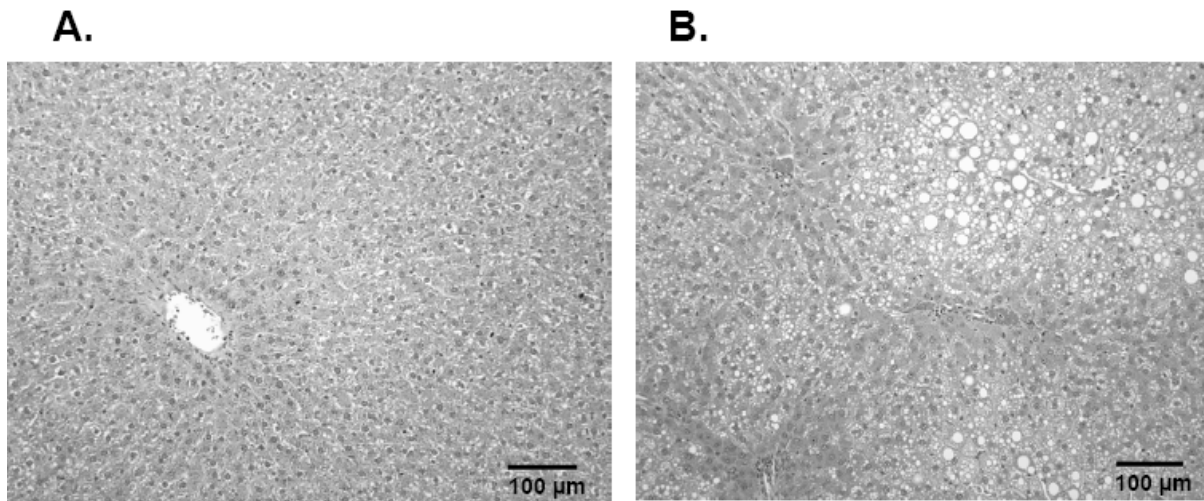
Figure 1. Chronic ethanol consumption causes liver steatosis. Light microscopy images from representative livers of control and ethanol-fed rats. (A) Representative image of hematoxylin-eosin stained liver section from a control-fed rat. (B) Representative image of hematoxylin-eosin stained liver section from ethanol-fed rat. Note that these images are from the same control and ethanol pair, and are representative of six pairs of control and ethanol-fed rats. Magnification is 20X.
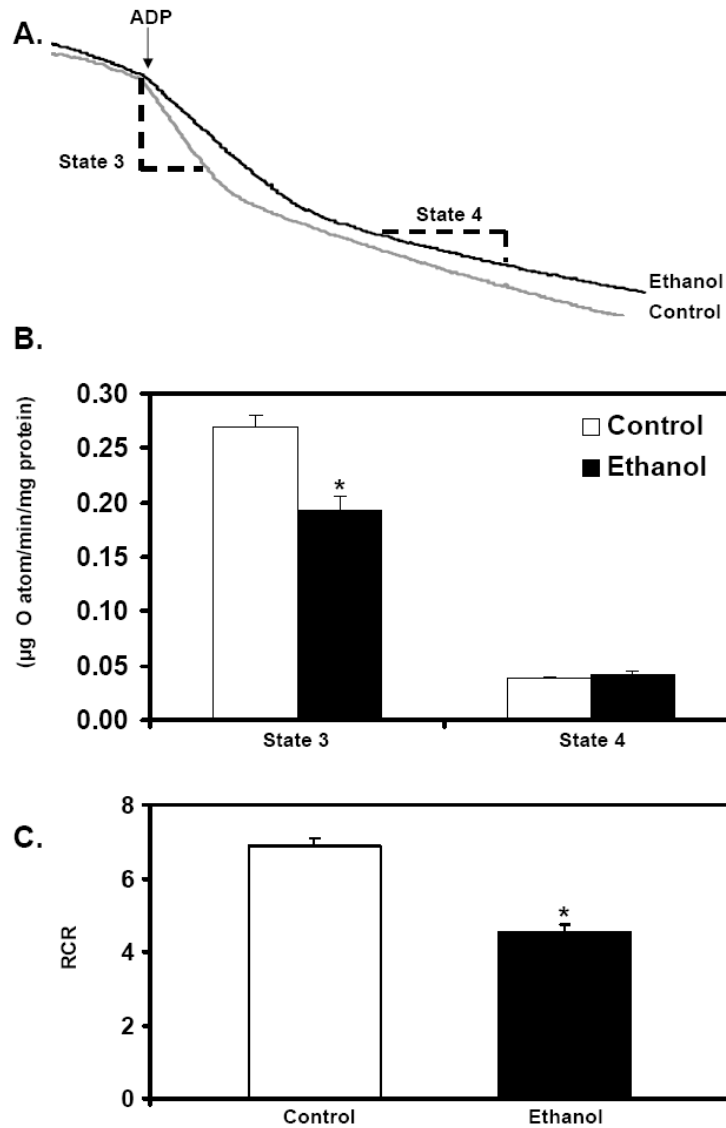
Chronic ethanol consumption decreases mitochondrial respiratory

function. Mitochondrial oxygen consumption in the presence of succinate and

ADP (i.e., state 3 respiration) was measured in freshly isolated liver mitochondria

from control and ethanol-fed animals. Note that the terms control mitochondria

and ethanol mitochondria are used in the manuscript and refer to mitochondria

isolated from livers of control-fed (i.e., ethanol-naïve) and ethanol-fed rats,

respectively. Figure 2A shows typical respiration results from mitochondria

isolated from an ethanol-fed rat and its pair-fed control. As shown in Figure 2B,

state 3 respiration was decreased in mitochondria isolated from the livers of

ethanol-fed rats compared to controls. A decrease in state 3 respiration is

notable because it indicates that chronic alcohol consumption decreases electron

transport and subsequently the rate at which liver mitochondria may synthesize

ATP. In contrast, state 4 respiration was unaffected by ethanol consumption

(Figure 2B), suggesting that uncoupling does not occur during the early stage of

the disease process and does not contribute to defects in mitochondrial

bioenergetics at this stage. In addition, the respiratory control ratio (i.e., RCR =

state3/state 4 respiration) was determined for each pair of ethanol and control-

fed rats. A higher RCR indicates mitochondria that are more tightly coupled with

better function (i.e., better quality of mitochondria), whereas a lower RCR

indicates that mitochondria are more loosely coupled with poorer function (i.e.,

damaged mitochondria) in response to treatment. The RCR was significantly

lower in the ethanol group compared to the control group (Figure 2C). These

data demonstrate that the bioenergetics of liver mitochondria are compromised in

the early, steatosis phase of alcoholic liver disease and are consistent with earlier studies done in our laboratory (10).

Mitochondria isolated from ethanol-fed rats are more sensitive to Ca^{2+}-induced swelling. We measured mitochondrial swelling in response to Ca^{2+}; a known inducer of the MPTP, to determine whether chronic ethanol consumption changes the sensitivity of MPTP induction. Figure 3A shows representative results of freshly isolated liver mitochondria from control and ethanol-fed rats incubated with 200 nmol Ca^{2+} to induce mitochondrial swelling. Both control and ethanol mitochondria were sensitive to Ca^{2+}-dependent swelling. However, mitochondria from ethanol-fed animals were more sensitive to Ca^{2+}-triggered swelling as shown by the faster rate of swelling (i.e., steeper slope) immediately following the addition of Ca^{2+} (Figure 3A, arrow). The rate of swelling was taken over the same time period, 180-330 sec, for each sample (Figure 3B). There was a 71% increase in the rate of Ca^{2+}-dependent swelling in ethanol mitochondria compared to control over this time frame. Pretreatment with CsA, a known inhibitor of the MPTP, blocked Ca^{2+}-induced swelling in both control and ethanol mitochondria, indicating that this is a MPTP-dependent process (data not shown).
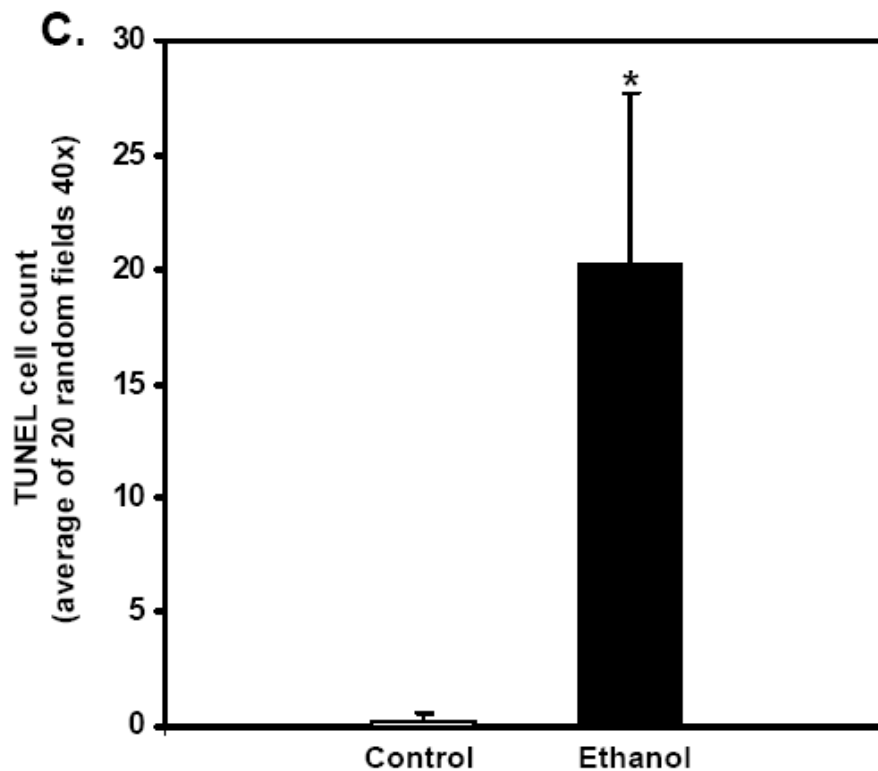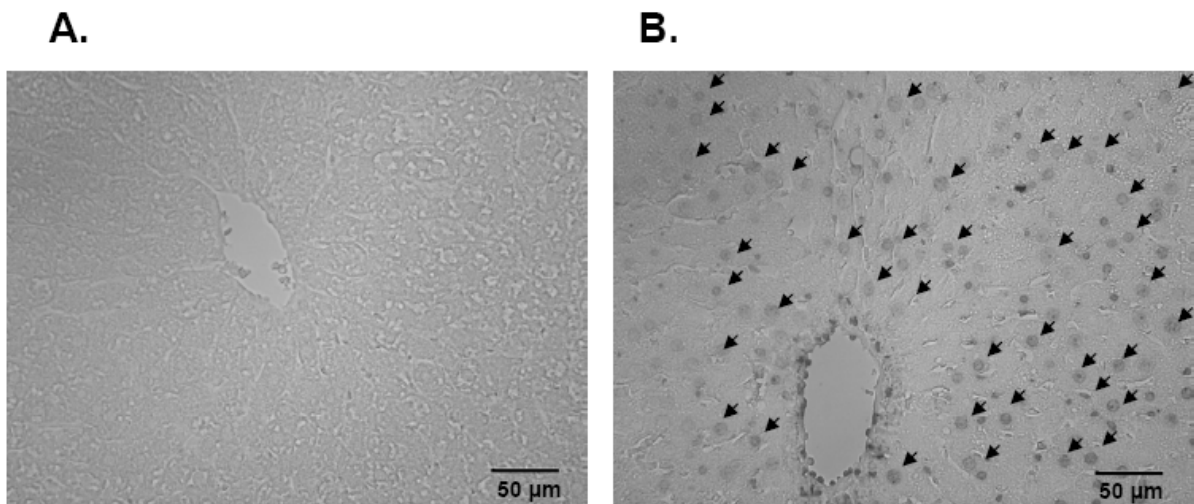
Figure 2. Chronic ethanol consumption decreases mitochondrial respiration. (A) Representative results from oxygen consumption studies from control (gray trace) and ethanol (black trace) mitochondria. Oxygen consumption was determined using succinate as the oxidizable substrate. ADP was added at the arrow to initiate 3 respiration (dashed line marking). After all ADP is converted to ATP, mitochondria enter state 4 respiration (lower rate of respiration), which is marked on the trace (dashed line marking). (B) State 3 respiration was significantly lower in ethanol mitochondria compared to controls, whereas there was no difference in state 4 respiration between groups. (C) The respiratory control ratio (RCR = state 3/state 4 respiration) was significantly lower in ethanol mitochondria compared to controls. Data are expressed as the mean ± S.E. for six pairs of control and ethanol fed rats, *$p<0.05$ compared to control.
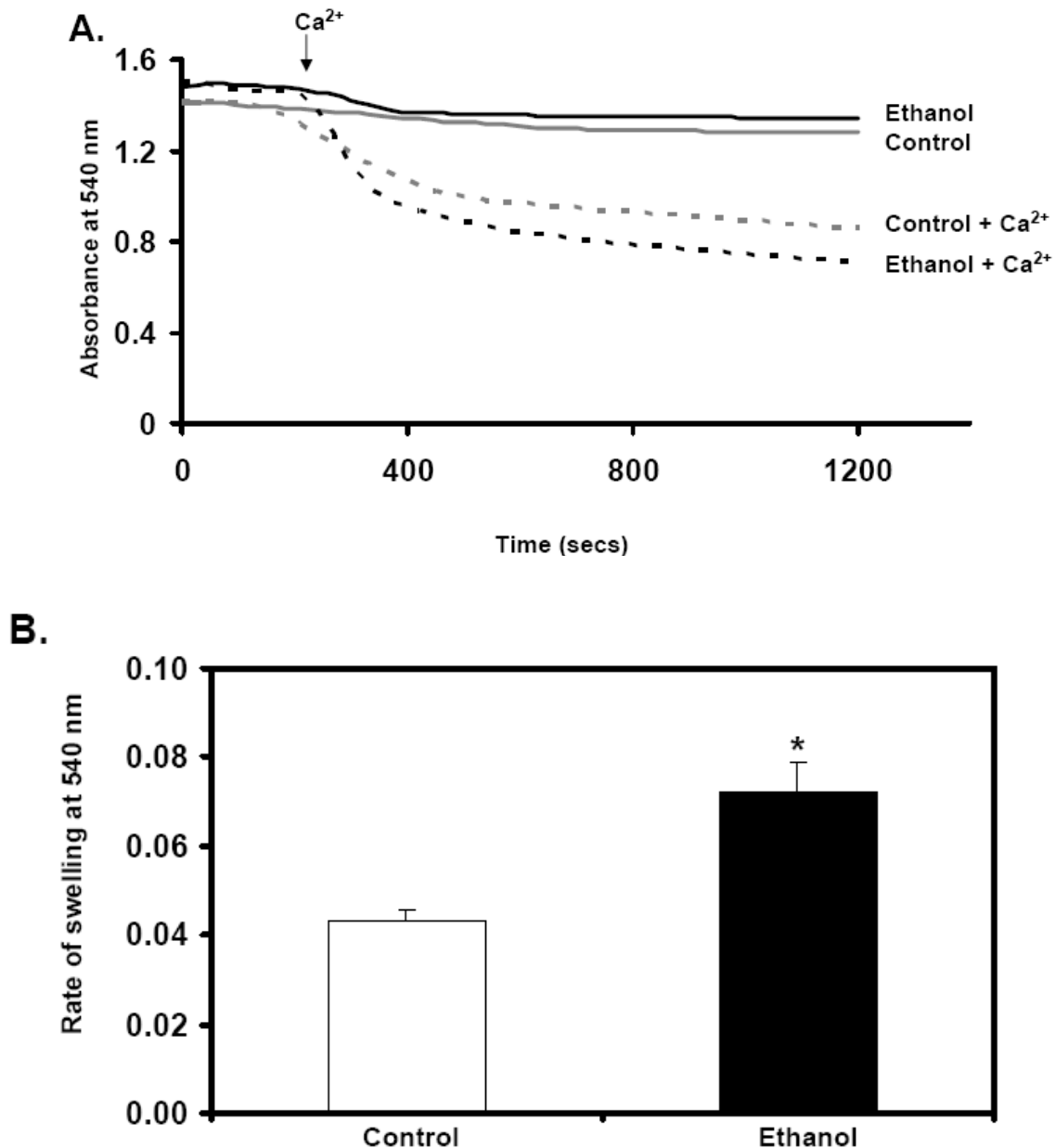
Figure 3. Chronic ethanol consumption increases sensitivity to Ca^{2+}-mediated mitochondrial swelling. Isolated mitochondria (0.25 mg/mL) were incubated in a KCl-based buffer containing 150 mM KCl, 25 mM $NaHCO_3$, 1 mM $MgCl_2$, 1 mM KH_2PO_4, and 20 mM HEPES, pH 7.4. (A) Representative results of mitochondrial swelling using 0 (solid lines) and 200 nmol Ca^{2+} (dashed lines) at an absorbance of 540 nm. (B) The decrease in absorbance was followed for 20 min and the rate of swelling was calculated from the initial slope of the decrease in absorbance (i.e., from 180-330 sec). Mitochondria from ethanol-treated animals (black dashed line) were significantly more sensitive to Ca^{2+}-mediated mitochondrial swelling than mitochondria from control animals (gray dashed line). Data are expressed as the mean ± S.E. for six pairs of control and ethanol fed rats, *$p < 0.05$ compared to control.

Chronic ethanol consumption induces cell death in the liver. Chronic

ethanol-dependent oxidative stress is thought to contribute to hepatocyte injury

and lead to apoptosis and/or necrosis. To determine whether cell death was

increased by chronic ethanol consumption, TUNEL staining was performed in

liver sections prepared from control and ethanol-fed rats. This method is used

for detecting DNA fragmentation, an indicator of cell death, by labeling the

terminal end of nucleic acids. We observed a significant increase in TUNEL-

positive cells in livers of ethanol-fed rats compared to controls (Figures 4A-C). It

is important to note that DNA fragmentation, as evidenced by the TUNEL

reaction, is not solely exclusive for apoptosis because DNA fragmentation may

occur during necrosis or DNA repair processes (43, 64), although both of these

alternative interpretations support the occurrence of ethanol-dependent cell injury

and death in this model of early alcoholic liver disease.

Effect of chronic ethanol consumption on select pro- and anti-apoptotic

proteins. Increased susceptibility to cell death may occur from an interaction

between pro-apoptotic proteins and components of the MPTP or from these

proteins inducing mitochondrial outer membrane permeability (MOMP)

independent of the classic MPTP process (1, 65). Therefore, we investigated the

impact of chronic alcohol consumption to alter the levels of three classic pro- and

anti-apoptotic proteins: cytochrome *c,* Bax, and Bcl-2, at the level of transcript

and protein. Alterations in the levels of pro-apoptotic Bax and anti-apoptotic Bcl-
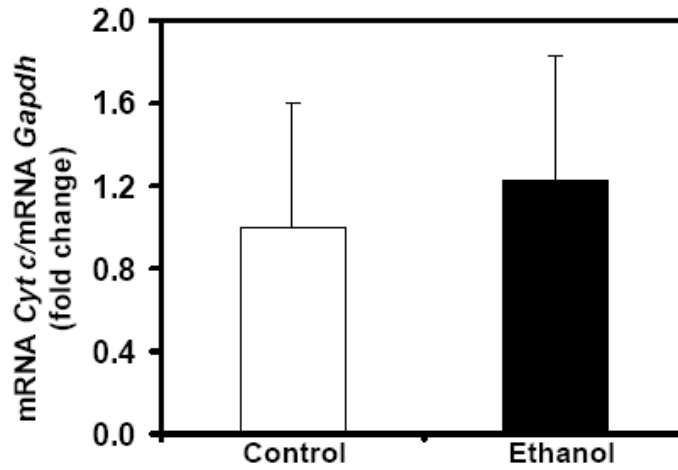
Figure 4. Chronic ethanol consumption increases hepatic TUNEL staining. TUNEL-positive nuclei were visualized in formalin-fixed liver sections for control (A) and ethanol (B)-fed rats. Images are representative of at least six rats per treatment group taken at 40X magnification. (C) For quantification, the number of TUNEL-positive cells was counted per liver sample from 20 random high-powered fields (40X magnification). Data are expressed as the mean ± S.E. for six pairs of control and ethanol fed rats, *p<0.05 compared to control.

2, in the mitochondrion, may be critical in determining the response to chronic

ethanol exposure and whether MPTP induction will occur. First, chronic alcohol

consumption had no effect on *Cytochrome c* gene expression between control

and ethanol groups (Figure 5A). Similarly, we observed no difference in

mitochondrial cytochrome *c* protein levels between control and ethanol groups

(Figure 5B) and we were unable to detect monomeric cytochrome *c* in cytosol

(data not shown). Like *Cytochrome c*, we observed no difference in *Bax* gene

expression between control and ethanol groups (Figure 6A). There was also no

difference in the cytosolic levels of Bax protein between control and ethanol

groups (Figure 6B). However, we observed a significant increase in

mitochondrial Bax protein levels in ethanol compared to control mitochondria

(Figure 6C). Lastly, we found a significant decrease in *Bcl*-2 gene expression in

ethanol compared to control liver (Figure 6D), whereas the levels of Bcl-2 protein

were increased in ethanol compared to control mitochondria (Figure 6E).

***Mitochondria from ethanol-fed rats have lower Ca^{2+} retention capacity than

control mitochondria.*** Mitochondria are recognized as an important cellular

Ca^{2+} store (2, 36) with mitochondrial Ca^{2+} able to stimulate electron transport,

increase ROS production, and induce the MPTP (21). Freshly isolated

mitochondria were incubated with the Ca^{2+}-sensitive fluorescent dye CaG5N (22,

72) to determine the effect of chronic ethanol consumption on mitochondrial Ca^{2+}

retention capacity. In this experiment, bolus additions of Ca^{2+} (20 nmol) were

added sequentially to energized mitochondria until MPTP induction, which results
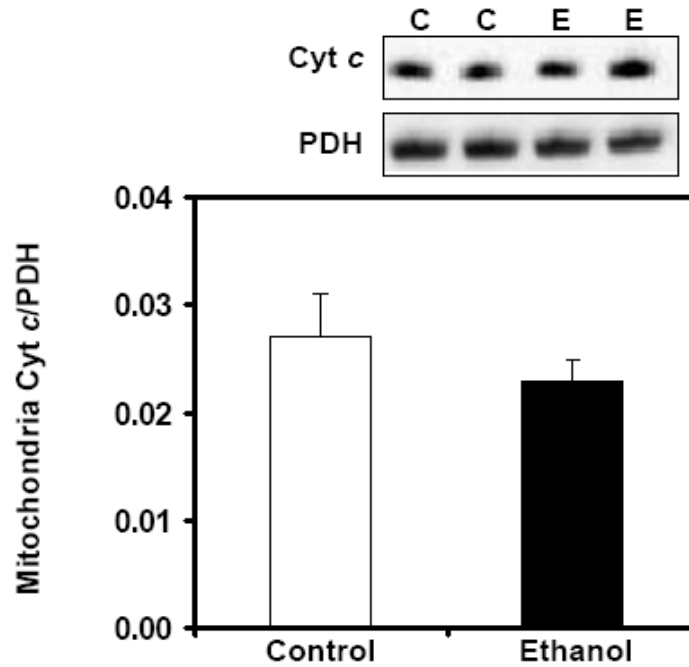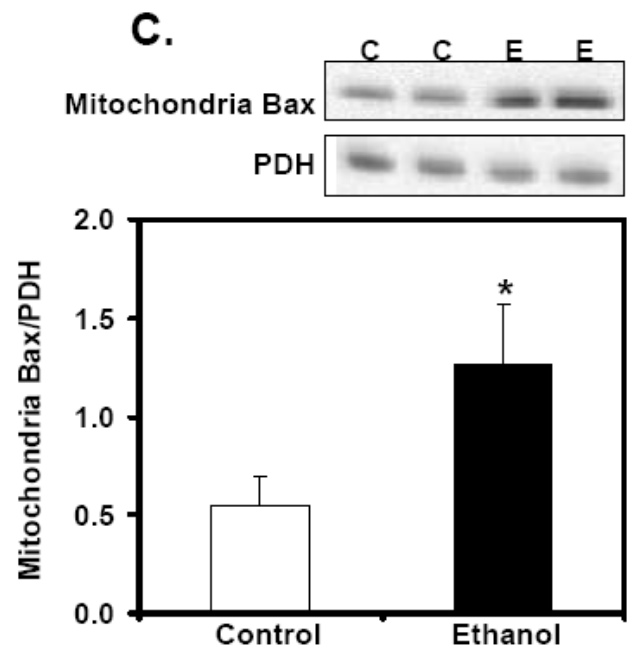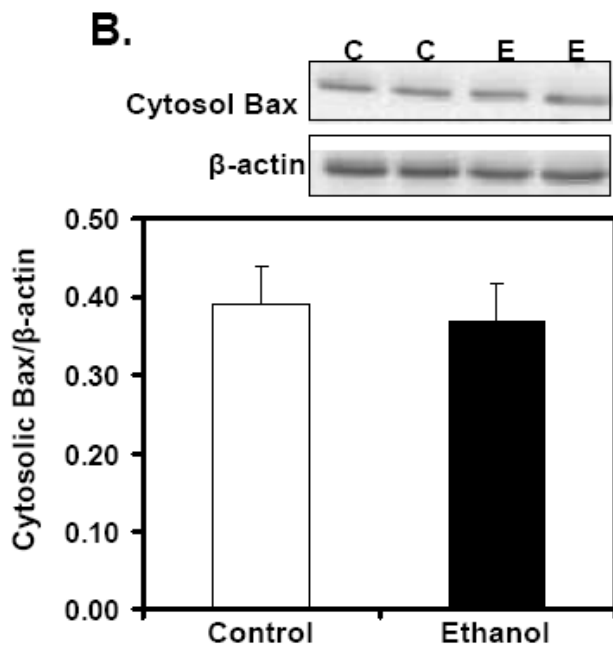
Figure 5. Effect of chronic ethanol consumption on cytochrome *c* transcript and protein levels. For gene expression analyses, total RNA was isolated and measured by real-time PCR. The relative amount of mRNA was determined using the comparative threshold (Ct) method by normalizing target cDNA levels to *Gapdh*. Protein was measured by western blotting technique and normalized to pyruvate dehydrogenase (PDH). (A) There was no difference in *Cytochrome c* gene expression between control and ethanol-fed animals. (B) There was no difference in mitochondrial cytochrome *c* protein between control and ethanol groups. Data are expressed as the mean ± S.E. for six pairs of control and ethanol fed rats.

A.

B.

Cytosol Bax

β-actin

C.

Mitochondria Bax

PDH
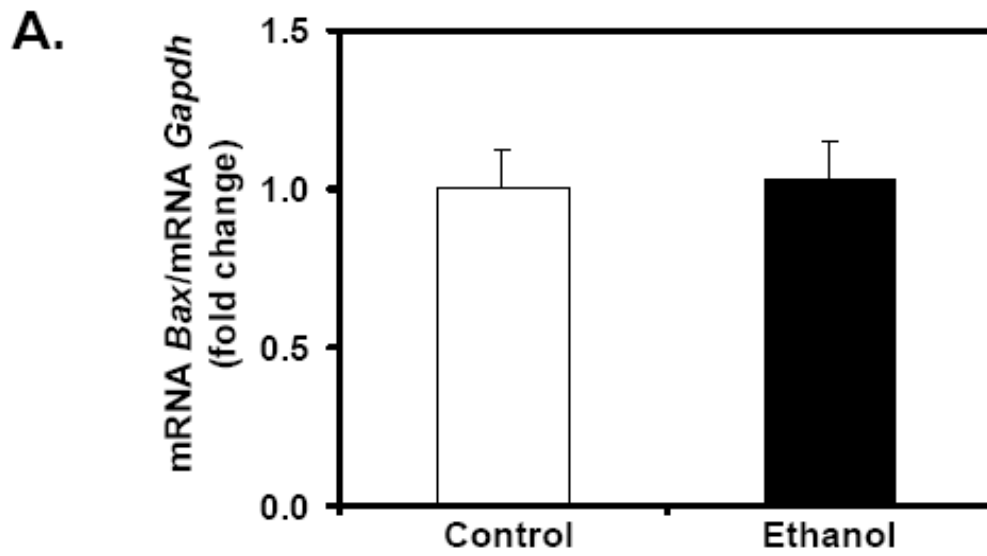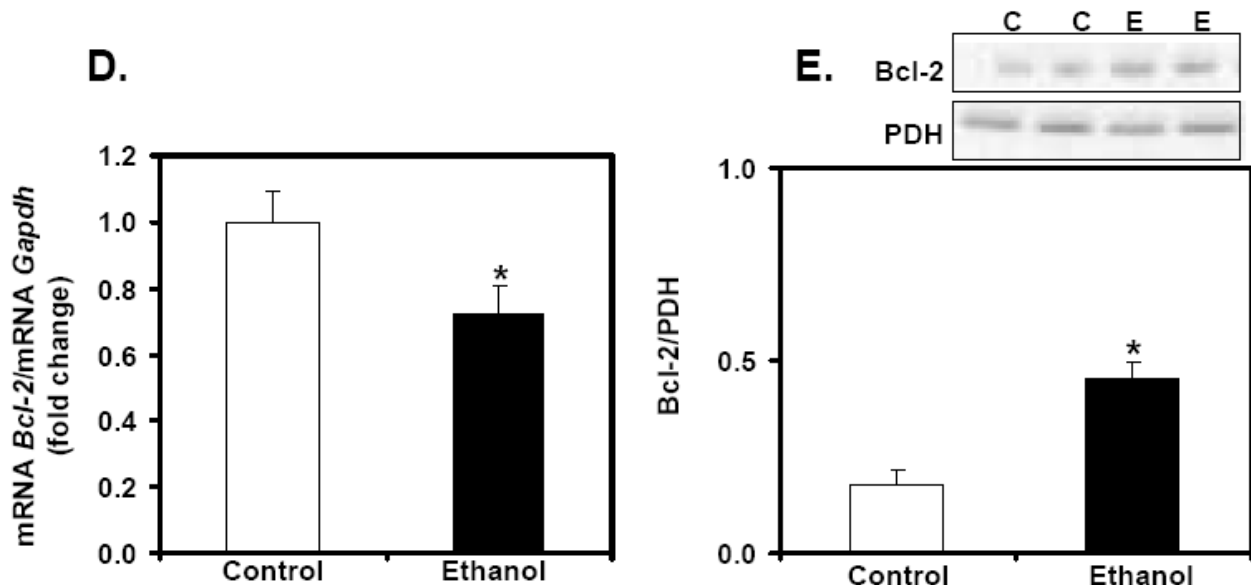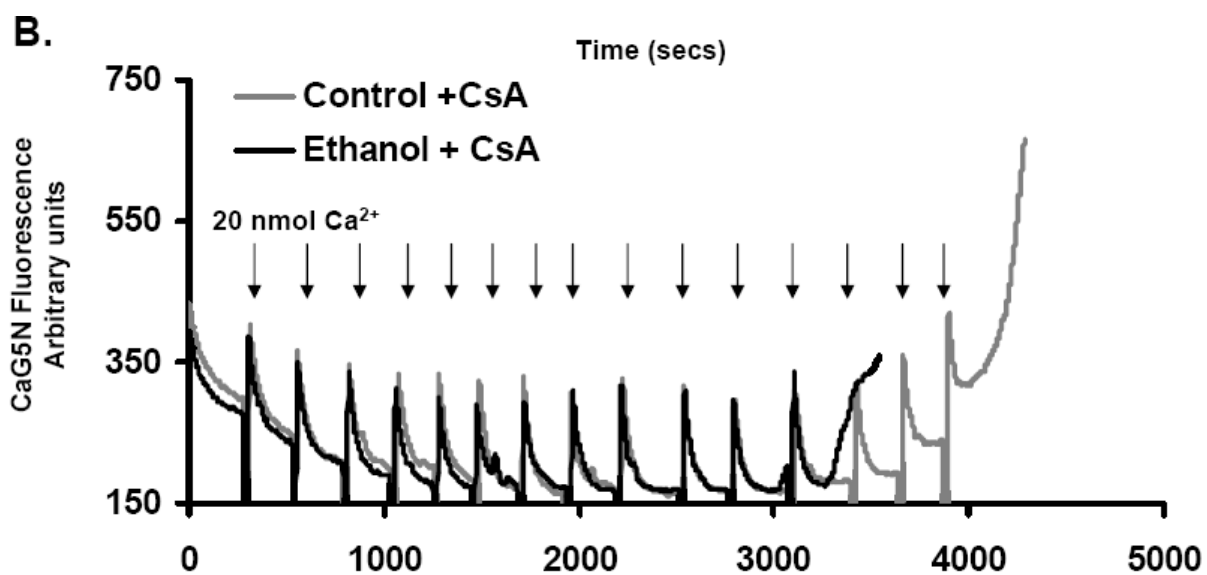
Figure 6. Effect of chronic ethanol consumption on transcript and protein levels of key pro- and anti-apoptotic mediators. For gene expression analyses, total RNA was isolated and measured by real-time PCR. The relative amount of mRNA was determined using the comparative threshold (Ct) method by normalizing target cDNA levels to *Gapdh*. Protein was measured by western blotting technique and normalized to either β-actin or pyruvate dehydrogenase (PDH). (A) There was no difference in *Bax* gene expression between control and ethanol-fed animals. The pro-apoptotic protein Bax was measured in cytosolic and mitochondrial fractions (B) and (C), respectively. There was no difference in cytosolic Bax protein between control and ethanol-fed rats. There was a significant increase in mitochondrial Bax protein in ethanol compared to control rats. (D) There was a significant decrease in *Bcl*-2 gene expression in ethanol compared to control animals. (E) Bcl-2 protein was significantly increased in liver mitochondria from ethanol-fed rats compared to controls. Data are expressed as mean ± S.E. for six pairs of control and ethanol fed rats, *p<0.05 compared to control.

116

in release of intra-mitochondrial Ca^{2+} (as indicated by a rapid rise in CaG5N fluorescence at the end of the experimental run). As shown in Figure 7A, initial aliquots of Ca^{2+} lead to a transient rise in extra-mitochondrial Ca^{2+} followed by a rapid return to baseline fluorescence as Ca^{2+} is taken up and sequestered by mitochondria. Note that Ca^{2+} retention was slower in mitochondria from ethanol-fed animals compared to control, and upon further additions of Ca^{2+}, mitochondria from ethanol-fed animals were unable to retain as much Ca^{2+} before undergoing induction of the MPTP (Figure 7A). Indeed, there was a significant decrease in the amount of Ca^{2+} stored prior to the induction of the MPTP in mitochondria from ethanol-fed animals (167 ± 21 nmol Ca^{2+} per mg protein) compared to mitochondria from control animals (317 ± 36 nmol Ca^{2+} per mg protein) (Figure 7C). When the Ca^{2+} retention capacity experiment was performed in the presence of CsA, both mitochondria from control and ethanol-fed animals stored more Ca^{2+} before induction of the MPTP (Figure 7B and D). For example, control + CsA and ethanol + CsA-treated mitochondria stored 883 ± 60 and 675 ± 120 nmol Ca^{2+} per mg protein, respectively. While mitochondria from ethanol-fed animals treated with CsA stored slightly less Ca^{2+} before pore induction, this difference was not statistically significant compared to control mitochondria treated with CsA ($p=0.17$). Together, these findings are noteworthy because they demonstrate that chronic ethanol ingestion increases the susceptibility of mitochondria to Ca^{2+} overload, which presumably increases sensitivity to the MPTP.

A.

CaG5N Fluorescence Arbitrary units

750

550

350

150

20 nmol Ca²⁺

Control
Ethanol

0   500   1000   1500   2000   2500

B.

Time (secs)

CaG5N Fluorescence Arbitrary units

750

550

350

150

20 nmol Ca²⁺

Control +CsA
Ethanol + CsA

0   1000   2000   3000   4000   5000
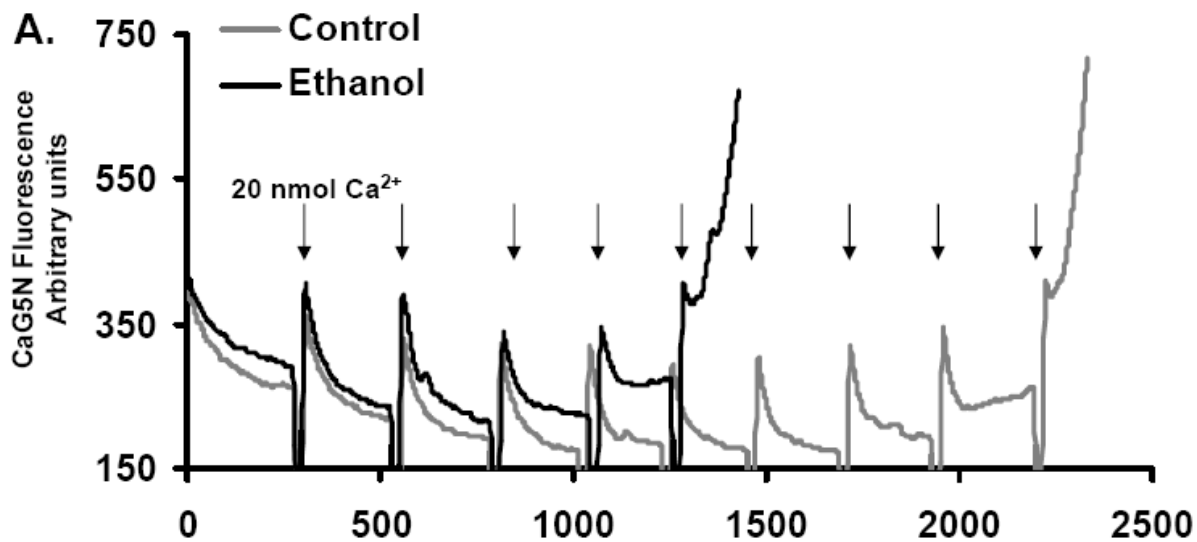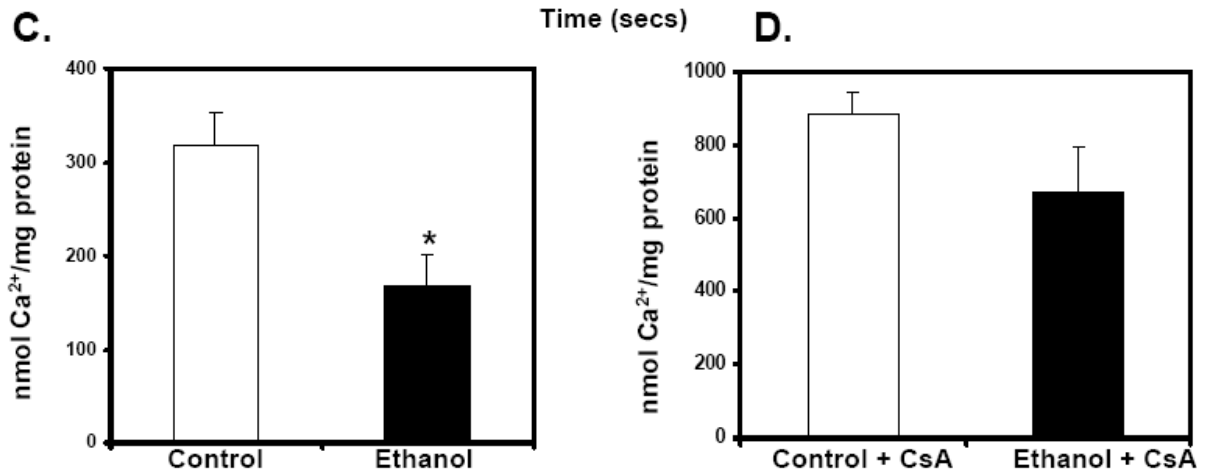
Figure 7. Effect of chronic ethanol consumption on liver mitochondria Ca^{2+} retention capacity. Liver mitochondria (0.2 mg/mL) were incubated in respiration buffer (130 mM KCl, 2 mM KH$_2$PO$_4$, 3 mM HEPES, and 2 mM MgCl$_2$) with 8 mM succinate, 1 μM rotenone, 0.2 mM ADP, 1 μg/mL oligomycin, and 0.2 μM CaG5N. (A) Representative results of Ca^{2+} uptake in control (gray line) and ethanol (black line) mitochondria. Ca^{2+} was added as 20 nmol additions every 240 sec (i.e., 20 nmol at each arrow). Mitochondrial Ca^{2+} retention capacity was lower in ethanol compared to control mitochondria before MPTP induction. (B) Representative results of Ca^{2+} uptake in control (gray line) and ethanol (black line) mitochondria pretreated with CsA. Ca^{2+} was added as 20 nmol additions every 240 sec (i.e., 20 nmol at each arrow). Note that in the presence of CsA, mitochondrial Ca^{2+} retention capacity was increased for both control and ethanol mitochondria. (C) Quantification of mitochondrial Ca^{2+} retention capacity in ethanol and control mitochondria. (D) Quantification of mitochondrial Ca^{2+} retention capacity in ethanol and control mitochondria pretreated with CsA. Data are expressed as the mean ± S.E. for six pairs of control and ethanol-fed rats, *$p < 0.005$ compared to control.

Chronic ethanol consumption causes an increase in cyclophilin D. The

exact composition of the pore is unknown; however, the MPT is proposed to

occur in response to the opening of a pore (i.e., the MPTP) involving the inner

and outer membrane proteins VDAC and ANT, the matrix protein Cyp D, and

other accessory proteins (80). To investigate the mechanisms that may

contribute to increased mitochondrial swelling and reduced Ca^{2+} retention

capacity in response to chronic ethanol exposure, components of the MPTP were

examined. Real-time PCR and western blots analysis was used to determine the

effect of chronic ethanol consumption on components of the MPTP. As shown in

Figures 8A and 8B, chronic ethanol consumption had no effect on *Vdac* gene

expression or VDAC protein levels between control and ethanol groups.

Similarly, chronic ethanol consumption had no effect on *Ant* gene expression or

ANT protein levels between control and ethanol groups (Figures 8C and 8D).

However, we observed a significant increase in *Cyp D* gene expression in

ethanol compared to control liver (Figure 8E) along with a significant increase in

Cyp D protein in ethanol compared to control mitochondria (Figure 8F).
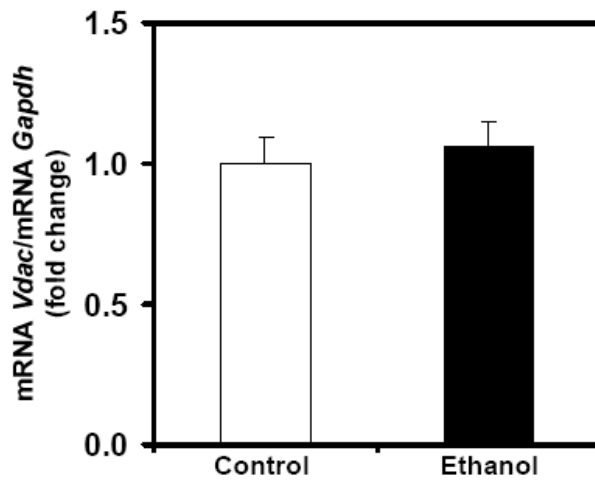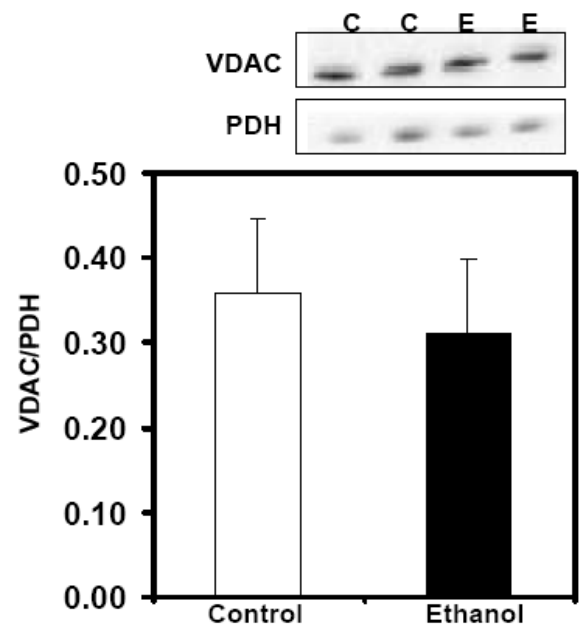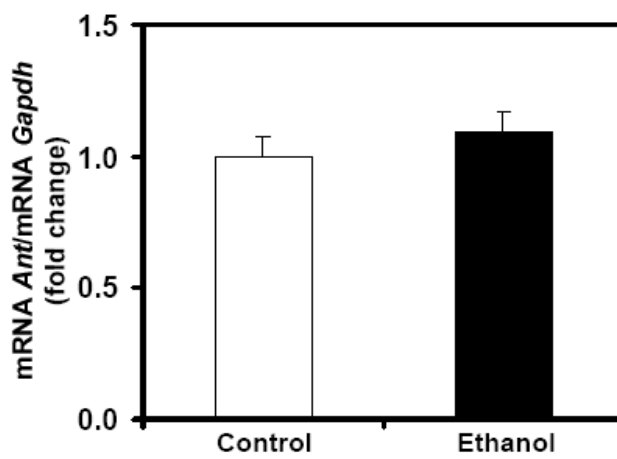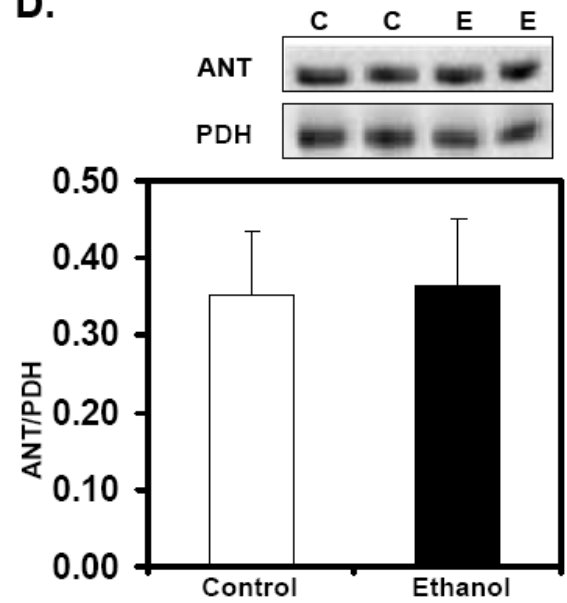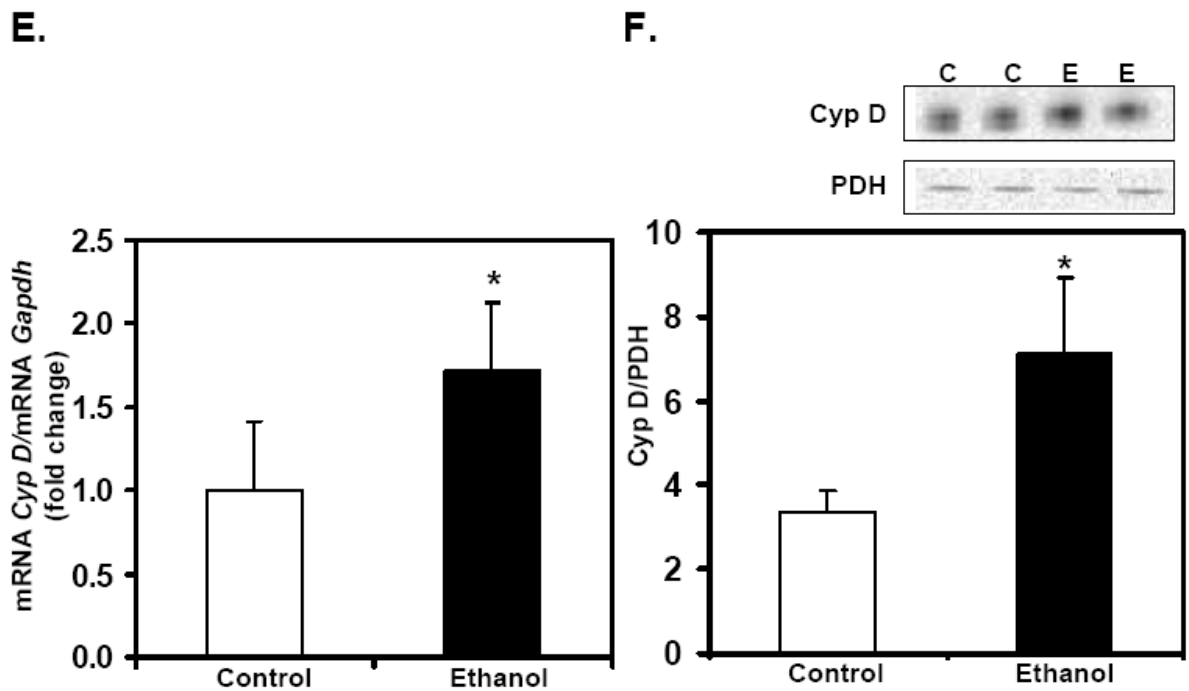
Figure 8. Chronic ethanol consumption increases cyclophilin D transcript and protein levels. For gene expression analyses total RNA was isolated and measured by real-time PCR. The relative amount of mRNA was determined using the comparative threshold (Ct) method by normalizing target cDNA levels to *Gapdh*. Protein was measured by western blotting technique and normalized to pyruvate dehydrogenase (PDH). (A) There was no difference in *Vdac* gene expression between control and ethanol groups. (B) There was no difference in VDAC protein between control and ethanol mitochondria. (C) There was no difference in *Ant* gene expression between control and ethanol groups. (D) There was no difference in ANT protein between control and ethanol mitochondria. (E) There was a significant increase in *Cyp D* gene expression in liver from ethanol-fed compared to control animals. (F) There was a significant increase in Cyp D protein in ethanol compared to control mitochondria. Data are expressed as the mean ± S.E. for six pairs of control and ethanol fed rats, *p<0.05 compared to control.

DISCUSSION

Previous studies from our laboratory and others have shown that chronic ethanol consumption causes mitochondrial dysfunction due to mtDNA and ribosomal damage, depressed oxidative phosphorylation (OxPhos), and increased ROS generation (59). The negative impact of chronic ethanol consumption on liver mitochondria bioenergetics is largely attributed to losses in both mitochondrial and nuclear encoded proteins that comprise several of the OxPhos complexes (4, 24, 74). The alcohol-dependent decrease in these subunits results in reduced respiratory complex activities and depressed rates of ADP-dependent respiration (i.e., state 3 respiration) (10). It is these alcohol-mediated changes at the molecular level that largely contribute to decreased ATP synthesis and levels in liver mitochondria following chronic alcohol consumption (8, 26). In addition to these changes, it is possible that increased liver fat following chronic ethanol consumption (Table 1 and Figure 1) contributes, in part, to increased mitochondrial ROS production and subsequent oxidative damage. For example, in steatotic liver there will be increased delivery of free fatty acids to mitochondria for β-oxidation, leading to increased transfer of reducing equivalents to the respiratory chain. This event, coupled with a damaged respiratory chain, will amplify electron "leak" to molecular oxygen thereby increasing the generation of superoxide anions and other ROS (7). Increased ROS/RNS are proposed to damage the respiratory complexes by posttranslational oxidative modifications (75). Thus, ROS-dependent damage is predicted to occur in response to chronic alcohol ingestion and cause oxidative

damage to the respiratory chain machinery resulting in impaired bioenergetic capacity and other key mitochondrial functions.

One critical mitochondrial function involves control of cellular Ca^{2+} levels to ensure proper functioning of numerous signal transduction and cell cycle systems (78). Ca^{2+} is also a key regulator of internal mitochondrial functions and acts at several levels within the organelle to control ATP synthesis and ROS production (20). Dysregulation of mitochondrial Ca^{2+} homeostasis is now recognized to play a key role in several pathologies including liver disease (55). It is known that mitochondria have the ability to rapidly sequester large amounts of Ca^{2+} in response to increased cytosolic Ca^{2+} levels (30, 38); however, the ability to store and retain Ca^{2+} may be impaired when mitochondrial function is negatively impacted during pathological states. Recently, Yan et al., (77) reported that chronic ethanol consumption increased intracellular Ca^{2+} levels in isolated hepatocytes when compared to levels measured in ethanol-naïve hepatocytes. The data presented in the current study show that liver mitochondria from animals fed ethanol chronically are more susceptible to Ca^{2+} overload than control mitochondria. Isolated mitochondria in the presence of phosphate will take up and sequester Ca^{2+} until buffering is reached (i.e., Ca^{2+} retention capacity). However, when mitochondria become overloaded with Ca^{2+}, they will undergo the MPTP, allowing Ca^{2+} to flood out of the matrix compartment back into the cytosol. Mitochondria isolated from livers of ethanol-fed animals have a lower threshold for Ca^{2+}-mediated induction of the MPTP and therefore have a reduced Ca^{2+} retention capacity as compared to control mitochondria

(Figure 7). Accordingly, we investigated whether alterations in the proposed

components that compromise and/or regulate the MPTP might be involved in the

increased sensitivity of mitochondria to undergo the MPT following chronic

ethanol exposure.

The MPTP is a non-selective pore that spans the inner and outer

membranes of the mitochondrion and allows for the passage of small molecular

solutes (16, 80). While controversial, studies suggest that the MPTP is

composed of VDAC, ANT, and Cyp D (16, 41, 80) with opening of the pore

enhanced by adenine nucleotide depletion, ROS, and Ca^{2+} (6, 46, 50). One

consequence of pore opening is that the inner mitochondrial membrane becomes

more permeable to H^+ and other ions leading to dissipation of the proton motive

force and decreased ATP generation. Similarly, opening of the MPTP will allow

small molecular solutes to equilibrate across the inner membrane resulting in

swelling of the mitochondrion. As the matrix compartment expands, it exerts

pressure on both the inner and outer membranes causing the outer membrane to

rupture (i.e., MOMP). This can result in the release of mitochondrial proteins

from the inter membrane space, which then engage other proteins in the cytosol

and nucleus initiating cell death pathways. While the mechanisms responsible

for MPTP and MOMP induction remain poorly defined (39), several theories have

been proposed and include changes in mitochondria membrane potential, Ca^{2+}

overload, increased ROS production, and posttranslational modification of MPTP

components (34, 57, 69).

With regards to alcohol-dependent changes in MPTP components, we observed no change in VDAC or ANT gene expression or protein levels. The lack of effect on ANT was predicted as previous studies showed no effect on ANT protein following chronic ethanol consumption (23). However, we can not exclude the possibility that chronic ethanol treatment may have altered VDAC functionality via posttranslational modification, e.g., phosphorylation (29). In contrast, whole liver mitochondria isolated from chronic ethanol-fed animals exhibited a higher content of Cyp D protein compared to control mitochondria (Figure 8F). This finding is mirrored at the gene level as higher transcript levels of *Cyp D* are also observed in liver from ethanol-fed rats compared to controls (Figure 8E). Cyp D is a member of the CsA-binding cyclophilin family of proteins that catalyzes *cis-trans* isomerization of peptidyl-prolyl bonds (3, 34). This activity participates in the correct folding, assembly, and transport of newly synthesized proteins (32). In addition to its chaperone function in mitochondria, Cyp D is believed to serve as a regulator or "sensitizer" of the MPTP (11, 34). The role of Cyp D in the MPTP was originally proposed by Halestrap and colleagues and based on studies showing that opening of the MPTP was inhibited by CsA after binding to Cyp D (40). These early studies also suggested that ROS promote MPTP formation through oxidation of critical ANT thiols, which presumably increased the affinity of ANT for Cyp D and sensitivity to undergo the MPTP (46, 60, 80). Based on this, it is possible that the chronic ethanol-mediated increase in oxidative stress (7) and Cyp D may contribute to increased MPTP sensitivity and impaired mitochondrial Ca^{2+} handling through increased

interactions among MPTP components. Previous studies have shown that tissues with high Cyp D content like synaptic mitochondria also have reduced mitochondrial Ca^{2+} retention capacity compared to tissues (i.e., non-synaptic mitochondria) that contain lower levels of Cyp D (62). Likewise, we observed a similar response of reduced Ca^{2+} retention capacity (Figures 7A and C) and increased Cyp D protein levels in liver mitochondria isolated from chronic ethanol-fed animals compared to ethanol-naïve controls (Figure 8E). Therefore, higher levels of Cyp D in response to chronic ethanol ingestion may contribute, in part, to reduce the mitochondrial Ca^{2+} threshold that initiates the MPTP (Figures 3 and 7).

More recently, the role of Cyp D in regulation of the MPTP has been supported in studies using Cyp D null mice. In these studies, genetic ablation of Cyp D increased mitochondrial Ca^{2+} buffering capacity to levels measured in CsA-treated mitochondria from wild-type controls, with no effect of CsA observed in Cyp D null mitochondria (12, 15). While this work supports the hypothesis that Cyp D regulates the MPTP, it is important to point out that new reservations have been raised concerning the significance of the VDAC-ANT-Cyp D interaction in MPTP regulation (13, 17, 34, 39). For example, the ANT-Cyp D interaction has only been shown using *in vitro* systems with detergent extracts of mitochondria and following ANT purification (76). Moreover, ANT null mitochondria display CsA-sensitive MPTP (49) and VDAC may be not required for MPTP opening (13). Also, studies show that the absence of Cyp D does not exclude Ca^{2+}-mediated MPTP induction but simply increases the amount of Ca^{2+} needed to

open the pore (49). Our data shows that while CsA treatment increases

mitochondria Ca^{2+} retention capacity, it does not block pore formation, but merely

delays onset of MPTP in both control and ethanol mitochondria (Figure 7 B and

D). Recent studies also suggest additional regulatory interactions of Cyp D with

the inorganic phosphate carrier (54), an Hsp90-TRAP-1 complex (45), and a

GSK-3-ERK complex (70) in mitochondria, with all these interactions having

possible implications for MPTP regulation. Lastly, some models even suggest

that it is the isomerase activity of Cyp D facilitating a conformational change in an

unknown inner membrane protein that is responsible for sensitizing pore

opening; however, this protein has not been identified (39). While these studies

do not exclude the involvement Cyp D in the MPTP, they do highlight an

emerging complexity of the mitochondrial effects of Cyp D, which are

independent of the MPTP. Thus, the role of Cyp D in mitochondrial Ca^{2+}

metabolism and MPTP regulation should be assumed to go beyond the classic

VDAC-ANT-Cyp D interaction model.

This intricacy in mitochondrial physiology is further highlighted by studies

showing that Cyp D may also play a role as a redox sensor in the mitochondrion.

Linard et al. (56) showed that oxidation of human Cyp D influences its

conformation and activity. Using site-directed mutagenesis, it was shown that

Cys^{157} and Cys^{203} influence the redox conformation of Cyp D through the

formation of an intra-molecular disulfide bridge. Whereas the reduced enzyme

functions as a chaperone; i.e., refolding proteins after import into the

mitochondrion, the oxidized enzyme may participate in the activation of cell death

pathways through MPTP induction. Whether these redox sensor characteristics of Cyp D contribute to the increased vulnerability to undergo MPT in response to chronic ethanol consumption is not known and will be the focus of future studies.

In considering these alcohol-dependent changes in the MPTP machinery, it is important to also evaluate whether chronic alcohol consumption affects levels of other proteins involved in controlling mitochondrial function and cell death/survival pathways. For example, pro-apoptotic proteins, including Bax, are responsible for the permeabilization of the mitochondrial outer membrane (i.e., MOMP), whereas anti-apoptotic proteins, including Bcl-2 and Bcl-x_L preserve mitochondrial integrity and prevent release of cytochrome c (5). The pro-apoptotic protein Bax is a cytosolic protein that translocates to the mitochondrion during apoptosis (5). After activation, Bax inserts into the outer mitochondrial membrane and forms larger oligomeric structures that may potentiate the MPTP (5, 61). Whereas we observed no change in total levels of Bax protein in the cytosol, we did see a significant increase in Bax in the mitochondrial compartment from ethanol-fed animals compared to controls. It is predicted that the alcohol-dependent increase in mitochondrial Bax may contribute to the defect in Ca^{2+} handling through interactions with the MPTP and/or other membrane components. In addition, Bax may directly affect respiratory chain function (66, 73). For example, activation of the Bax pathway alters intracellular pH causing matrix alkalinization and cytosolic acidification, which could disrupt mitochondrial respiration or ATP synthase activity (5). Moreover, when Bax was expressed in respiration-competent yeast strains mitochondrial oxygen consumption was

decreased, suggesting that Bax may directly inhibit respiratory complex activities
(42). Our data presented herein also show decreased respiration in isolated liver
mitochondria from ethanol-fed animals that contain increased Bax protein in the
mitochondrial compartment. While preliminary, these results suggest that, in
addition to aiding in membrane permeabilization and disruption in mitochondrial
Ca^{2+} handling, the mitochondrial localization of Bax may have directs effects on
the individual respiratory complexes, interfering with respiration and/or ATP
production in mitochondria from chronic ethanol-exposed animals.

Important to this, is also the concept that the balance between pro- and
anti-apoptotic proteins can determine cell fate. In contrast to Bax, the Bcl-2
family proteins, Bcl-2 and Bcl-x_L, inhibit cell death, depending upon the
intracellular location of these proteins. For example, Bcl-2 is located on the
cytoplasmic face of the outer mitochondrial membrane where it is proposed to
prevent the release of pro-apoptotic proteins (52, 79). Studies show that Bcl-2
over-expression can affect mitochondrial-mediated cell death by preventing
oxidative stress and inhibiting the release of pro-apoptotic mitochondrial inter-
membrane proteins (52). One protein regulated by the Bcl-2 family proteins is
cytochrome *c*, a peripheral protein of the inner mitochondrial membrane that
functions as an electron shuttle between complexes III and IV of the electron
transport chain. Upon an apoptotic stimulus, cytochrome *c* can be released from
mitochondria into the cytosol where it mediates activation and oligomerization of
the adaptor molecule apoptosis-protease activating factor 1 (Apaf-1) forming the
apoptosome and initiating apoptosis (33). Consistent with the central role of the

mitochondrion in regulating apoptosis, several studies report that Bcl-2 prevents cytochrome *c* release (48, 79). In the current study, we observed increased mitochondrial Bcl-2 protein in mitochondria from ethanol-treated animals compared to controls. This increase may reflect a compensatory response to lessen apoptosis induced by chronic ethanol consumption. In addition, cells that over-express Bcl-x_L do not accumulate cytosolic cytochrome *c* during apoptosis as cytochrome *c* can be sequestered by binding to Bcl-x_L (47). Interestingly, Cyp D over-expression may also decrease cytochrome *c* release from mitochondria via interaction with Bcl-2; a function of Cyp D independent of it presumed role in the MPTP (31). Together, these data are important as they provide a possible explanation for why we observed no overt loss in mitochondrial cytochrome *c* in ethanol-fed groups and our inability to detect the monomeric (12-15 kDa) cytochrome *c* in cytosol from both ethanol and control groups. These data also support the idea that increased cell death (as measured by TUNEL staining) observed in livers of ethanol-fed animals may be independent of the cytochrome *c*/Apaf-1 pathway, and more likely reflect necrotic cell death due to the inability to maintain adequate ATP (8). Interestingly, studies suggest that Cyp D-dependent MPTP regulates necrotic, but not apoptotic cell death (63). Together, these findings support a model in which release of cytochrome *c* from mitochondria during ethanol-mediated stress may be limited by interaction with anti-apoptotic proteins like Bcl-2 and/or Bcl-x_L, or in response to increased Cyp D in mitochondria from ethanol-fed rats.

In conclusion, we show higher Cyp D levels in liver mitochondria following chronic ethanol consumption. One possible consequence of increased Cyp D may be dysregulation of mitochondrial Ca^{2+} handling capability and increased sensitivity for MPTP induction in response to chronic ethanol ingestion. However, as highlighted in previous sections, our understanding of the complex biologic functions of Cyp D in mitochondria is rapidly evolving and extends beyond the classic idea that Cyp D only functions via interactions with the MPTP. Thus, experimental findings involving Cyp D and its presumed role in the MPTP should be interpreted with caution, as recommended in (17, 34, 39). In the current study, we observed a significant reduction in the ability of mitochondria to retain Ca^{2+} that was matched by increased Ca^{2+}-induced swelling in liver mitochondria from chronic ethanol-fed animals compared to control groups. Moreover, we show decreased mitochondrial respiration and increased Bax protein in mitochondria in response to chronic ethanol ingestion. In total, these results are significant as they provide a more comprehensive understanding of the molecular changes that contribute to chronic ethanol-induced mitochondrial dysfunction and damage. By more easily undergoing the MPT, chronic ethanol-exposed mitochondria may instigate hepatocyte death leading to liver disease. Although the precise mechanisms responsible for the Ca^{2+} handling differences between liver mitochondria from control and ethanol groups remain to be determined, the results provided herein begin to provide a more complete explanation for the increased vulnerability of mitochondria from chronic ethanol exposure. These findings also suggest that normalization of Cyp D levels may

132

be an effective therapeutic strategy to treat diseases in which mitochondrial dysfunction is linked to pathogenesis, like that seen in alcoholic fatty liver disease.

GRANTS

DISCLOSURES

The authors have no conflicts of interest and no disclosures.

References:

1. Adachi M, Higuchi H, Miura S, Azuma T, Inokuchi S, Saito H, Kato S, and Ishii H. Bax interacts with the voltage-dependent anion channel and mediates ethanol-induced apoptosis in rat hepatocytes. *Am J Physiol Gastrointest Liver Physiol* 287: G695-705, 2004.

2. Albano E. Alcohol, oxidative stress and free radical damage. *Proc Nutr Soc* 65: 278-290, 2006.

3. Andreeva L, Heads R, and Green CJ. Cyclophilins and their possible role in the stress response. *Int J Exp Pathol* 80: 305-315, 1999.

4. Andringa KK, King AL, Eccleston HB, Mantena SK, Landar A, Jhala NC, Dickinson DA, Squadrito GL, and Bailey SM. Analysis of the liver mitochondrial proteome in response to ethanol and S-adenosylmethionine treatments: novel molecular targets of disease and hepatoprotection. *Am J Physiol Gastrointest Liver Physiol* 298: G732-745, 2010.

5. Antonsson B. Bax and other pro-apoptotic Bcl-2 family "killer-proteins" and their victim the mitochondrion. *Cell Tissue Res* 306: 347-361, 2001.

6. Armstrong JS. The role of the mitochondrial permeability transition in cell death. *Mitochondrion* 6: 225-234, 2006.

7. Bailey SM, and Cunningham CC. Acute and chronic ethanol increases reactive oxygen species generation and decreases viability in fresh, isolated rat hepatocytes. *Hepatology* 28: 1318-1326, 1998.

8. Bailey SM, and Cunningham CC. Effect of dietary fat on chronic ethanol-induced oxidative stress in hepatocytes. *Alcohol Clin Exp Res* 23: 1210-1218, 1999.

9. Bailey SM, Pietsch EC, and Cunningham CC. Ethanol stimulates the production of reactive oxygen species at mitochondrial complexes I and III. *Free Radic Biol Med* 27: 891-900, 1999.

10. Bailey SM, Robinson G, Pinner A, Chamlee L, Ulasova E, Pompilius M, Page GP, Chhieng D, Jhala N, Landar A, Kharbanda KK, Ballinger S, and Darley-Usmar V. S-adenosylmethionine prevents chronic alcohol-induced mitochondrial dysfunction in the rat liver. *Am J Physiol Gastrointest Liver Physiol* 291: G857-867, 2006.

11. Baines CP. The molecular composition of the mitochondrial permeability transition pore. *J Mol Cell Cardiol* 46: 850-857, 2009.

12.   Baines CP, Kaiser RA, Purcell NH, Blair NS, Osinska H, Hambleton MA, Brunskill EW, Sayen MR, Gottlieb RA, Dorn GW, Robbins J, and Molkentin JD. Loss of cyclophilin D reveals a critical role for mitochondrial permeability transition in cell death. *Nature* 434: 658-662, 2005.

13.   Baines CP, Kaiser RA, Sheiko T, Craigen WJ, and Molkentin JD. Voltage-dependent anion channels are dispensable for mitochondrial-dependent cell death. *Nat Cell Biol* 9: 550-555, 2007.

14.   Bambrick LL, Chandrasekaran K, Mehrabian Z, Wright C, Krueger BK, and Fiskum G. Cyclosporin A increases mitochondrial calcium uptake capacity in cortical astrocytes but not cerebellar granule neurons. *J Bioenerg Biomembr* 38: 43-47, 2006.

15.   Basso E, Fante L, Fowlkes J, Petronilli V, Forte MA, and Bernardi P. Properties of the permeability transition pore in mitochondria devoid of Cyclophilin D. *J Biol Chem* 280: 18558-18561, 2005.

16.   Bernardi P, Colonna R, Costantini P, Eriksson O, Fontaine E, Ichas F, Massari S, Nicolli A, Petronilli V, and Scorrano L. The mitochondrial permeability transition. *Biofactors* 8: 273-281, 1998.

17.   Bernardi P, Krauskopf A, Basso E, Petronilli V, Blachly-Dyson E, Di Lisa F, and Forte MA. The mitochondrial permeability transition from in vitro artifact to disease target. *FEBS J* 273: 2077-2099, 2006.

18.   Bradford MM. A rapid and sensitive method for the quantitation of microgram quantities of protein utilizing the principle of protein-dye binding. *Anal Biochem* 72: 248-254, 1976.

19.   Broekemeier KM, Dempsey ME, and Pfeiffer DR. Cyclosporin A is a potent inhibitor of the inner membrane permeability transition in liver mitochondria. *J Biol Chem* 264: 7826-7830, 1989.

20.   Brookes PS, Yoon Y, Robotham JL, Anders MW, and Sheu SS. Calcium, ATP, and ROS: a mitochondrial love-hate triangle. *Am J Physiol Cell Physiol* 287: C817-833, 2004.

21.   Camello-Almaraz C, Gomez-Pinilla PJ, Pozo MJ, and Camello PJ. Mitochondrial reactive oxygen species and Ca2+ signaling. *Am J Physiol Cell Physiol* 291: C1082-1088, 2006.

22.   Chalmers S, and Nicholls DG. The relationship between free and total calcium concentrations in the matrix of liver and brain mitochondria. *J Biol Chem* 278: 19062-19070, 2003.

23. Coleman WB, Cahill A, Ivester P, and Cunningham CC. Differential effects of ethanol consumption on synthesis of cytoplasmic and mitochondrial encoded subunits of the ATP synthase. *Alcohol Clin Exp Res* 18: 947-950, 1994.

24. Coleman WB, and Cunningham CC. Effects of chronic ethanol consumption on the synthesis of polypeptides encoded by the hepatic mitochondrial genome. *Biochim Biophys Acta* 1019: 142-150, 1990.

25. Crompton M, Virji S, and Ward JM. Cyclophilin-D binds strongly to complexes of the voltage-dependent anion channel and the adenine nucleotide translocase to form the permeability transition pore. *Eur J Biochem* 258: 729-735, 1998.

26. Cunningham CC, Coleman WB, and Spach PI. The effects of chronic ethanol consumption on hepatic mitochondrial energy metabolism. *Alcohol Alcohol* 25: 127-136, 1990.

27. Cunningham CC, and Spach PI. The effect of chronic ethanol consumption on the lipids in liver mitochondria. *Ann N Y Acad Sci* 492: 181-192, 1987.

28. Dahout-Gonzalez C, Nury H, Trezeguet V, Lauquin GJ, Pebay-Peyroula E, and Brandolin G. Molecular, functional, and pathological aspects of the mitochondrial ADP/ATP carrier. *Physiology (Bethesda)* 21: 242-249, 2006.

29. Das S, Wong R, Rajapakse N, Murphy E, and Steenbergen C. Glycogen synthase kinase 3 inhibition slows mitochondrial adenine nucleotide transport and regulates voltage-dependent anion channel phosphorylation. *Circ Res* 103: 983-991, 2008.

30. Duchen MR. Mitochondria and Ca(2+)in cell physiology and pathophysiology. *Cell Calcium* 28: 339-348, 2000.

31. Eliseev RA, Malecki J, Lester T, Zhang Y, Humphrey J, and Gunter TE. Cyclophilin D interacts with Bcl2 and exerts an anti-apoptotic effect. *J Biol Chem* 284: 9692-9699, 2009.

32. Galat A. Peptidylproline cis-trans-isomerases: immunophilins. *Eur J Biochem* 216: 689-707, 1993.

33. Garrido C, Galluzzi L, Brunet M, Puig PE, Didelot C, and Kroemer G. Mechanisms of cytochrome c release from mitochondria. *Cell Death Differ* 13: 1423-1433, 2006.

34. Giorgio V, Soriano ME, Basso E, Bisetto E, Lippe G, Forte MA, and Bernardi P. Cyclophilin D in mitochondrial pathophysiology. *Biochim Biophys Acta* 2009.

35. Graier WF, Frieden M, and Malli R. Mitochondria and Ca(2+) signaling: old guests, new functions. *Pflugers Arch* 455: 375-396, 2007.

36. Gunter TE, Buntinas L, Sparagna G, Eliseev R, and Gunter K. Mitochondrial calcium transport: mechanisms and functions. *Cell Calcium* 28: 285-296, 2000.

37. Gunter TE, and Pfeiffer DR. Mechanisms by which mitochondria transport calcium. *Am J Physiol* 258: C755-786, 1990.

38. Hajnoczky G, Csordas G, Das S, Garcia-Perez C, Saotome M, Sinha Roy S, and Yi M. Mitochondrial calcium signalling and cell death: approaches for assessing the role of mitochondrial Ca2+ uptake in apoptosis. *Cell Calcium* 40: 553-560, 2006.

39. Halestrap AP. What is the mitochondrial permeability transition pore? *J Mol Cell Cardiol* 46: 821-831, 2009.

40. Halestrap AP, and Davidson AM. Inhibition of Ca2(+)-induced large-amplitude swelling of liver and heart mitochondria by cyclosporin is probably caused by the inhibitor binding to mitochondrial-matrix peptidyl-prolyl cis-trans isomerase and preventing it interacting with the adenine nucleotide translocase. *Biochem J* 268: 153-160, 1990.

41. Halestrap AP, McStay GP, and Clarke SJ. The permeability transition pore complex: another view. *Biochimie* 84: 153-166, 2002.

42. Harris MH, Vander Heiden MG, Kron SJ, and Thompson CB. Role of oxidative phosphorylation in Bax toxicity. *Mol Cell Biol* 20: 3590-3596, 2000.

43. Hewitson TD, Bisucci T, and Darby IA. Histochemical localization of apoptosis with in situ labeling of fragmented DNA. *Methods Mol Biol* 326: 227-234, 2006.

44. Jacobson J, and Duchen MR. Interplay between mitochondria and cellular calcium signalling. *Mol Cell Biochem* 256-257: 209-218, 2004.

45. Kang BH, Plescia J, Dohi T, Rosa J, Doxsey SJ, and Altieri DC. Regulation of tumor cell mitochondrial homeostasis by an organelle-specific Hsp90 chaperone network. *Cell* 131: 257-270, 2007.

46. Kanno T, Sato EE, Muranaka S, Fujita H, Fujiwara T, Utsumi T, Inoue M, and Utsumi K. Oxidative stress underlies the mechanism for Ca(2+)-induced permeability transition of mitochondria. *Free Radic Res* 38: 27-35, 2004.

47. Kharbanda S, Pandey P, Schofield L, Israels S, Roncinske R, Yoshida K, Bharti A, Yuan ZM, Saxena S, Weichselbaum R, Nalin C, and Kufe D. Role for Bcl-xL as an inhibitor of cytosolic cytochrome C accumulation in DNA damage-induced apoptosis. *Proc Natl Acad Sci U S A* 94: 6939-6942, 1997.

48. Kluck RM, Bossy-Wetzel E, Green DR, and Newmeyer DD. The release of cytochrome c from mitochondria: a primary site for Bcl-2 regulation of apoptosis. *Science* 275: 1132-1136, 1997.

49. Kokoszka JE, Waymire KG, Levy SE, Sligh JE, Cai J, Jones DP, MacGregor GR, and Wallace DC. The ADP/ATP translocator is not essential for the mitochondrial permeability transition pore. *Nature* 427: 461-465, 2004.

50. Kowaltowski AJ, Castilho RF, and Vercesi AE. Mitochondrial permeability transition and oxidative stress. *FEBS Lett* 495: 12-15, 2001.

51. Kowaltowski AJ, de Souza-Pinto NC, Castilho RF, and Vercesi AE. Mitochondria and reactive oxygen species. *Free Radic Biol Med* 47: 333-343, 2009.

52. Kowaltowski AJ, Fenton RG, and Fiskum G. Bcl-2 family proteins regulate mitochondrial reactive oxygen production and protect against oxidative stress. *Free Radic Biol Med* 37: 1845-1853, 2004.

53. Landar A, Shiva S, Levonen AL, Oh JY, Zaragoza C, Johnson MS, and Darley-Usmar VM. Induction of the permeability transition and cytochrome c release by 15-deoxy-Delta12,14-prostaglandin J2 in mitochondria. *Biochem J* 394: 185-195, 2006.

54. Leung AW, Varanyuwatana P, and Halestrap AP. The mitochondrial phosphate carrier interacts with cyclophilin D and may play a key role in the permeability transition. *J Biol Chem* 283: 26312-26323, 2008.

55. Li Y, Boehning DF, Qian T, Popov VL, and Weinman SA. Hepatitis C virus core protein increases mitochondrial ROS production by stimulation of Ca2+ uniporter activity. *FASEB J* 2007.

56. Linard D, Kandlbinder A, Degand H, Morsomme P, Dietz KJ, and Knoops B. Redox characterization of human cyclophilin D: identification of a new mammalian mitochondrial redox sensor? *Arch Biochem Biophys* 491: 39-45, 2009.

57. Ly JD, Grubb DR, and Lawen A. The mitochondrial membrane potential (deltapsi(m)) in apoptosis; an update. *Apoptosis* 8: 115-128, 2003.

58.   Mann RE, Smart RG, and Govoni R. The epidemiology of alcoholic liver disease. *Alcohol Res Health* 27: 209-219, 2003.

59.   Mantena SK, King AL, Andringa KK, Eccleston HB, and Bailey SM. Mitochondrial dysfunction and oxidative stress in the pathogenesis of alcohol- and obesity-induced fatty liver diseases. *Free Radic Biol Med* 44: 1259-1272, 2008.

60.   McStay GP, Clarke SJ, and Halestrap AP. Role of critical thiol groups on the matrix surface of the adenine nucleotide translocase in the mechanism of the mitochondrial permeability transition pore. *Biochem J* 367: 541-548, 2002.

61.   Mizuta T, Shimizu S, Matsuoka Y, Nakagawa T, and Tsujimoto Y. A Bax/Bak-independent mechanism of cytochrome c release. *J Biol Chem* 282: 16623-16630, 2007.

62.   Naga KK, Sullivan PG, and Geddes JW. High cyclophilin D content of synaptic mitochondria results in increased vulnerability to permeability transition. *J Neurosci* 27: 7469-7475, 2007.

63.   Nakagawa T, Shimizu S, Watanabe T, Yamaguchi O, Otsu K, Yamagata H, Inohara H, Kubo T, and Tsujimoto Y. Cyclophilin D-dependent mitochondrial permeability transition regulates some necrotic but not apoptotic cell death. *Nature* 434: 652-658, 2005.

64.   Pang Z, and Geddes JW. Mechanisms of cell death induced by the mitochondrial toxin 3-nitropropionic acid: acute excitotoxic necrosis and delayed apoptosis. *J Neurosci* 17: 3064-3073, 1997.

65.   Pastorino JG, Marcineviciute A, Cahill A, and Hoek JB. Potentiation by chronic ethanol treatment of the mitochondrial permeability transition. *Biochem Biophys Res Commun* 265: 405-409, 1999.

66.   Perier C, Tieu K, Guegan C, Caspersen C, Jackson-Lewis V, Carelli V, Martinuzzi A, Hirano M, Przedborski S, and Vila M. Complex I deficiency primes Bax-dependent neuronal apoptosis through mitochondrial oxidative damage. *Proc Natl Acad Sci U S A* 102: 19126-19131, 2005.

67.   Petrosillo G, Ruggiero FM, Pistolese M, and Paradies G. Ca2+-induced reactive oxygen species production promotes cytochrome c release from rat liver mitochondria via mitochondrial permeability transition (MPT)-dependent and MPT-independent mechanisms: role of cardiolipin. *J Biol Chem* 279: 53103-53108, 2004.

68.   Pfeiffer DR, Gunter TE, Eliseev R, Broekemeier KM, and Gunter KK. Release of Ca2+ from mitochondria via the saturable mechanisms and the permeability transition. *IUBMB Life* 52: 205-212, 2001.

69. Rasola A, and Bernardi P. The mitochondrial permeability transition pore and its involvement in cell death and in disease pathogenesis. *Apoptosis* 12: 815-833, 2007.

70. Rasola A, Sciacovelli M, Chiara F, Pantic B, Brusilow WS, and Bernardi P. Activation of mitochondrial ERK protects cancer cells from death through inhibition of the permeability transition. *Proc Natl Acad Sci U S A* 107: 726-731.

71. Rimessi A, Giorgi C, Pinton P, and Rizzuto R. The versatility of mitochondrial calcium signals: from stimulation of cell metabolism to induction of cell death. *Biochim Biophys Acta* 1777: 808-816, 2008.

72. Takahashi A, Camacho P, Lechleiter JD, and Herman B. Measurement of intracellular calcium. *Physiol Rev* 79: 1089-1125, 1999.

73. Teles AV, Ureshino RP, Dorta DJ, Lopes GS, Hsu YT, and Smaili SS. Bcl-x(L) inhibits Bax-induced alterations in mitochondrial respiration and calcium release. *Neurosci Lett* 442: 96-99, 2008.

74. Venkatraman A, Landar A, Davis AJ, Chamlee L, Sanderson T, Kim H, Page G, Pompilius M, Ballinger S, Darley-Usmar V, and Bailey SM. Modification of the mitochondrial proteome in response to the stress of ethanol-dependent hepatotoxicity. *J Biol Chem* 279: 22092-22101, 2004.

75. Venkatraman A, Landar A, Davis AJ, Ulasova E, Page G, Murphy MP, Darley-Usmar V, and Bailey SM. Oxidative modification of hepatic mitochondria protein thiols: effect of chronic alcohol consumption. *Am J Physiol Gastrointest Liver Physiol* 286: G521-527, 2004.

76. Woodfield K, Ruck A, Brdiczka D, and Halestrap AP. Direct demonstration of a specific interaction between cyclophilin-D and the adenine nucleotide translocase confirms their role in the mitochondrial permeability transition. *Biochem J* 336 (Pt 2): 287-290, 1998.

77. Yan M, Zhu P, Liu HM, Zhang HT, and Liu L. Ethanol induced mitochondria injury and permeability transition pore opening: role of mitochondria in alcoholic liver disease. *World J Gastroenterol* 13: 2352-2356, 2007.

78. Yan Y, Wei CL, Zhang WR, Cheng HP, and Liu J. Cross-talk between calcium and reactive oxygen species signaling. *Acta Pharmacol Sin* 27: 821-826, 2006.

79.   Yang J, Liu X, Bhalla K, Kim CN, Ibrado AM, Cai J, Peng TI, Jones DP, and Wang X. Prevention of apoptosis by Bcl-2: release of cytochrome c from mitochondria blocked. *Science* 275: 1129-1132, 1997.

80.   Zoratti M, and Szabo I. The mitochondrial permeability transition. *Biochim Biophys Acta* 1241: 139-176, 1995.

CHAPTER 4

CYCLOPHILIN D GENE ABLATION IS NOT PROTECTIVE AGAINST
MITOCHONDRIAL DYSFUNCTION IN ALCOHOL LIVER DISEASE

ADRIENNE L. KING[1], ZHENGKUAN MAO[1], TELISHA M. SWAIN[1], MATHIEU J.
LESORT[2], AND SHANNON M. BAILEY[1]

Departments of [1]Environmental Health Sciences and [2]Psychiatry and Behavioral
Neurobiology, Center for Free Radical Biology, University of Alabama at
Birmingham, Birmingham AL, 35294

Format adapted for dissertation

ABSTRACT

Chronic alcohol consumption increases the sensitivity for the induction of the mitochondrial permeability transition pore (MPTP). The exact composition of the pore remains elusive; however, it is thought to consist of the voltage dependent anion channel (VDAC), adenine nucleotide translocator (ANT) and cyclophilin D (Cyp D). Our recent findings show increased Cyp D gene and protein levels in liver ethanol fed rats compared to controls. Therefore, to investigate the role of Cyp D in alcohol-mediated sensitivity to MPTP induction and mitochondrial dysfunction, male wild-type (i.e., C57BL/6) and Cyp D null mice (Cyp D$^{-/-}$) mice were fed an alcohol-containing diet for 6 wk. Liver mitochondria were isolated from the four treatment groups: 1) wild-type mice fed control diet; 2) Cyp D$^{-/-}$ mice fed control diet; 3) wild-type mice fed ethanol diet; and 4) Cyp D$^{-/-}$ mice fed ethanol; and Ca^{2+}-mediated induction of the MPTP, as well as, mitochondrial respiratory function were measured. In addition, body weight, liver weight, liver to body ratio, and liver histology was assessed as indictors of alcohol-dependent liver injury. Steatosis was present in livers of both wild-type and Cyp D$^{-/-}$ mice fed the ethanol-containing diet. We saw an increased liver to body ratio in Cyp D$^{-/-}$ mice fed the ethanol-containing diet compared to Cyp D$^{-/-}$ fed the control diet and wild-type mice fed the ethanol diet. State 4 respiration (ADP-independent) was increased in liver mitochondria

143

isolated from both ethanol-fed wild-type and Cyp D$^{-/-}$ mice. Liver mitochondria

from wild-type control and ethanol-fed mice were both more sensitive to Ca^{2+}-

mediated MPTP induction than Cyp D$^{-/-}$ mice fed the ethanol diet. In addition,

liver mitochondria from ethanol-fed Cyp D$^{-/-}$ were more sensitive than control-fed

Cyp D$^{-/-}$ to Ca^{2+}-mediated MPTP induction. These findings suggest that Cyp D

gene ablation is not protective against alcohol induced mitochondrial dysfunction.

INTRODUCTION

Chronic alcohol consumption causes liver injury with some of the earliest

pathological changes observed at the level of the mitochondrion (7, 13, 21). It is

well known that chronic alcohol consumption causes alterations in the structure

and function of mitochondria, which results in the production of reactive oxygen

species (ROS) (3, 4). Mitochondria, a major intracellular source of ROS, are

recognized as a critical site in the cellular stress response induced by chronic

ethanol exposure. It is well known that chronic exposure to alcohol causes

mitochondrial DNA damage (mtDNA), inhibition of mitochondrial protein

synthesis, defects in oxidative phosphorylation, and depressed ATP synthesis (7,

14, 15, 21). Studies by Pastorino et al. (33) showed that chronic alcohol

consumption increases the sensitivity to the induction of the mitochondrial

permeability transition pore (MPTP); however, the mechanisms responsible were

not defined.

MPTP induction is defined as increased permeability of the inner

mitochondrial membrane to water and solutes. This leads to mitochondrial

membrane depolarization, swelling of the mitochondria, and rupture of the outer membrane, which indirectly participates in the release of apoptotic proteins such as cytochrome *c*. Although the precise structure of the pore is not known it is thought to consist of 3 main proteins: the voltage dependent anion channel (VDAC), adenine nucleotide translocase (ANT), and the key regulator of the MPTP, cyclophilin D (Cyp D). Recent studies in mice lacking Cyp D (gene name *ppif*, peptidylprolyl *cis-trans* isomerase f) revealed an important role for Cyp D as a key regulator of the induction of the MPTP. Baines et al. (8) reported that *ppif* null mice were protected from ischemia/reperfusion-induced cell death *in vivo*. In addition, mitochondria isolated from livers, hearts, and brains of *ppif* null mice were resistant to mitochondrial swelling and permeability transition *in vitro*. From these findings it is suggested that Cyp D dependent regulation of the MPTP may play a crucial role in cellular responses to specific stresses directly relevant to human disease, especially, those induced by calcium (Ca^{2+}) overload toxicity and oxidative stress.

As an extension of previous studies (33), we observed an alcohol-dependent increase in Cyp D at both the gene and protein level in liver whereas VDAC and ANT were unchanged by chronic alcohol feeding (25). This finding suggests that increased Cyp D levels could predispose liver mitochondria to increased probability to undergo MPTP formation and opening in response to chronic ethanol exposure (25). To further examine the role of Cyp D in alcohol-mediated mitochondrial dysfunction, we examined liver mitochondrial bioenergetics and Ca^{2+}-mediated induction of the MPTP in liver mitochondria

from wild-type and Cyp D$^{-/-}$ mice fed an alcohol containing diet for a 5-6 week period. These functional experiments were complemented by ethanol-dependent changes on liver weight, liver to body ratio, and histology. These studies aimed at determining alcohol-mediated alterations represent an appealing approach to interrogate molecular events responsible for alcohol toxicity.

MATERIALS AND METHODS

Materials: All chemicals were of the highest analytical grade and purchased from Sigma (St. Louis, MO) unless otherwise noted. Lieber-DeCarli control and ethanol liquid diets were purchased from Bio-Serv (Frenchtown, NJ).

Generation and characterization of Cyclophilin D (Ppif$^{-/-}$) KO mice: Cyclophilin D null mice (Cyp D$^{-/-}$) on a C57BL/6 genetic background mice were created using homologous recombination in embryonic stem cells (10). Male chimeras were subsequently mated with black, non-agouti C57BL/6 female mice, and F1 heterozygotes were then back-crossed on to C57BL/6 genetic background with isogenic heterozygotes intercrossed to generate congenic homozygotes Cyp D$^{-/-}$ animals (10). Cyp D$^{-/-}$ pups are born at the expected mendelian frequency, revealing that Cyp D is dispensable for embryonic development and viability of adult mice (10). Further, the baseline morphology and cristae organization of heart mitochondria isolated from Cyp D$^{-/-}$ mice is unaffected compared to wild-type mice (8).

Feeding protocol: C57BL/6 (i.e., wild-type) and Cyp D$^{-/-}$ mice were housed in pairs and maintained under a 12 h light/dark cycle for the duration of the experiment. Animals were fed a standard chow diet for approximately 1 wk after procurement and weighed approximately 25 g at the start of the feeding protocol. Lieber-DeCarli nutritionally adequate liquid control and ethanol containing diets were formulated by Bio-Serv (Frenchtown, NJ). Mice were fed a 4% (w/v) ethanol diet containing 28.8% of the total daily calories as ethanol, 35% as fat, 18.2% as carbohydrate, and 18% of as protein. The control diet is an identical formulation with the ethanol calories substituted by carbohydrate (dextrin maltose). Control animals were pair-fed to their ethanol counterparts so that each pair of mice was iso-caloric. Animals were maintained on the feeding protocols for at least 31 days before experiments were begun. All animal protocols were approved by the institutional animal care and use committee, and experiments conducted in accordance with the National Institutes of Health (NIH) *Guide for the Care and Use of Laboratory Animals* (NIH Publication No. 86-23).

Mitochondria isolation and respiration measurements: Liver mitochondria were isolated by differential centrifugation techniques (17). Oxygen consumption of isolated liver mitochondria was monitored using a Clark-type oxygen electrode (Hansatech Instruments, Amesbury, MA) as discussed in (25). Respiratory capacity was assessed by measuring state 3 (ADP-dependent) and state 4 (ADP-independent) respiration using glutamate-malate as the oxidizable

substrates. The respiratory control ratio (RCR) was calculated by determining the ratio between state 3 and state 4 respiration rates.

Liver histology: Liver sections from control and ethanol-fed rats were fixed in 10% formalin, sectioned, and stained with hematoxylin-eosin for detection of steatosis (1).

Mitochondrial swelling assay: For measurements, mitochondria were re-suspended in a Ca^{2+}-depletion buffer (5 mM HEPES, 3 mM $MgCl_2$, 250 mM sucrose, pH 7.4) and centrifuged for 7 min at 10,000xg at 4ºC. The final mitochondrial protein pellet was then re-suspended in a KCl buffer (150 mM KCl, 25 mM $NaHCO_3$, 1 mM $MgCl_2$, 3 mM KH_2PO_4, and 20 mM HEPES, pH 7.4). The protein concentration was determined by the Bradford protein assay (11). Isolated mitochondria (1 mg/mL) were incubated in a KCl-based buffer (150 mM KCl, 25 mM $NaHCO_3$, 1 mM $MgCl_2$, 1 mM KH_2PO_4, and 20 mM HEPES, pH 7.4) and were energized with the oxidizable substrate glutamate-malate (1 mM). Ca^{2+} (8 nmol) was added and swelling was monitored by recording the decrease in absorbance for 1 hour and 80 minutes using a 96-well Biotek Synergy HT plate reader (Bio-Tek Instruments, Inc.). Cyclosporin A (CsA, 1 µM) was added to select samples prior to the addition of Ca^{2+} and swelling was monitored as described (18). CsA was used to demonstrate involvement of the MPTP, as CsA is an inhibitor of the MPTP (12). Inclusion of CsA allows for increased Ca^{2+} accumulation before induction of the MPTP (9).

Statistical analysis: Data represent the mean ± S.E.M. for 6-8 pairs of animals per group. The two-way analysis of variance using SPSS software and the significant differences between groups were obtained using paired Student's t-test. The level of statistical significance was set at $p<0.05$.

RESULTS

Animals and liver histology. For these experiments, mice were pair-fed a control or an ethanol-containing diet for 5-6 wk to induce steatosis and mitochondrial dysfunction (5). Histologic examination of livers clearly indicates that wild-type mice fed the control diet showed no overt pathology or steatosis (Figure 1A); whereas livers from mice fed the ethanol diet showed accumulation of macrovesicular, as well as microvesicular fat (Figure 1B). There was no overt pathology in the liver of Cyp D$^{-/-}$ mice fed the control diet (Figure 1C); however there were increased liver lipid droplets in Cyp D$^{-/-}$ mice fed the ethanol diet (Figure 1D). In addition, serum and liver triglyceride levels were measured (Figure 2). There was a significant effect of ethanol treatment on serum and liver triglyceride levels ($p<0.005$). There was a significant increase in serum triglycerides levels in wild-type mice fed the ethanol diet compared to control-wild-type (Figure 2A). In addition, there was a significant increase in serum triglycerides levels in Cyp D$^{-/-}$ mice fed the ethanol diet compared to control-fed Cyp D$^{-/-}$ mice as well as ethanol-wild-type (Figure 2A). There was significant increase in liver triglycerides levels in wild-type mice fed the ethanol diet compared to control-fed wild-type. In addition, there was a significant increase in

A.   Control-WT

B.   Ethanol-WT

C.   Control-Cyp D$^{-/-}$

D.   Ethanol-Cyp D$^{-/-}$
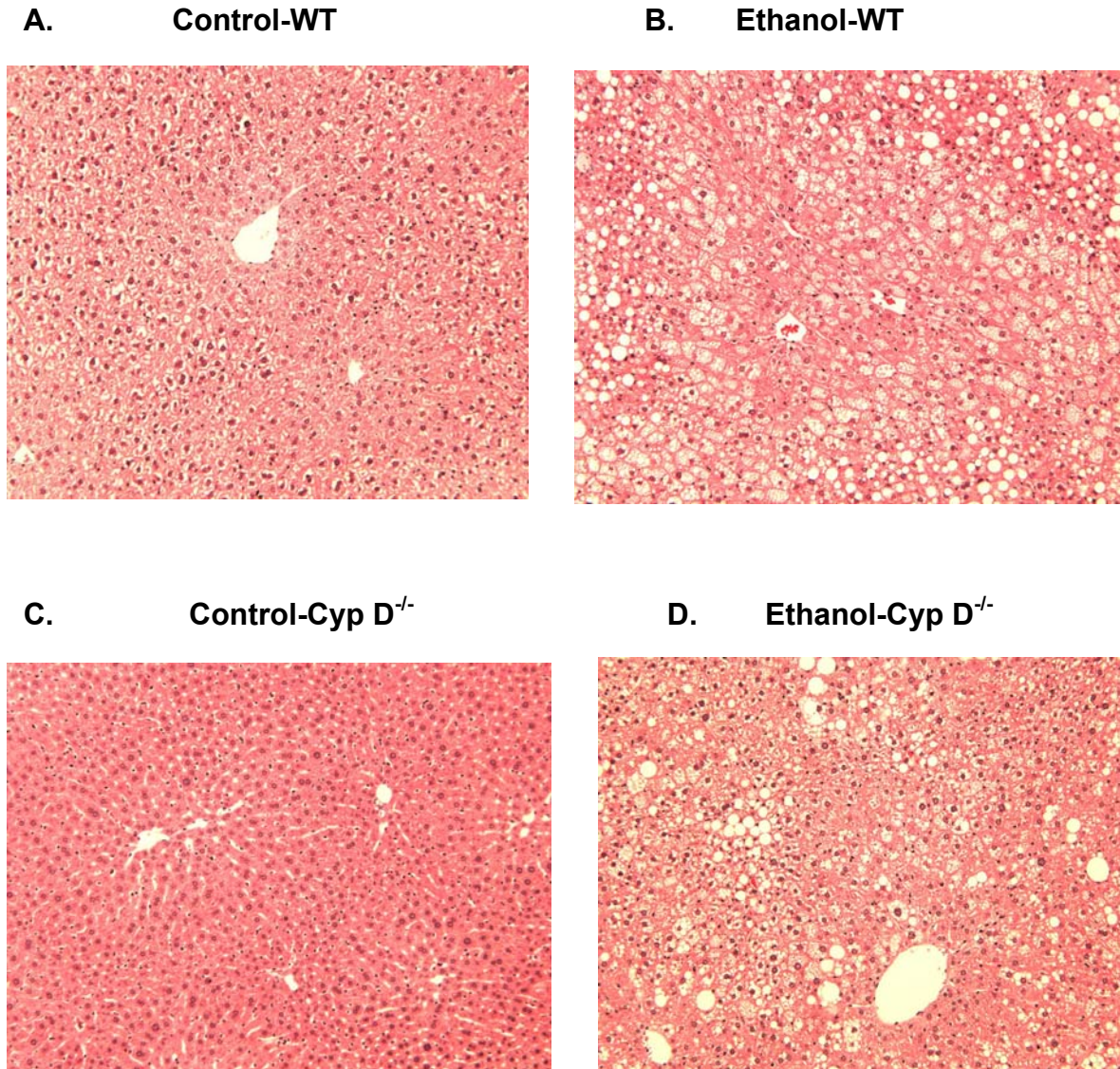
Figure 1. Chronic alcohol consumption causes steatosis in wild-type and Cyp D$^{-/-}$ mice. Liver sections were fixed in 10% buffered formalin, embedded in paraffin, sectioned, and stained with hematoxylin eosin. Panel A, liver from mice fed control diet show no pathological changes or fat deposition in hepatocytes. Panel B, liver from mice fed an ethanol-containing diet shows mild steatosis. Panel C, liver from Cyp D$^{-/-}$ mice fed a control diet show no pathological changes. Panel D, liver from Cyp D$^{-/-}$ mice fed an ethanol diet shows mild steatosis. Magnification is 20X.

A.
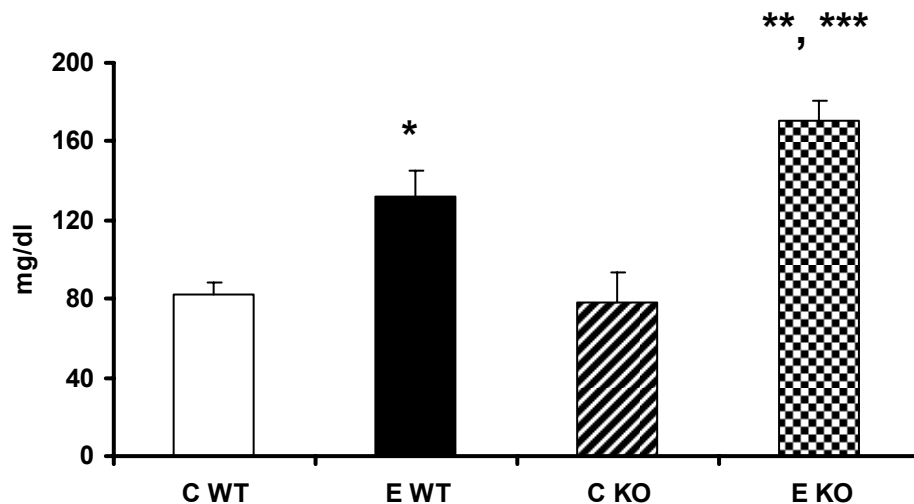
B.
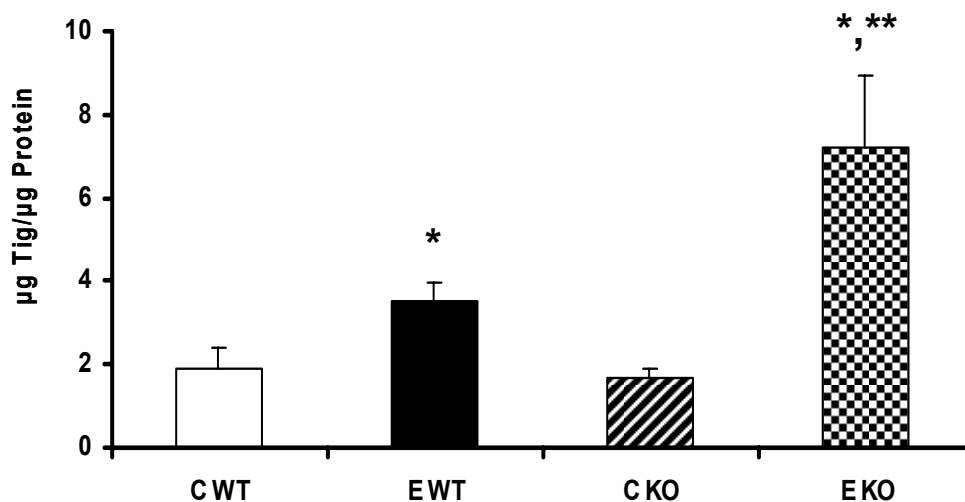
Figure 2. Ethanol increases triglyceride levels. Mice were pair-fed control (C) and ethanol (E)-containing diets for 6 weeks. (A) Ethanol exposure increased the serum triglyceride levels in ethanol-fed wild-type and ethanol-fed Cyp D$^{-/-}$ mice. 2 factor ANOVA; ethanol P = 0.000, genotype P = 0.168, and interaction (ethanol x genotype) P = 0.09. (B) Ethanol exposure increased the liver triglyceride levels in ethanol-fed wild-type and ethanol-fed Cyp D$^{-/-}$ mice. 2 factor ANOVA; ethanol P = 0.001, genotype P = 0.08, and interaction (ethanol x genotype) P = 0.06. Data represent the mean ± SEM for 6-8 mice per group. *p<0.05, compared to C WT; **p<0.05, compared to E WT; ***p<0.05, compared to C KO.

A.
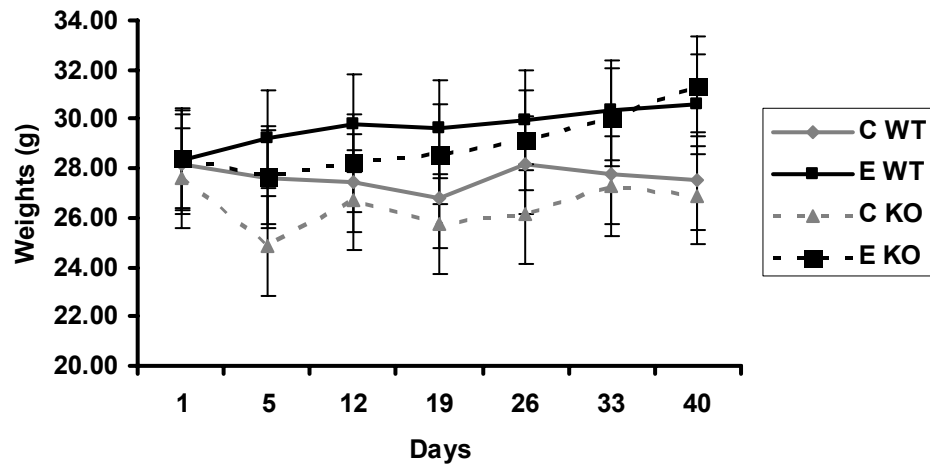
B.
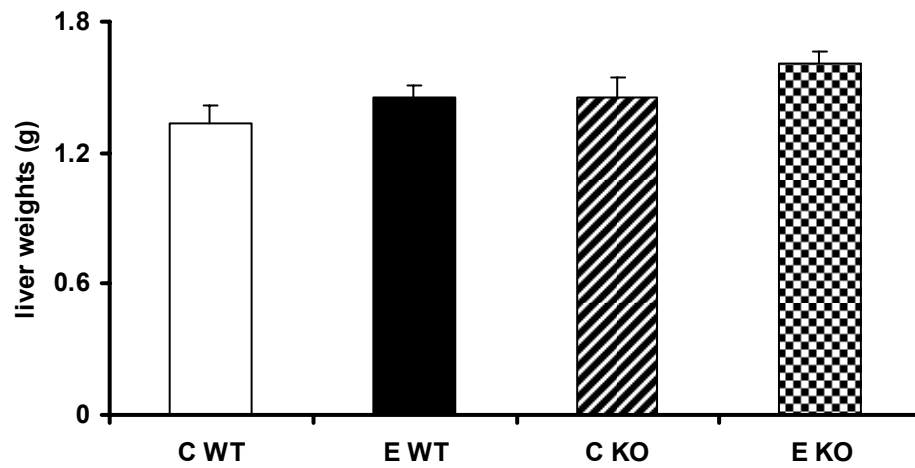
C.
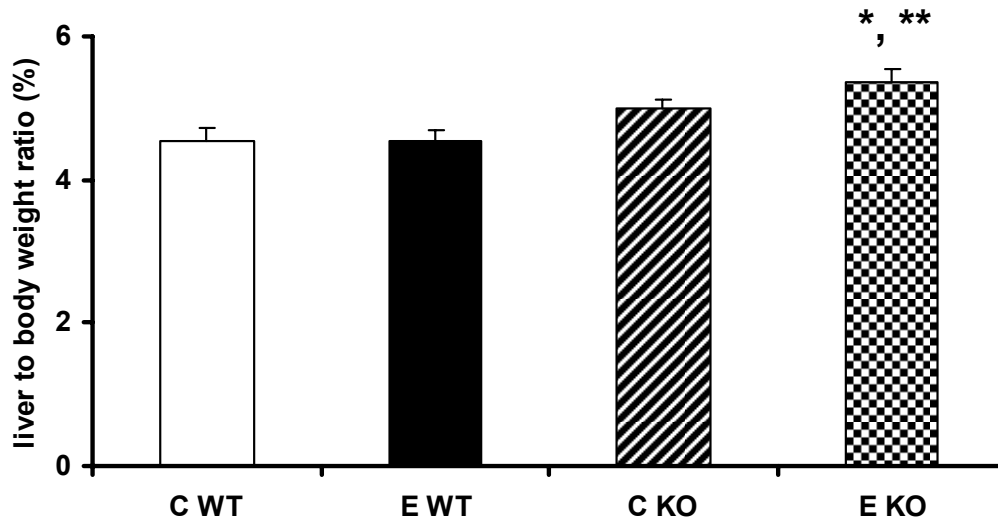
Figure 3. **Ethanol increases liver and liver/body weight ratio.** Mice were pair-fed control (C) and ethanol (E)-containing diets for 6 weeks. (A) Ethanol fed animals weighed more than control fed animals. (B) Ethanol exposure increased the liver weight. 2 factor ANOVA; ethanol $P = 0.08$, genotype $P = 0.08$, and interaction (ethanol x genotype) $P = 0.80$. (C) Ethanol increased the liver/body weight ratio. 2 factor ANOVA; ethanol $P = 0.25$, genotype $P = 0.001$, and interaction (ethanol x genotype) $P = 0.25$. Data represent the mean ± SEM for 6-8 mice per group. *$p<0.05$, compared to E WT; **$p<0.05$, compared to C KO.

liver triglycerides levels in Cyp D$^{-/-}$ mice fed the ethanol diet compared to control-fed Cyp D$^{-/-}$ mice (Figure 2B).

In addition the body weight, liver weight, and liver to body ratio were measured in all groups. At the beginning of the study, all mice weighed approximately 28 g.   There was no difference in ethanol consumption between wild-type and Cyp D$^{-/-}$ mice (p=0.46). The genotype had a significant effect on the liver to body ratio (p < 0.005). Moreover, there was a significant increase in liver to body ratio in the Cyp D$^{-/-}$ mice fed the ethanol diet compared to ethanol-fed wild-type and control- fed Cyp D$^{-/-}$ mice (Figure 3C).

Chronic ethanol consumption decreases mitochondrial respiratory function.
Mitochondria from wild-type and Cyp D$^{-/-}$ mice fed control and ethanol-containing diets were incubated in the presence of glutamate-malate and ADP to initiate State 3 respiration. Figure 4A shows typical respiration results from mitochondria isolated from wild-type and Cyp D$^{-/-}$ mice fed control and ethanol-containing diets. As shown in Figure 4B, state 3 respiration was unaffected by ethanol consumption in the wild-type and Cyp D$^{-/-}$ mice. There was a significant effect of ethanol treatment on state 4 respiration and RCR (p < 0.001). Moreover, there was a significant increase in state 4 respiration (i.e. respiration in the absence of ADP) in mitochondria from the liver of ethanol-fed wild-type compared to control-fed wild-type and ethanol-fed Cyp D$^{-/-}$ compared to control-fed Cyp D$^{-/-}$ (Figure 4B).   This increase in state 4 respiration indicates that mitochondria are

154

A.

B.

155
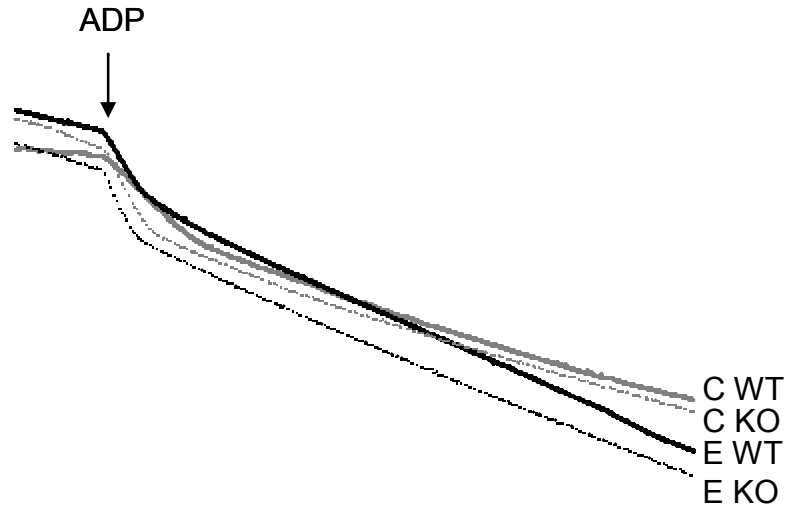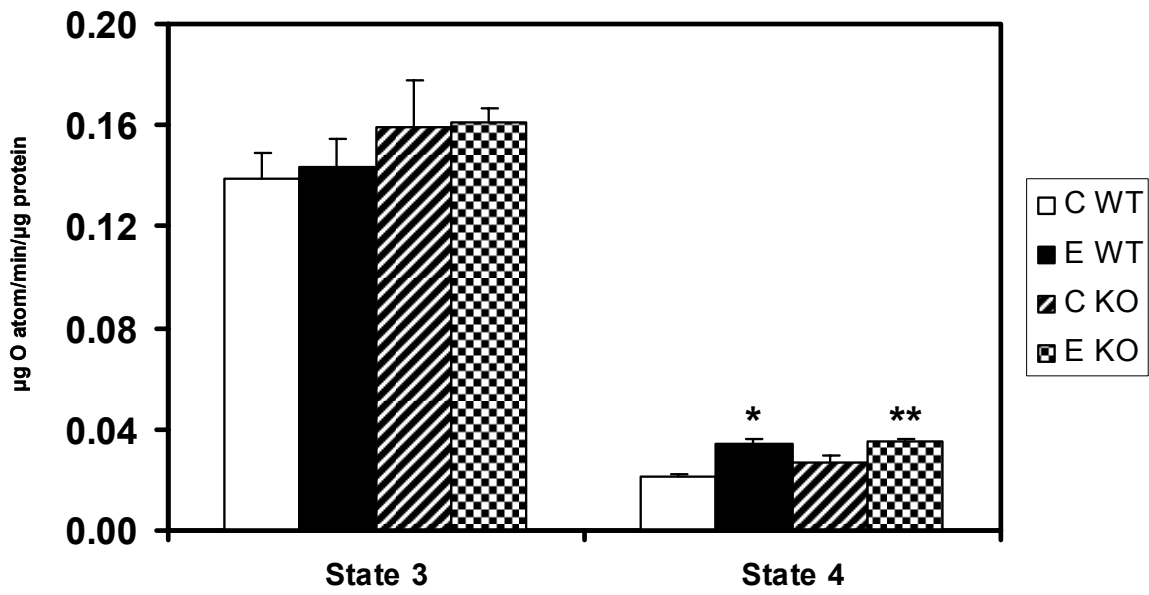
C.
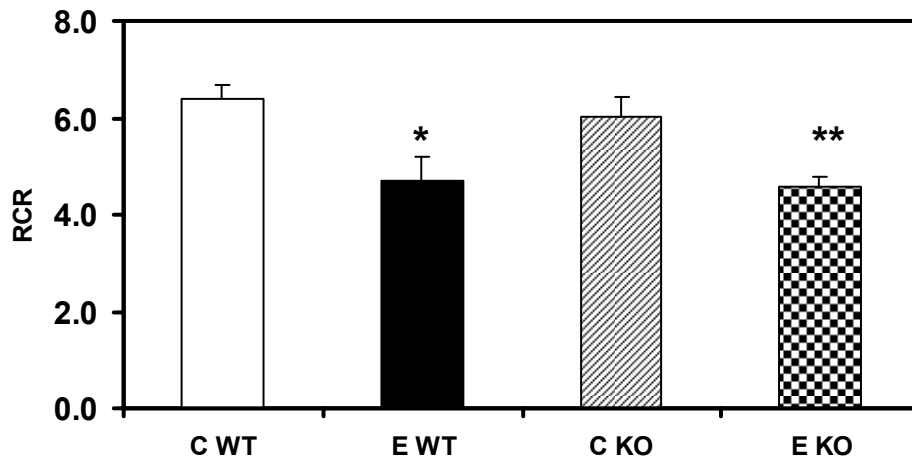
Figure 4. Chronic alcohol consumption increase state 4 respiration and decreases RCR. (A) Representative trace from oxygen consumption studies using isolated mitochondria. Oxygen consumption was determined using glutamate-malate as the oxidizable substrate. ADP was added at the arrow to initiate 3 respiration. After all ADP is converted to ATP, mitochondria enter state 4 respiration (lower rate of respiration). (B) There was no difference in state 3 respiration; whereas, there was a significant increase in state 4 respiration in mitochondria from the liver of ethanol compared to control and ethanol-KO compared to control-KO. 2 factor ANOVA for state 4; ethanol P = 0.000, genotype P = 0.16, and interaction (ethanol x genotype) P = 0.37. (C) The respiratory control ratio (RCR = state 3/state 4 respiration) was significantly lower in the ethanol-wt group compared to the control-wt group, as well as in the ethanol-KO compared to the control-KO. 2 factor ANOVA; ethanol P = 0.000, genotype P = 0.50, and interaction (ethanol x genotype) P = 0.76. Data are expressed as the mean ± S.E. for 6-8 pairs of mice, *p<0.05 compared to C WT, **p<0.05 compared to C KO.

uncoupled and will be less able to conserve the proton gradient generated by electron transfer. In addition, the respiratory control ratio (RCR = state3/state 4 respiration) was determined for wild-type and Cyp $D^{-/-}$ mice fed control and ethanol-containing diets. A higher RCR indicates better quality of mitochondria (i.e., more tightly coupled with better function) whereas a lower RCR indicates that mitochondria are damaged (i.e., more loosely coupled with poorer function) in response to treatment. The RCR was significantly lower in the ethanol fed-wild-type group compared to the control-fed wild-type group, as well as in the ethanol-fed Cyp $D^{-/-}$ compared to control-fed Cyp $D^{-/-}$ (Figure 4C). These data show that isolated liver mitochondria from Cyp $D^{-/-}$ mice fed an alcohol diet were not protected from alcohol-dependent impairment in respiratory function.

Mitochondria isolated from Cyp $D^{-/-}$ fed alcohol mice are not fully protected against Ca^{2+}-induced swelling as compared to Cyp $D^{-/-}$ mice fed a control diet. To determine whether chronic alcohol consumption changes the sensitivity to induction of the MPTP, we measured mitochondrial swelling in response to Ca^{2+}; a known inducer of the MPT pore. Figure 5A shows a representative trace of freshly isolated liver mitochondria from control wild-type, control-fed Cyp $D^{-/-}$, ethanol wild-type, and ethanol-Cyp $D^{-/-}$ fed mice incubated with 8 nmol of Ca^{2+} to induce swelling and subsequently the MPT pore. Both control and ethanol

A.
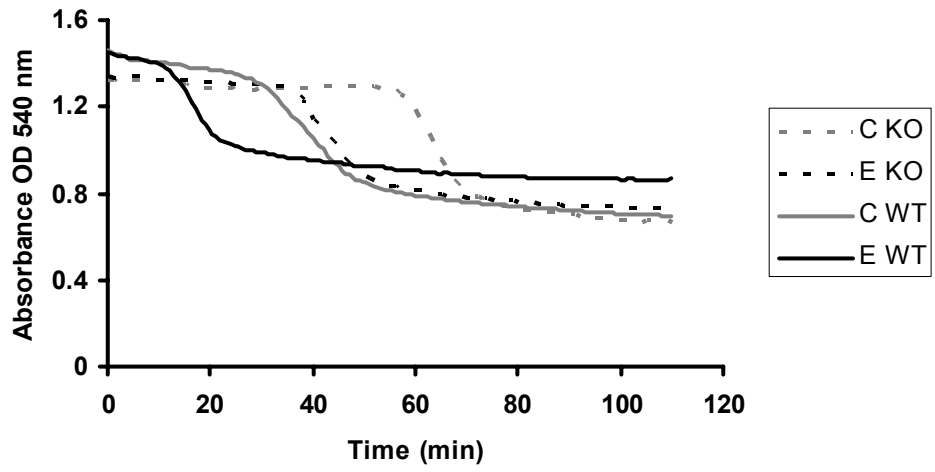
B.
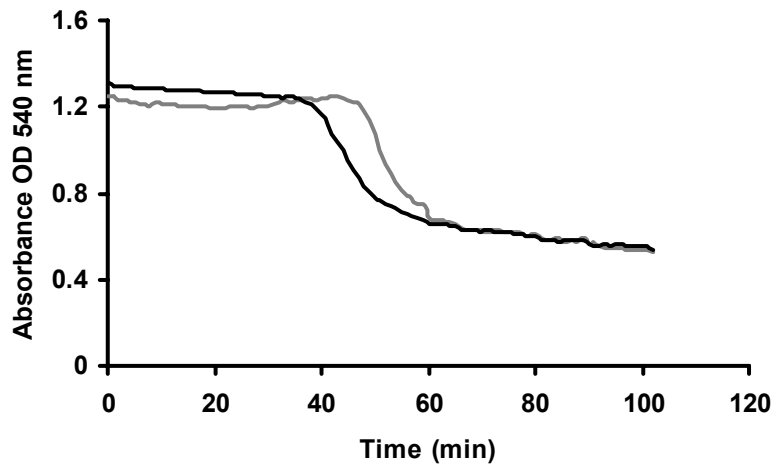
C.
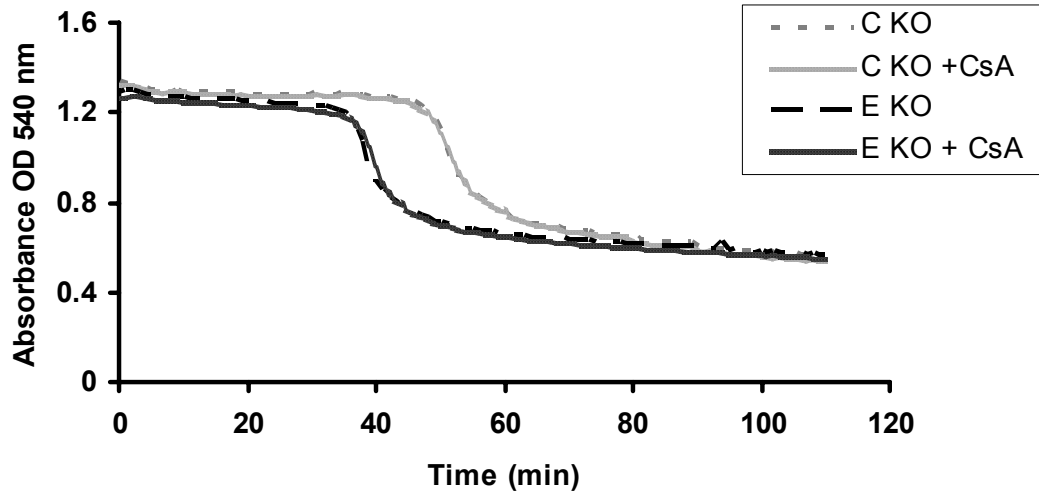
Figure 5. Chronic ethanol consumption increases sensitivity to Ca^{2+}-mediated mitochondrial swelling. Isolated mitochondria (1 mg/mL) were incubated in a KCl-based buffer (150 mM KCl, 25 mM $NaHCO_3$, 1 mM $MgCl_2$, 1 mM KH_2PO_4, and 20 mM HEPES, pH 7.4) and were energized with the oxidizable substrate glutmate and malate (1 mM). (A) Representative results of mitochondrial swelling using 8 nmol Ca^{2+} at an absorbance of 540 nm. (B) Representative results of mitochondrial swelling for control and ethanol using 40 nmol Ca^{2+} and 1 μM CsA at an absorbance of 540 nm. (C) Representative results of mitochondrial swelling for C KO, C KO + CsA, E KO and E KO + CsA using 40 nmol Ca^{2+} and 1 μM CsA at an absorbance of 540 nm. The decrease in absorbance was followed for 1hour 80 min.

mitochondria were sensitive to swelling in response to Ca^{2+} with ethanol

mitochondria being more sensitive to swelling. This data is supportive

of previous data conducted in our laboratory using a rat model (25). Notably,

mitochondria from control and ethanol-fed Cyp D$^{-/-}$ animals were more resistant

to Ca^{2+}-mediated swelling compared to mitochondria from control-wild-type and

ethanol-wild-type fed mice (Figure 5A). However, mitochondria from ethanol-fed

Cyp D$^{-/-}$ mice are still more sensitive than mitochondria from control-fed Cyp D$^{-/-}$

mice. Using 40 nmol Ca^{2+} and pretreatment with 1 μM CsA delayed Ca^{2+}-

induced swelling in both control and ethanol mitochondria (Figure 5B). However,

pretreatment with CsA in Cyp D$^{-/-}$ mice made no difference in delaying Ca^{2+}-

induced swelling indicating this is a Cyp D dependent process (Figure 5C).

DISCUSSION

Previous studies in our laboratory and many others have shown that

chronic consumption of alcohol causes steatosis in various rodent models (25).

Steatosis, also known as fatty liver disease, occurs in the beginning stage of ALD

where there is an accumulation of fat in the hepatocytes. Various mechanisms

have been proposed as to why chronic alcohol consumption leads to fat

accumulation. Excess fat could result from all, some, or a combination of the

following: increased fatty acid synthesis; decreased fatty acid synthesis;

increased transport of fatty acids from peripheral organs to the liver; blunted

transport of fatty acids from the liver. Thus, the accumulation of fat sensitizes the

liver to other toxic agents for further injury.   In the current study, we saw an

increase in lipid droplets in the ethanol-wild-type compared to control-wild-type as well as the ethanol-fed Cyp D$^{-/-}$ compared to control-fed Cyp D$^{-/-}$ (Figure 1). Body weight, liver weight, and liver to body ratio were assessed. We observed an increase in the body weight of Cyp D$^{-/-}$ mice fed the ethanol diet compared to Cyp D$^{-/-}$ mice fed the control diet. Recently, Luvisetto et al. (30) reported an increase in body weight in Cyp D$^{-/-}$ mice as well as adult-onset obesity. White adipose tissue (WAT) accumulated subcutaneously and intraperitoneally with a large mass of WAT infiltrating the thoracic cavity in Cyp D$^{-/-}$ mice (30) with no change in brown adipose tissue. In the current study, Cyp D$^{-/-}$ mice fed the ethanol diet had a significant increase in liver to body ratio as compared to ethanol-fed wild-type and Cyp D$^{-/-}$ mice fed the control diet (Figure 3C). These findings are important because obesity and adiposity may increase alcoholic liver disease. The potential protective effect of Cyp D ablation may be nullified because of an increase in adiposity (31).

It is well documented that chronic consumption of alcohol causes mitochondrial dysfunction (2, 6, 7, 21). Specifically, our laboratory has shown using a rat model that liver mitochondria have decreased state 3 respiration with no change in state 4 respiration following chronic alcohol consumption (25). In contrast, we have also shown that chronic alcohol consumption in mice has no effect on state 3 respiration but significantly increased state 4 respiration in liver mitochondria (35). This may be due to multiple factors, including the species difference (rats vs. mice) and/or a lower dose of ethanol (28.8% of total calories) in the diet. To extend our previous work, we measured respiration in liver

161

mitochondria isolated from wild-type and Cyp D$^{-/-}$ mice fed control and ethanol containing diets. As shown in Figure 4B, state 3 respiration was unaffected by ethanol consumption in both wild-type and Cyp D$^{-/-}$ mice. However, there was a significant increase in state 4 respiration (i.e. respiration in the absence of ADP) in liver mitochondria of ethanol-fed wild-type mice compared to control-fed wild-type mice. Moreover, ethanol-fed Cyp D$^{-/-}$ mice compared to control-fed Cyp D$^{-/-}$ mice had a significant increase in state 4 respiration (Figure 4B). Previously, Basso et al. (10) reported that Cyp D$^{-/-}$ mice have basal, ADP and uncoupler-stimulated rates of respiration that were indistinguishable from those of mitochondria prepared from wild-type mice (10). These findings suggest that Cyp D does not affect energy conservation and ATP synthesis under normal conditions. Moreover, Du et al. (22) showed that isolated brain mitochondria from Cyp D$^{-/-}$ mice showed no difference in RCR compared to nontransgenic mice. Additionally, the isolated mitochondria from Cyp D$^{-/-}$ mice had similar cytochrome *c* oxidase activity and ATP levels compared to nontransgenic mice (22). Our results are similar to the previous studies showing no difference between control-fed wild-type and control-fed Cyp D$^{-/-}$ mice. Because we saw no differences in state 3 and state 4 respiration between control-fed wild-type and control-fed Cyp D$^{-/-}$, the differences that we did see are due to the effect of ethanol consumption.

Accumulating evidence demonstrates a protective role of Cyp D deletion in different disease models. Baines et al. (8) using wild-type and Cyp D$^{-/-}$ mice subjected to cardiac ischaemia/reperfusion injury, found a 40% reduction in

infarction area observed in the Cyp D$^{-/-}$ mice.   Du et al. (22) revealed that Cyp D deficient cortical mitochondria were resistant to amyloid-β protein (Aβ) toxicity which is a key protein found in the brain of Alzheimer's disease patients. In addition, mitochondria were also resistant to Ca^{2+} induced mitochondrial swelling and permeability transition (22). Moreover, Cyp D deficiency improved learning and memory in an Alzheimer's disease mouse model in which mitochondrial dysfunction has been implicated (22). However, an accurate assessment of the effect of Cyp D deletion on mitochondrial function in the context of induction of the MPTP in an alcoholic liver disease model and other liver disease is not known. Therefore, due to the increased Cyp D levels we observed in alcohol fed rats (25) we wanted to investigate the role of Cyp D in alcohol-mediated sensitivity to the MPTP induction.

In the present study, mitochondria isolated from Cyp D$^{-/-}$ mice chronically fed alcohol are more resistant to Ca^{2+}-induced swelling compared to control-fed wild-type and ethanol-fed wild-type mice. However, isolated mitochondria from Cyp D$^{-/-}$ ethanol-fed mice were not as resistant to Ca^{2+}-induced swelling as compared to control-fed Cyp D$^{-/-}$ mice (Figure 5A). These findings reveal that the loss of Cyp D did not fully protect against alcohol mediated induction of the MPTP. These results so far suggest that ethanol might be inducing or changing proteins (i.e., Bax, Bcl-2, and BNIP3) other than Cyp D levels to induce changes in mitochondrial outer membrane permeabilization and sensitivity to the MPTP.

Recently, genetic ablation of the *ppif* gene which encodes for Cyp D has demonstrated that Cyp D is responsible for the modulation of the MPTP (8).

Therefore, the ability of Cyp D to interact with various components of the MPTP is an inherent feature. Cyp D has been shown to interact with the ANT and to promote an open conformation of the MPTP, which allows for the passage of solutes up to 1.5 kDa (19, 24). In addition, it is known that Ca^{2+} strongly promotes binding of Cyp D to the ANT and may be responsible for the induction of the MPTP (34). Recently, the mitochondrial phosphate carrier (PiC), another abundant inner mitochondrial membrane has been identified as a possible player in the MPTP (28). Therefore, understanding the role of Cyp D and the interaction of different components of the MPTP will be necessary in understanding the role of the MPTP in alcoholic liver disease.

A consequence of induction of the MPTP is cell death by way of apoptosis or necrosis. The MPTP results in mitochondrial depolarization and increased ROS production, which can trigger autophagy (20). Autophagy is now well recognized as a major intracellular pathway for degrading long-lived cytoplasmic proteins and damaged organelles (20, 32). Autophagy is necessary to control the quality of proteins and organelles to maintain cellular function. However, the knockout of autophagy genes can lead to multiple cellular abnormalities and deformed mitochondria (36). Mitochondria are known to be degraded by the autophagosomal-lysosomal pathway, but the basis for individually targeted autophagy of mitochondria is not known. Dysfunctional mitochondria are selected through rounds of fission followed by selective fusion which leads to the removal of defective mitochondria by autophagy (20, 27). A study done by Carreira et al. (16) showed that cardiomyocytes isolated from Cyp D$^{-/-}$ mice did

not increase autophagy in response to starvation. In addition, cardiomyocytes isolated from Cyp D over-expressing mice exhibited enhanced levels of autophagy. These data implicate Cyp D and the MPTP in the induction of autophagy. With increasing metabolic stress induced by chronic alcohol consumption, the protective process of mitophagy may not be functional in Cyp D$^{-/-}$ mice. Therefore, damaged and dysfunctional mitochondria may remain and disease ensues.

Disagreement persists as to the function of the MPTP in mediating apoptotic and or necrotic cell death. Gunter and colleagues found that Cyp D/Bcl-2 interaction is important for limiting cytochrome *c* release from mitochondria and inhibiting cytochrome *c* dependent apoptosis (23). In a previous study done in our laboratory we found increased mitochondrial Bcl-2 protein in mitochondria from ethanol-treated animals compared to controls and were unable to detect the monomeric (12-15 kDa) cytochrome *c* in cytosol from both ethanol and control groups (25). Thus, Cyp D may play a role as a survival molecule, possibly acting on targets other than the MPTP. This dual function of Cyp D could lead to a balance of its pro- and anti-apoptotic effects in animals lacking Cyp D. Baines et al. (8) reported mitochondria isolated from the livers, hearts, and brains of *ppif* null mice were resistant to mitochondrial swelling and MPTP *in vitro*. However, in the same study it was reported that Bcl-2 family member-induced cell death does not depend on Cyp D and *ppif* null fibroblasts were not protected from staurosporine or TNF-α induced cell death (8). This may be important as TNF-α is critical for alcoholic liver disease (26). These studies

concluded that the MPTP only plays a role in necrotic, rather than apoptotic, responses (29). Therefore, pro- and anti-apoptotic proteins as well as gene transcript levels in the chronic alcoholic consumption Cyp D$^{-/-}$ model must be investigated.

In conclusion, in the current study we show that wild-type and Cyp D$^{-/-}$ mice chronically fed alcohol develop steatosis, which is known to be seen in the early stages of alcoholic liver disease. In addition, we observed mitochondrial dysfunction indicated by an increase in state 4 respiration and an increase in mitochondrial swelling in Cyp D$^{-/-}$ mice chronically fed alcohol. Future studies will investigate the role of pro- and anti-apoptotic proteins in the Cyp D$^{-/-}$ model fed alcohol chronically and what implication this may have on apoptotic and or necrotic cell death. Due to the protective role of genetic ablation of Cyp D in other disease models we proposed that Cyp D$^{-/-}$ mice fed the ethanol diet would be protective. However, even though Cyp D$^{-/-}$ mice fed the ethanol diet had delayed Ca^{2+} mediated induction of the MPTP these mice were not protected against liver respiratory damage and steatosis. Further studies are needed to better identify the mechanisms that are involved in the induction of the MPTP. The potential unknown roles of Cyp D in the MPTP and other processes such autophagy in the context of alcoholic liver disease remain elusive and need further investigation.

ACKNOWLEDGMENTS

References:

1.   Andringa KK, King AL, Eccleston HB, Mantena SK, Landar A, Jhala NC, Dickinson DA, Squadrito GL, and Bailey SM. Analysis of the liver mitochondrial proteome in response to ethanol and S-adenosylmethione treatments: novel molecular targets of disease and hepatoprotection. *Am J Physiol Gastrointest Liver Physiol* 298: G732-745.

2.   Arteel GE, Iimuro Y, Yin M, Raleigh JA, and Thurman RG. Chronic enteral ethanol treatment causes hypoxia in rat liver tissue in vivo. *Hepatology* 25: 920-926, 1997.

3.   Bailey SM, and Cunningham CC. Acute and chronic ethanol increases reactive oxygen species generation and decreases viability in fresh, isolated rat hepatocytes. *Hepatology* 28: 1318-1326, 1998.

4.   Bailey SM, and Cunningham CC. Effect of dietary fat on chronic ethanol-induced oxidative stress in hepatocytes. *Alcohol Clin Exp Res* 23: 1210-1218, 1999.

5.   Bailey SM, Mantena SK, Millender-Swain T, Cakir Y, Jhala NC, Chhieng D, Pinkerton KE, and Ballinger SW. Ethanol and tobacco smoke increase hepatic steatosis and hypoxia in the hypercholesterolemic apoE(-/-) mouse: implications for a "multihit" hypothesis of fatty liver disease. *Free Radic Biol Med* 46: 928-938, 2009.

6.   Bailey SM, Pietsch EC, and Cunningham CC. Ethanol stimulates the production of reactive oxygen species at mitochondrial complexes I and III. *Free Radic Biol Med* 27: 891-900, 1999.

7.   Bailey SM, Robinson G, Pinner A, Chamlee L, Ulasova E, Pompilius M, Page GP, Chhieng D, Jhala N, Landar A, Kharbanda KK, Ballinger S, and Darley-Usmar V. S-adenosylmethionine prevents chronic alcohol-induced mitochondrial dysfunction in the rat liver. *Am J Physiol Gastrointest Liver Physiol* 291: G857-867, 2006.

8.   Baines CP, Kaiser RA, Purcell NH, Blair NS, Osinska H, Hambleton MA, Brunskill EW, Sayen MR, Gottlieb RA, Dorn GW, Robbins J, and Molkentin JD. Loss of cyclophilin D reveals a critical role for mitochondrial permeability transition in cell death. *Nature* 434: 658-662, 2005.

9.   Bambrick LL, Chandrasekaran K, Mehrabian Z, Wright C, Krueger BK, and Fiskum G. Cyclosporin A increases mitochondrial calcium uptake capacity in cortical astrocytes but not cerebellar granule neurons. *J Bioenerg Biomembr* 38: 43-47, 2006.

10.   Basso E, Fante L, Fowlkes J, Petronilli V, Forte MA, and Bernardi P. Properties of the permeability transition pore in mitochondria devoid of Cyclophilin D. *J Biol Chem* 280: 18558-18561, 2005.

11.   Bradford MM. A rapid and sensitive method for the quantitation of microgram quantities of protein utilizing the principle of protein-dye binding. *Anal Biochem* 72: 248-254, 1976.

12.   Broekemeier KM, Dempsey ME, and Pfeiffer DR. Cyclosporin A is a potent inhibitor of the inner membrane permeability transition in liver mitochondria. *J Biol Chem* 264: 7826-7830, 1989.

13.   Cahill A, Hershman S, Davies A, and Sykora P. Ethanol feeding enhances age-related deterioration of the rat hepatic mitochondrion. *Am J Physiol Gastrointest Liver Physiol* 289: G1115-1123, 2005.

14.   Cahill A, Stabley GJ, Wang X, and Hoek JB. Chronic ethanol consumption causes alterations in the structural integrity of mitochondrial DNA in aged rats. *Hepatology* 30: 881-888, 1999.

15.   Cahill A, Wang X, and Hoek JB. Increased oxidative damage to mitochondrial DNA following chronic ethanol consumption. *Biochem Biophys Res Commun* 235: 286-290, 1997.

16.   Carreira RS, Lee Y, Ghochani M, Gustafsson AB, and Gottlieb RA. Cyclophilin D is required for mitochondrial removal by autophagy in cardiac cells. *Autophagy* 6.

17.   Choo YS, Johnson GV, MacDonald M, Detloff PJ, and Lesort M. Mutant huntingtin directly increases susceptibility of mitochondria to the calcium-induced permeability transition and cytochrome c release. *Hum Mol Genet* 13: 1407-1420, 2004.

18.   Choo YS, Mao Z, Johnson GV, and Lesort M. Increased glutathione levels in cortical and striatal mitochondria of the R6/2 Huntington's disease mouse model. *Neurosci Lett* 386: 63-68, 2005.

19.   Crompton M, Virji S, and Ward JM. Cyclophilin-D binds strongly to complexes of the voltage-dependent anion channel and the adenine nucleotide translocase to form the permeability transition pore. *Eur J Biochem* 258: 729-735, 1998.

20.   Cuervo AM. Autophagy: in sickness and in health. *Trends Cell Biol* 14: 70-77, 2004.

21.   Cunningham CC, Coleman WB, and Spach PI. The effects of chronic ethanol consumption on hepatic mitochondrial energy metabolism. *Alcohol Alcohol* 25: 127-136, 1990.

22.   Du H, Guo L, Fang F, Chen D, Sosunov AA, McKhann GM, Yan Y, Wang C, Zhang H, Molkentin JD, Gunn-Moore FJ, Vonsattel JP, Arancio O, Chen JX, and Yan SD. Cyclophilin D deficiency attenuates mitochondrial and neuronal perturbation and ameliorates learning and memory in Alzheimer's disease. *Nat Med* 14: 1097-1105, 2008.

23.   Eliseev RA, Malecki J, Lester T, Zhang Y, Humphrey J, and Gunter TE. Cyclophilin D interacts with Bcl2 and exerts an anti-apoptotic effect. *J Biol Chem* 284: 9692-9699, 2009.

24.   Halestrap AP, Kerr PM, Javadov S, and Woodfield KY. Elucidating the molecular mechanism of the permeability transition pore and its role in reperfusion injury of the heart. *Biochim Biophys Acta* 1366: 79-94, 1998.

25.   King AL, Swain TM, Dickinson DA, Lesort MJ, and Bailey SM. Chronic ethanol consumption enhances sensitivity to Ca2+-mediated opening of the mitochondrial permeability transition pore and increases cyclophilin D in liver. *Am J Physiol Gastrointest Liver Physiol*.

26.   Kono H, Enomoto N, Connor HD, Wheeler MD, Bradford BU, Rivera CA, Kadiiska MB, Mason RP, and Thurman RG. Medium-chain triglycerides inhibit free radical formation and TNF-alpha production in rats given enteral ethanol. *Am J Physiol Gastrointest Liver Physiol* 278: G467-476, 2000.

27.   Kroemer G, Galluzzi L, and Brenner C. Mitochondrial membrane permeabilization in cell death. *Physiol Rev* 87: 99-163, 2007.

28.   Leung AW, Varanyuwatana P, and Halestrap AP. The mitochondrial phosphate carrier interacts with cyclophilin D and may play a key role in the permeability transition. *J Biol Chem* 283: 26312-26323, 2008.

29.   Li Y, Johnson N, Capano M, Edwards M, and Crompton M. Cyclophilin-D promotes the mitochondrial permeability transition but has opposite effects on apoptosis and necrosis. *Biochem J* 383: 101-109, 2004.

30.   Luvisetto S, Basso E, Petronilli V, Bernardi P, and Forte M. Enhancement of anxiety, facilitation of avoidance behavior, and occurrence of adult-onset obesity in mice lacking mitochondrial cyclophilin D. *Neuroscience* 155: 585-596, 2008.

31.   Mandal P, Pritchard MT, and Nagy LE. Anti-inflammatory pathways and alcoholic liver disease: role of an adiponectin/interleukin-10/heme oxygenase-1 pathway. *World J Gastroenterol* 16: 1330-1336.

32.   Mizushima N, Ohsumi Y, and Yoshimori T. Autophagosome formation in mammalian cells. *Cell Struct Funct* 27: 421-429, 2002.

33.   Pastorino JG, Marcineviciute A, Cahill A, and Hoek JB. Potentiation by chronic ethanol treatment of the mitochondrial permeability transition. *Biochem Biophys Res Commun* 265: 405-409, 1999.

34.   Petrosillo G, Ruggiero FM, Pistolese M, and Paradies G. Ca2+-induced reactive oxygen species production promotes cytochrome c release from rat liver mitochondria via mitochondrial permeability transition (MPT)-dependent and MPT-independent mechanisms: role of cardiolipin. *J Biol Chem* 279: 53103-53108, 2004.

35.   Venkatraman A, Shiva S, Wigley A, Ulasova E, Chhieng D, Bailey SM, and Darley-Usmar VM. The role of iNOS in alcohol-dependent hepatotoxicity and mitochondrial dysfunction in mice. *Hepatology* 40: 565-573, 2004.

36.   Yamamoto A, Cremona ML, and Rothman JE. Autophagy-mediated clearance of huntingtin aggregates triggered by the insulin-signaling pathway. *J Cell Biol* 172: 719-731, 2006.

CHAPTER 5

CONCLUSIONS AND FUTURE WORK

Alcoholic liver disease is a serious health problem in the United States (1, 102).   Chronic alcohol consumption causes injury to the liver and other tissues, but despite years of intensive study there are no FDA approved therapies for the treatment of alcoholic liver disease. There is considerable evidence that alcohol consumption enhances oxidative stress and the mitochondrion is recognized as a site critical in the cellular stress response induced by chronic alcohol exposure (11, 13, 14, 29, 44, 134). Key functions of the mitochondrion in healthy cells are: 1) production of ATP to support the normal cell metabolism and 2) controlled generation of ROS for redox sensitive signaling pathways. However, in recent years the role of mitochondria in apoptotic and necrotic cell death has become more apparent, and a major player in this process is the mitochondrial permeability transition pore (MPTP). Therefore, in this dissertation Chapter 2 and Chapter 3 provide detailed methods for assessing mitochondrial function by measuring mitochondrial bioenergetics and Ca^{2+}-mediated induction of the MPTP (i.e., Ca^{2+} accumulation and Ca^{2+}-induced swelling).

In Chapter 3, we proposed that chronic alcohol consumption causes increased Ca^{2+}-mediated mitochondrial swelling and lower Ca^{2+} retention

172

capacity.   We observed that liver mitochondria from ethanol-fed animals had increased Ca^{2+}-mediated mitochondrial swelling (Figure 3). In addition, liver mitochondria from ethanol-fed animals were not able to retain as much Ca^{2+} as mitochondria from control-fed animals before induction of the MPTP (Figure 7). Pore opening is proposed to be regulated by changes in membrane potential, increased ROS production, and possible oxidation of critical thiol groups present on the adenine nucleotide translocase (ANT) (96). Lipid peroxidation products such as malondialdehyde and 4-hydroxynonenal, which are formed as a consequence of ethanol-induced oxidative stress, can accumulate in the liver and trigger the MPTP in isolated mitochondria (74). As chronic alcohol consumption increases hepatocyte ROS production (11, 14), it is highly likely that alcohol-dependent oxidative stress promotes opening of the MPTP in liver mitochondria. In addition, studies show that ROS promote formation of the MPTP presumably through the oxidation of critical ANT thiols (100, 138).

This modification of critical thiols on the ANT is thought to play a critical role in the induction of the MPTP. The ANT has three critical thiols with cross linking between the Cys^{160} and Cys^{257} shown to increase the affinity of ANT for cyclophilin D (Cyp D). It is this binding between ANT and Cyp D that is proposed to facilitate the induction of the MPTP through inhibition of the ADP/ATP exchange reaction (77, 100). Specifically, these authors proposed that cross-linking of Cys^{160} and Cys^{257} stabilizes the 'c' conformation of the ANT, which enhances Cyp D binding to the ANT and antagonizes ADP binding. However, Costantini et al. (40) proposed that cross-linking of Cys^{57} causes the formation of

173

ANT dimers that are involved in induction of the MPTP. Inducers of the pore, such as Ca^{2+}, may also cause a conformational change in the ANT, which presumably leads to increased binding of Cyp D (90).

Cyp D binding to mitochondrial membranes is also reported to increase with oxidative stress and thereby regulate pore opening (73). Interestingly, studies show that Cyp D may also play a role as a redox sensor in the mitochondrion. Linard et al. (95) showed that oxidation of human Cyp D influences its conformation and the activity. Using site-directed mutagenesis, it was shown that Cys^{157} and Cys^{203} influence the redox conformation of Cyp D through the formation of an intra-molecular disulfide bridge. Whereas the reduced enzyme functions as a chaperone; (i.e., refolding proteins after import into the mitochondrion) the oxidized enzyme may lead to cell death via the induction of the MPTP. Whether these redox sensor characteristics of Cyp D contribute to the increased vulnerability to undergo the MPTP in response to chronic alcohol consumption are not known and require further investigation. Finally, studies report that Ca^{2+} forms a complex with cardiolipin, an inner membrane phospholipid, on the matrix side of the ANT. It is thought that the negative charges of the cardiolipin headgroups bind to the positive charges of the lysines on the ANT located on the matrix side (27). It is well known that Ca^{2+} binds to cardiolipin and this complex will compete with the lysines of the ANT to give an excess positive charge, which participates in inducing the MPTP (27, 111).

Therefore, to improve understanding of the negative impacts of chronic alcohol on liver mitochondria physiology we investigated the effects of chronic alcohol consumption on the components of the MPTP. As shown in Chapter 3, Figure 8A and 8B we did not observe a change in VDAC gene transcript or protein level. In addition, we did observe change in ANT gene transcript or protein level (Figure 8C and 8D). However, chronic alcohol consumption increased Cyp D transcript and protein levels (Figure 8E and 8F) (84). It is well known that oxidative stress is a trigger for the induction of the MPTP (16, 68, 116). Oxidative stress may modify critical thiols on the ANT which may allow for increased binding of Cyp D to the ANT (100). With the increase in Cyp D that was observed in our study (84), this may lead to the increased probability of binding to ANT and increased induction of the MPTP. Taken together, these studies provide insight on the proposed components of the MPTP and data shown in this dissertation show what effect chronic alcohol consumption has on the proteins that make up the MPTP.

A consequence of induction of the MPTP is cell death by way of apoptosis or necrosis. We investigated what effect chronic alcohol consumption would have on cell death using the TUNEL assay. Data in Chapter 3, Figure 4 show that chronic consumption of alcohol increased cell death (84). This prompted us to investigate specific pro- and anti-apoptotic proteins, which are presented in Chapter 3, Figure 6. We observed no difference in *Bax* gene expression between control and ethanol groups. There was also no difference in the cytosolic levels of Bax protein between control and ethanol groups. However, we

observed a significant increase in mitochondrial Bax protein levels in ethanol compared to control mitochondria. Lastly, we found a significant decrease in *Bcl-2* gene expression in ethanol compared to control liver, whereas the levels of Bcl-2 protein were increased in ethanol compared to control mitochondria (84).

There are many proposed theories that suggest a close functional and physical link between pro- and anti-apoptotic proteins allowing these proteins to control the MPTP. Several models have been proposed for permeabilization of the outer membrane that includes: (1) Bax forms channels itself (92, 107), (2) Bax forms channels with the VDAC or ANT, and (3) Bax triggers the opening of the MPTP. Using confocal and electron microscopy, Bax was found to form large clusters protruding out from the mitochondrial outer membrane during apoptosis (107). A co-immunoprecipitation study done by Narita et al. (106) showed Bax interacting with VDAC, which is a component of the MPTP. In addition, Bax induced mitochondrial membrane loss, swelling, and cytochrome *c* release. Bax-induced mitochondrial changes were inhibited by recombinant antiapoptotic Bcl-xL (106). Furthermore, studies done by Marzo et al. (99) showed that after mitochondrial translocation, Bax would form a pore upon interaction with ANT. These modes of Bax-mediated MPTP are not mutually exclusive and may coexist during cell death signals. Future studies should be directed at investigating the interaction of Bax with VDAC to see whether this interaction contributes to increased vulnerability to MPT in response to chronic alcohol exposure.

There is also debate over the way the anti-apoptotic members of the Bcl-2 family inhibit the MPTP. It has been shown that the over-expression of Bcl-2 in

cells or the addition of Bcl-2 to isolated mitochondria reduces the MPTP

probability (121). Moreover, recombinant Bcl-2 can inhibit the formation of pores

by purified ANT or VDAC reconstituted into artificial membranes (121).

Therefore, these data provide two possible functions of Bcl-2 proteins. Bcl-2

proteins may inhibit the pore by interacting with Bax. The other possible function

of the Bcl-2 proteins may be interacting with proteins from the MPTP such as

ANT and VDAC to inhibit the pore. In summary, mitochondrial membrane

permeabilization is the decisive event that determines cell survival or death.

Components that determine the propensity to permeabilization include pro- and

anti-apoptotic members of the Bcl-2 family as well as the proteins that make up

the MPTP and how these proteins interact with one another.

Our findings in Chapter 3 lead us further to investigate the role of Cyp D in

alcohol-mediated sensitivity to MPTP induction. Therefore, to investigate the role

of Cyp D in alcohol-mediated sensitivity to MPTP induction wild-type and Cyp D$^{-/-}$

mice were fed an alcohol-containing diet for 6 weeks and data is presented in

Chapter 4. The significant findings were that liver mitochondria of both wild-type

and Cyp D$^{-/-}$ mice fed alcohol chronically had increased state 4 respiration and

decreased RCR compared to wild-type and Cyp D$^{-/-}$ mice fed control diets (Figure

4). As presented in Chapter 4 Figure 5A, liver mitochondria from ethanol-fed

wild-type mice were more sensitive than control-fed wild-type and ethanol-fed

Cyp D$^{-/-}$ mice were more sensitive than control-fed Cyp D$^{-/-}$ mice to Ca^{2+}-mediated

MPTP opening. In addition, liver mitochondria from wild-type control-fed and

ethanol-fed mice were both more sensitive than Cyp D$^{-/-}$ mice to Ca^{2+}-mediated

177

MPTP opening. The Cyp D$^{-/-}$ mice fed a control diet were the most resistant to Ca^{2+}-mediated MPTP opening. These findings are preliminary and suggest Cyp D gene ablation may not provide complete protection against alcohol induced mitochondrial dysfunction.

Recently, studies have been shown an interaction between Cyp D and the mitochondrial phosphate carrier (PiC), which is an inner mitochondrial protein (91). Using co-immunoprecipitation studies with a specific PiC carrier antibody and GST-Cyp D pull down experiments demonstrated that the PiC binds Cyp D (91). It is will known that phosphate is an activator of the MPTP and thus the phosphate bound form of the PiC is more susceptible to the conformation change that is needed for induction of the MPTP. Therefore, understanding the role of Cyp D and the interaction of different components of the MPTP like the PiC will be necessary in understanding the role of the MPTP in alcoholic liver disease.

As mentioned, there are no FDA approved treatments for alcoholic liver disease. There are some candidate treatments such as Vitamin A, E, C, and beta-carotene, gene-based therapies agents to modify pathways of fibrosis, and insulin-sensitizing agents, PPAR agonists. Some other promising candidates include the methionine metabolites S-Adenosylmethionine (SAM) and betaine. Methionine is an essential amino acid that is primarily metabolized in the liver. The first step in methionine metabolism is the formation of SAM. This reaction helps to maintain an adequate supply of liver methionine for the synthesis of SAM. SAM is an important methyl donor that is needed for the methylation of DNA, RNA, and other proteins. In addition, SAM is a precursor for the

antioxidant glutathione. Our laboratory has shown that SAM prevents chronic alcohol induced mitochondrial dysfunction in liver and the mitochondrial proteome (4, 15). Also, preliminary data shows that SAM co-administration blocks ethanol-induced MPTP (Mantena, King, and Bailey, unpublished data). Therefore, finding therapeutic treatments such as SAM and treatments aimed at regulating the MPTP may be promising in treating alcoholic liver disease.

In summary, this dissertation has provided detailed methods for measuring mitochondrial bioenergetics, Ca^{2+}-mediated induction of the MPTP and Ca^{2+} accumulation (i.e., Ca^{2+} retention capacity) using an alcoholic liver disease animal model. The most significant findings in this body of work were that chronic consumption of alcohol: 1) increased MPTP opening; 2) decreased Ca^{2+} retention capacity; 3) increase pro-apoptotic Bax in mitochondrial membrane; and 4) possibly altered the molecular composition of the MPTP by increased Cyp D transcript and protein levels in a rat model of chronic alcohol consumption (84). There are multiple relationships that exist among factors that are affected by chronic consumption of alcohol (Figure 1). Chronic alcohol consumption can cause dysfunction of the electron transport chain, particularly resulting in increased generation of ROS causing bioenergetic stress. Oxidative stress and excess Ca^{2+} are known triggers for the induction of the MPTP (77, 112). Pore opening results in mitochondrial dysfunction with uncoupled oxidative phosphorylation and ATP hydrolysis (16, 20). These two events may be acting independently of each other or may be occurring simultaneously. A
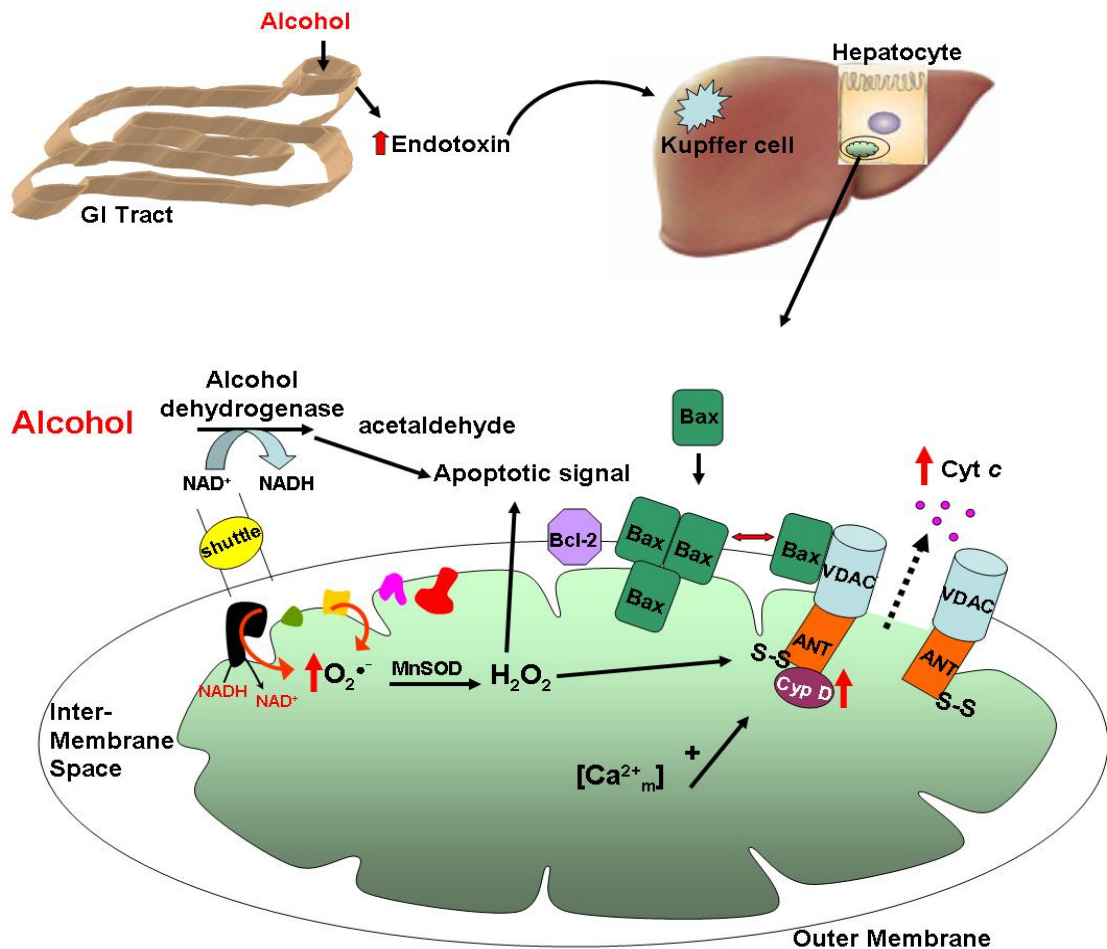
Figure 1. Proposed scheme of alcohol-dependent alterations in mitochondrial function and its impact on the mitochondrial permeability transition pore (MPTP). Chronic alcohol consumption increases gut permeability, which increases leakage of endotoxin from the gut into the hepatic portal circulation. Endotoxin travels to the liver through the portal vein where it activates Kupffer cells, the resident macrophages of the liver. Activation of Kupffer cells results in the production of a variety of soluble bio-active factors, which can damage hepatocytes. During chronic alcohol consumption, alcohol is metabolized in the cytosol of hepatocytes to acetaldehyde, which increases the

180

ratio of NADH/NAD$^+$. These excess reducing equivalents (i.e., electrons) from NADH are transported into the mitochondrion via the malate-aspartate shuttle. As a consequence of the increased flux of reducing equivalents, the redox-active components of respiratory complexes I and III will be in a more reduced state, which will facilitate the production of superoxide (O_2^-) and the subsequent production of hydrogen peroxide (H_2O_2). It is proposed that increased reactive oxygen species (ROS) production may cause the oxidation of critical vicinal thiols on the adenine nucleotide translocase (ANT). This modification of the ANT thiols is proposed to increase cyclophilin D (Cyp D) binding to the ANT, which will facilitate formation of the MPTP. These events will also increase sensitivity to calcium (Ca^{2+})-mediated activation of the MPTP. Moreover, the pro-apoptotic protein Bax is present as inactive monomers in the cytosol with the anti-apoptotic protein Bcl-2 present in the outer membrane of the mitochondrion. Increased acetaldehyde and ROS may serve as pro-apoptotic signals that are received by Bax causing Bax to become activated and translocate to the outer membrane of the mitochondion. Once Bax translocates it can form oligomers with itself or it may directly interact with the MPTP components. This will contribute to increased outer membrane permeability, release of cytochrome c (cyt c), and the initiation of cell death pathways. Note that Bcl-2 can function to inhibit the MPTP by binding to and inhibiting Bax.

consequence of induction of the MPTP is outer membrane permeabilization (7, 88). Two fundamentally different, but not mutually exclusive, mechanisms can potentially underlie outer membrane permeabilization. One mechanism is the MPTP which is accompanied by extensive colloid osmotic swelling of the matrix, leading to mechanical rupture of the outer membrane. The second mechanisminvolves the formation of large pores in the outer membrane and is directly promoted by proapoptotic members of the Bcl-2 family of proteins, such as Bax (5, 92). Our findings presented in this body of work show that alcohol alters mitochondrial function and the MPTP. These findings are significant as they provide a more comprehensive understanding of the molecular defects that contribute to chronic ethanol-induced mitochondrial dysfunction and damage.

FUTURE WORK

The findings in Chapter 4 must be complemented by additional mitochondrial functional studies. For example, isolated liver mitochondria from Cyp D$^{-/-}$ mice fed an ethanol-containing diet were not as resistant to mitochondrial swelling as compared to Cyp D$^{-/-}$ mice fed a control diet. How do these results compare to Ca^{2+} retention capacity? We would like to use the methods described in Chapter 2 to measure Ca^{2+} retention capacity in liver mitochondria isolated from four treatment groups: 1) wild-type mice fed control diet; 2) Cyp D$^{-/-}$ mice fed control diet; 3) wild-type mice fed ethanol diet; and 4) Cyp D$^{-/-}$ mice fed ethanol diet. Additional studies would include using the TUNEL assay to measure cell death in the 4 treatment groups since a consequence of

the MPTP is cell death. Moreover, studies also should include measuring pro-
and anti-apoptotic proteins as well as on the gene level.

The majority of data presented in this dissertation was carried out in
isolated mitochondria. Measurements on isolated mitochondria tell us what type
of behavior can be mediated by the mitochondria themselves, independently of
the presence of the rest of the cell. But, what happens on the cellular level? An
advantage of working on the cellular level is that mitochondrial structures and the
concentrations of components of medium around the mitochondria are more like
those *in vivo.* In addition, there are other organelles and structures at the cell
level that could show important interactions with mitochondria like the
endoplasmic reticulum. This is important as mitochondria-ER interactions are
intimately linked and involved in processes of maintaining calcium homeostasis
(66). Therefore, using primary hepatocytes from control and ethanol fed animals
would mimic the *in vivo* situation better than isolated mitochondria. Using
isolated hepatocytes, the functional capacity of mitochondria could be explored
using high resolution respirometry or the Seahorse XF24 Analyzer. In addition,
MPTP opening in intact cells could be visualized using compounds that do not
enter mitochondria unless the MPTP is open. For example, cells could be loaded
with calcein acetoxymethyl ester which does not load into mitochondria (89).
Calcein fluorescence is compartmentalized outside mitochondria and MPTP
opening could be visualized by the distribution of calcein inside mitochondria
(89). In addition, using heptaocytes from control and ethanol fed animals could
provide useful insights to the role of apoptosis and or necrosis in alcoholic liver

disease. The use of isolated mitochondria provides useful information for calculating estimates of necessary energies or effects of process that are difficult to measure directly in cells. On the other hand, the intact cell can provide important insights and modifications to data obtained from isolated mitochondria, particularly with respect to interactions with other organelles. Therefore, having information from isolated mitochondria as well as on a cellular level will advance our understanding of molecular aspects that contribute to alcoholic liver disease.

In conclusion, the factors that contribute to alcoholic liver disease are far from resolved and still remain elusive. These studies, in combination with those highlighted or reviewed here; serve to support a role of mitochondrial dysfunction in alcoholic liver disease. Continued studies into the mechanisms underlying alcoholic liver disease with an emphasis on pathophysiology will continue to allow us to consider therapeutic approaches to this important disease.

General References:

1.   Adachi M, and Brenner DA. Clinical syndromes of alcoholic liver disease. *Dig Dis* 23: 255-263, 2005.

2.   Albano E. Alcohol, oxidative stress and free radical damage. *Proc Nutr Soc* 65: 278-290, 2006.

3.   Andreeva L, Heads R, and Green CJ. Cyclophilins and their possible role in the stress response. *Int J Exp Pathol* 80: 305-315, 1999.

4.   Andringa KK, King AL, Eccleston HB, Mantena SK, Landar A, Jhala NC, Dickinson DA, Squadrito GL, and Bailey SM. Analysis of the liver mitochondrial proteome in response to ethanol and S-adenosylmethionine treatments: novel molecular targets of disease and hepatoprotection. *Am J Physiol Gastrointest Liver Physiol* 298: G732-745.

5.   Antonsson B. Bax and other pro-apoptotic Bcl-2 family "killer-proteins" and their victim the mitochondrion. *Cell Tissue Res* 306: 347-361, 2001.

6.   Arber S, Krause KH, and Caroni P. s-cyclophilin is retained intracellularly via a unique COOH-terminal sequence and colocalizes with the calcium storage protein calreticulin. *J Cell Biol* 116: 113-125, 1992.

7.   Armstrong JS. The role of the mitochondrial permeability transition in cell death. *Mitochondrion* 6: 225-234, 2006.

8.   Aronis A, Komarnitsky R, Shilo S, and Tirosh O. Membrane depolarization of isolated rat liver mitochondria attenuates permeability transition pore opening and oxidant production. *Antioxid Redox Signal* 4: 647-654, 2002.

9.   Arteel GE, Iimuro Y, Yin M, Raleigh JA, and Thurman RG. Chronic enteral ethanol treatment causes hypoxia in rat liver tissue in vivo. *Hepatology* 25: 920-926, 1997.

10.   Bailey SM. A review of the role of reactive oxygen and nitrogen species in alcohol-induced mitochondrial dysfunction. *Free Radic Res* 37: 585-596, 2003.

11.   Bailey SM, and Cunningham CC. Acute and chronic ethanol increases reactive oxygen species generation and decreases viability in fresh, isolated rat hepatocytes. *Hepatology* 28: 1318-1326, 1998.

12. Bailey SM, and Cunningham CC. Contribution of mitochondria to oxidative stress associated with alcoholic liver disease. *Free Radic Biol Med* 32: 11-16, 2002.

13. Bailey SM, Patel VB, Young TA, Asayama K, and Cunningham CC. Chronic ethanol consumption alters the glutathione/glutathione peroxidase-1 system and protein oxidation status in rat liver. *Alcohol Clin Exp Res* 25: 726-733, 2001.

14. Bailey SM, Pietsch EC, and Cunningham CC. Ethanol stimulates the production of reactive oxygen species at mitochondrial complexes I and III. *Free Radic Biol Med* 27: 891-900, 1999.

15. Bailey SM, Robinson G, Pinner A, Chamlee L, Ulasova E, Pompilius M, Page GP, Chhieng D, Jhala N, Landar A, Kharbanda KK, Ballinger S, and Darley-Usmar V. S-adenosylmethionine prevents chronic alcohol-induced mitochondrial dysfunction in the rat liver. *Am J Physiol Gastrointest Liver Physiol* 291: G857-867, 2006.

16. Baines CP. The molecular composition of the mitochondrial permeability transition pore. *J Mol Cell Cardiol* 46: 850-857, 2009.

17. Baines CP, Kaiser RA, Purcell NH, Blair NS, Osinska H, Hambleton MA, Brunskill EW, Sayen MR, Gottlieb RA, Dorn GW, Robbins J, and Molkentin JD. Loss of cyclophilin D reveals a critical role for mitochondrial permeability transition in cell death. *Nature* 434: 658-662, 2005.

18. Baines CP, Kaiser RA, Sheiko T, Craigen WJ, and Molkentin JD. Voltage-dependent anion channels are dispensable for mitochondrial-dependent cell death. *Nat Cell Biol* 9: 550-555, 2007.

19. Basso E, Fante L, Fowlkes J, Petronilli V, Forte MA, and Bernardi P. Properties of the permeability transition pore in mitochondria devoid of Cyclophilin D. *J Biol Chem* 280: 18558-18561, 2005.

20. Batandier C, Leverve X, and Fontaine E. Opening of the mitochondrial permeability transition pore induces reactive oxygen species production at the level of the respiratory chain complex I. *J Biol Chem* 279: 17197-17204, 2004.

21. Bergsma DJ, Eder C, Gross M, Kersten H, Sylvester D, Appelbaum E, Cusimano D, Livi GP, McLaughlin MM, Kasyan K, and et al. The cyclophilin multigene family of peptidyl-prolyl isomerases. Characterization of three separate human isoforms. *J Biol Chem* 266: 23204-23214, 1991.

22.   Bianchi K, Rimessi A, Prandini A, Szabadkai G, and Rizzuto R. Calcium and mitochondria: mechanisms and functions of a troubled relationship. *Biochim Biophys Acta* 1742: 119-131, 2004.

23.   Bottenus RE, Spach PI, Filus S, and Cunningham CC. Effect of chronic ethanol consumption of energy-linked processes associated with oxidative phosphorylation: proton translocation and ATP-Pi exchange. *Biochem Biophys Res Commun* 105: 1368-1373, 1982.

24.   Broekemeier KM, Dempsey ME, and Pfeiffer DR. Cyclosporin A is a potent inhibitor of the inner membrane permeability transition in liver mitochondria. *J Biol Chem* 264: 7826-7830, 1989.

25.   Brookes PS, and Darley-Usmar VM. Role of calcium and superoxide dismutase in sensitizing mitochondria to peroxynitrite-induced permeability transition. *Am J Physiol Heart Circ Physiol* 286: H39-46, 2004.

26.   Brookes PS, Salinas EP, Darley-Usmar K, Eiserich JP, Freeman BA, Darley-Usmar VM, and Anderson PG. Concentration-dependent effects of nitric oxide on mitochondrial permeability transition and cytochrome c release. *J Biol Chem* 275: 20474-20479, 2000.

27.   Brustovetsky N, and Klingenberg M. Mitochondrial ADP/ATP carrier can be reversibly converted into a large channel by Ca2+. *Biochemistry* 35: 8483-8488, 1996.

28.   Cahill A, and Cunningham CC. Effects of chronic ethanol feeding on the protein composition of mitochondrial ribosomes. *Electrophoresis* 21: 3420-3426, 2000.

29.   Cahill A, Cunningham CC, Adachi M, Ishii H, Bailey SM, Fromenty B, and Davies A. Effects of alcohol and oxidative stress on liver pathology: the role of the mitochondrion. *Alcohol Clin Exp Res* 26: 907-915, 2002.

30.   Cahill A, Hershman S, Davies A, and Sykora P. Ethanol feeding enhances age-related deterioration of the rat hepatic mitochondrion. *Am J Physiol Gastrointest Liver Physiol* 289: G1115-1123, 2005.

31.   Cahill A, Wang X, and Hoek JB. Increased oxidative damage to mitochondrial DNA following chronic ethanol consumption. *Biochem Biophys Res Commun* 235: 286-290, 1997.

32.   Capobianco L, Brandolin G, and Palmieri F. Transmembrane topography of the mitochondrial phosphate carrier explored by peptide-specific antibodies and enzymatic digestion. *Biochemistry* 30: 4963-4969, 1991.

33.   Caro AA, and Cederbaum AI. Oxidative stress, toxicology, and pharmacology of CYP2E1. *Annu Rev Pharmacol Toxicol* 44: 27-42, 2004.

34.   Carroll AK, Clevenger WR, Szabo T, Ackermann LE, Pei Y, Ghosh SS, Glasco S, Nazarbaghi R, Davis RE, and Anderson CM. Ectopic expression of the human adenine nucleotide translocase, isoform 3 (ANT-3). Characterization of ligand binding properties. *Mitochondrion* 5: 1-13, 2005.

35.   Cederbaum AI. Cytochrome P450 2E1-dependent oxidant stress and upregulation of anti-oxidant defense in liver cells. *J Gastroenterol Hepatol* 21 Suppl 3: S22-25, 2006.

36.   Cederbaum AI, Lu Y, and Wu D. Role of oxidative stress in alcohol-induced liver injury. *Arch Toxicol* 83: 519-548, 2009.

37.   Chipuk JE, and Green DR. How do BCL-2 proteins induce mitochondrial outer membrane permeabilization? *Trends Cell Biol* 18: 157-164, 2008.

38.   Coleman WB, Cahill A, Ivester P, and Cunningham CC. Differential effects of ethanol consumption on synthesis of cytoplasmic and mitochondrial encoded subunits of the ATP synthase. *Alcohol Clin Exp Res* 18: 947-950, 1994.

39.   Coleman WB, and Cunningham CC. Effect of chronic ethanol consumption on hepatic mitochondrial transcription and translation. *Biochim Biophys Acta* 1058: 178-186, 1991.

40.   Costantini P, Belzacq AS, Vieira HL, Larochette N, de Pablo MA, Zamzami N, Susin SA, Brenner C, and Kroemer G. Oxidation of a critical thiol residue of the adenine nucleotide translocator enforces Bcl-2-independent permeability transition pore opening and apoptosis. *Oncogene* 19: 307-314, 2000.

41.   Crews FT, Bechara R, Brown LA, Guidot DM, Mandrekar P, Oak S, Qin L, Szabo G, Wheeler M, and Zou J. Cytokines and alcohol. *Alcohol Clin Exp Res* 30: 720-730, 2006.

42.   Crompton M. The mitochondrial permeability transition pore and its role in cell death. *Biochem J* 341 (Pt 2): 233-249, 1999.

43.   Crompton M, Virji S, and Ward JM. Cyclophilin-D binds strongly to complexes of the voltage-dependent anion channel and the adenine nucleotide translocase to form the permeability transition pore. *Eur J Biochem* 258: 729-735, 1998.

44. Cunningham CC, Coleman WB, and Spach PI. The effects of chronic ethanol consumption on hepatic mitochondrial energy metabolism. *Alcohol Alcohol* 25: 127-136, 1990.

45. Demaurex N, Poburko D, and Frieden M. Regulation of plasma membrane calcium fluxes by mitochondria. *Biochim Biophys Acta* 1787: 1383-1394, 2009.

46. Dey A, and Cederbaum AI. Alcohol and oxidative liver injury. *Hepatology* 43: S63-74, 2006.

47. Domschke S, Domschke W, and Lieber CS. Hepatic redox state: attenuation of the acute effects of ethanol induced by chronic ethanol consumption. *Life Sci* 15: 1327-1334, 1974.

48. Du H, Guo L, Fang F, Chen D, Sosunov AA, McKhann GM, Yan Y, Wang C, Zhang H, Molkentin JD, Gunn-Moore FJ, Vonsattel JP, Arancio O, Chen JX, and Yan SD. Cyclophilin D deficiency attenuates mitochondrial and neuronal perturbation and ameliorates learning and memory in Alzheimer's disease. *Nat Med* 14: 1097-1105, 2008.

49. Duchen MR. Mitochondria and Ca(2+)in cell physiology and pathophysiology. *Cell Calcium* 28: 339-348, 2000.

50. Enomoto N, Ikejima K, Yamashina S, Hirose M, Shimizu H, Kitamura T, Takei Y, Sato, and Thurman RG. Kupffer cell sensitization by alcohol involves increased permeability to gut-derived endotoxin. *Alcohol Clin Exp Res* 25: 51S-54S, 2001.

51. Ermak G, and Davies KJ. Calcium and oxidative stress: from cell signaling to cell death. *Mol Immunol* 38: 713-721, 2002.

52. Fischer G, Bang H, and Mech C. [Determination of enzymatic catalysis for the cis-trans-isomerization of peptide binding in proline-containing peptides]. *Biomed Biochim Acta* 43: 1101-1111, 1984.

53. Fischer G, Wittmann-Liebold B, Lang K, Kiefhaber T, and Schmid FX. Cyclophilin and peptidyl-prolyl cis-trans isomerase are probably identical proteins. *Nature* 337: 476-478, 1989.

54. Freskgard PO, Bergenhem N, Jonsson BH, Svensson M, and Carlsson U. Isomerase and chaperone activity of prolyl isomerase in the folding of carbonic anhydrase. *Science* 258: 466-468, 1992.

55.	Frezza M, di Padova C, Pozzato G, Terpin M, Baraona E, and Lieber CS. High blood alcohol levels in women. The role of decreased gastric alcohol dehydrogenase activity and first-pass metabolism. *N Engl J Med* 322: 95-99, 1990.

56.	Friedman J, Trahey M, and Weissman I. Cloning and characterization of cyclophilin C-associated protein: a candidate natural cellular ligand for cyclophilin C. *Proc Natl Acad Sci U S A* 90: 6815-6819, 1993.

57.	Galat A. Peptidylproline cis-trans-isomerases: immunophilins. *Eur J Biochem* 216: 689-707, 1993.

58.	Giorgio V, Soriano ME, Basso E, Bisetto E, Lippe G, Forte MA, and Bernardi P. Cyclophilin D in mitochondrial pathophysiology. *Biochim Biophys Acta* 2009.

59.	Graier WF, Frieden M, and Malli R. Mitochondria and Ca(2+) signaling: old guests, new functions. *Pflugers Arch* 455: 375-396, 2007.

60.	Grimm S, and Brdiczka D. The permeability transition pore in cell death. *Apoptosis* 12: 841-855, 2007.

61.	Gunter TE, Buntinas L, Sparagna G, Eliseev R, and Gunter K. Mitochondrial calcium transport: mechanisms and functions. *Cell Calcium* 28: 285-296, 2000.

62.	Gunter TE, Gunter KK, Sheu SS, and Gavin CE. Mitochondrial calcium transport: physiological and pathological relevance. *Am J Physiol* 267: C313-339, 1994.

63.	Gunter TE, and Pfeiffer DR. Mechanisms by which mitochondria transport calcium. *Am J Physiol* 258: C755-786, 1990.

64.	Gunter TE, and Sheu SS. Characteristics and possible functions of mitochondrial Ca(2+) transport mechanisms. *Biochim Biophys Acta* 1787: 1291-1308, 2009.

65.	Gunter TE, Yule DI, Gunter KK, Eliseev RA, and Salter JD. Calcium and mitochondria. *FEBS Lett* 567: 96-102, 2004.

66.	Hajnoczky G, Csordas G, Das S, Garcia-Perez C, Saotome M, Sinha Roy S, and Yi M. Mitochondrial calcium signalling and cell death: approaches for assessing the role of mitochondrial Ca2+ uptake in apoptosis. *Cell Calcium* 40: 553-560, 2006.

67.   Halestrap AP. Mitochondrial permeability: dual role for the ADP/ATP translocator? *Nature* 430: 1 p following 983, 2004.

68.   Halestrap AP. What is the mitochondrial permeability transition pore? *J Mol Cell Cardiol* 46: 821-831, 2009.

69.   Halestrap AP, Clarke SJ, and Javadov SA. Mitochondrial permeability transition pore opening during myocardial reperfusion--a target for cardioprotection. *Cardiovasc Res* 61: 372-385, 2004.

70.   Halestrap AP, Connern CP, Griffiths EJ, and Kerr PM. Cyclosporin A binding to mitochondrial cyclophilin inhibits the permeability transition pore and protects hearts from ischaemia/reperfusion injury. *Mol Cell Biochem* 174: 167-172, 1997.

71.   Halestrap AP, and Davidson AM. Inhibition of Ca2(+)-induced large-amplitude swelling of liver and heart mitochondria by cyclosporin is probably caused by the inhibitor binding to mitochondrial-matrix peptidyl-prolyl cis-trans isomerase and preventing it interacting with the adenine nucleotide translocase. *Biochem J* 268: 153-160, 1990.

72.   Halestrap AP, Kerr PM, Javadov S, and Woodfield KY. Elucidating the molecular mechanism of the permeability transition pore and its role in reperfusion injury of the heart. *Biochim Biophys Acta* 1366: 79-94, 1998.

73.   He L, and Lemasters JJ. Regulated and unregulated mitochondrial permeability transition pores: a new paradigm of pore structure and function? *FEBS Lett* 512: 1-7, 2002.

74.   Hoek JB, Cahill A, and Pastorino JG. Alcohol and mitochondria: a dysfunctional relationship. *Gastroenterology* 122: 2049-2063, 2002.

75.   Hoek JB, and Pastorino JG. Ethanol, oxidative stress, and cytokine-induced liver cell injury. *Alcohol* 27: 63-68, 2002.

76.   Hoffmann K, and Handschumacher RE. Cyclophilin-40: evidence for a dimeric complex with hsp90. *Biochem J* 307 (Pt 1): 5-8, 1995.

77.   Kanno T, Sato EE, Muranaka S, Fujita H, Fujiwara T, Utsumi T, Inoue M, and Utsumi K. Oxidative stress underlies the mechanism for Ca(2+)-induced permeability transition of mitochondria. *Free Radic Res* 38: 27-35, 2004.

78.   Karaa A, Kamoun WS, and Clemens MG. Chronic ethanol sensitizes the liver to endotoxin via effects on endothelial nitric oxide synthase regulation. *Shock* 24: 447-454, 2005.

79.   Kern D, Drakenberg T, Wikstrom M, Forsen S, Bang H, and Fischer G. The cis/trans interconversion of the calcium regulating hormone calcitonin is catalyzed by cyclophilin. *FEBS Lett* 323: 198-202, 1993.

80.   Kessova IG, and Cederbaum AI. Mitochondrial alterations in livers of Sod1-/- mice fed alcohol. *Free Radic Biol Med* 42: 1470-1480, 2007.

81.   Kieffer LJ, Seng TW, Li W, Osterman DG, Handschumacher RE, and Bayney RM. Cyclophilin-40, a protein with homology to the P59 component of the steroid receptor complex. Cloning of the cDNA and further characterization. *J Biol Chem* 268: 12303-12310, 1993.

82.   Kieffer LJ, Thalhammer T, and Handschumacher RE. Isolation and characterization of a 40-kDa cyclophilin-related protein. *J Biol Chem* 267: 5503-5507, 1992.

83.   Kiessling KH, and Tobe U. Degeneration of Liver Mitochondria in Rats after Prolonged Alcohol Consumption. *Exp Cell Res* 33: 350-354, 1964.

84.   King AL, Swain TM, Dickinson DA, Lesort MJ, and Bailey SM. Chronic ethanol consumption enhances sensitivity to Ca2+-mediated opening of the mitochondrial permeability transition pore and increases cyclophilin D in liver. *Am J Physiol Gastrointest Liver Physiol*.

85.   Kluck RM, Bossy-Wetzel E, Green DR, and Newmeyer DD. The release of cytochrome c from mitochondria: a primary site for Bcl-2 regulation of apoptosis. *Science* 275: 1132-1136, 1997.

86.   Kokoszka JE, Waymire KG, Levy SE, Sligh JE, Cai J, Jones DP, MacGregor GR, and Wallace DC. The ADP/ATP translocator is not essential for the mitochondrial permeability transition pore. *Nature* 427: 461-465, 2004.

87.   Krauskopf A, Eriksson O, Craigen WJ, Forte MA, and Bernardi P. Properties of the permeability transition in VDAC1(-/-) mitochondria. *Biochim Biophys Acta* 1757: 590-595, 2006.

88.   Kroemer G, Galluzzi L, and Brenner C. Mitochondrial membrane permeabilization in cell death. *Physiol Rev* 87: 99-163, 2007.

89.   Lemasters JJ. V. Necrapoptosis and the mitochondrial permeability transition: shared pathways to necrosis and apoptosis. *Am J Physiol* 276: G1-6, 1999.

90.   Lemasters JJaA-LN. *Mitochondria in Pathogenesis.* Kluwer Academic, 2001.

91. Leung AW, Varanyuwatana P, and Halestrap AP. The mitochondrial phosphate carrier interacts with cyclophilin D and may play a key role in the permeability transition. *J Biol Chem* 283: 26312-26323, 2008.

92. Li T, Brustovetsky T, Antonsson B, and Brustovetsky N. Oligomeric BAX induces mitochondrial permeability transition and complete cytochrome c release without oxidative stress. *Biochim Biophys Acta* 2008.

93. Li Y, Boehning DF, Qian T, Popov VL, and Weinman SA. Hepatitis C virus core protein increases mitochondrial ROS production by stimulation of Ca2+ uniporter activity. *Faseb J* 2007.

94. Li Y, Johnson N, Capano M, Edwards M, and Crompton M. Cyclophilin-D promotes the mitochondrial permeability transition but has opposite effects on apoptosis and necrosis. *Biochem J* 383: 101-109, 2004.

95. Linard D, Kandlbinder A, Degand H, Morsomme P, Dietz KJ, and Knoops B. Redox characterization of human cyclophilin D: identification of a new mammalian mitochondrial redox sensor? *Arch Biochem Biophys* 491: 39-45, 2009.

96. Ly JD, Grubb DR, and Lawen A. The mitochondrial membrane potential (deltapsi(m)) in apoptosis; an update. *Apoptosis* 8: 115-128, 2003.

97. Mann RE, Smart RG, and Govoni R. The epidemiology of alcoholic liver disease. *Alcohol Res Health* 27: 209-219, 2003.

98. Mantena SK, King AL, Andringa KK, Eccleston HB, and Bailey SM. Mitochondrial dysfunction and oxidative stress in the pathogenesis of alcohol- and obesity-induced fatty liver diseases. *Free Radic Biol Med* 44: 1259-1272, 2008.

99. Marzo I, Brenner C, Zamzami N, Jurgensmeier JM, Susin SA, Vieira HL, Prevost MC, Xie Z, Matsuyama S, Reed JC, and Kroemer G. Bax and adenine nucleotide translocator cooperate in the mitochondrial control of apoptosis. *Science* 281: 2027-2031, 1998.

100. McStay GP, Clarke SJ, and Halestrap AP. Role of critical thiol groups on the matrix surface of the adenine nucleotide translocase in the mechanism of the mitochondrial permeability transition pore. *Biochem J* 367: 541-548, 2002.

101. Mizuta T, Shimizu S, Matsuoka Y, Nakagawa T, and Tsujimoto Y. A Bax/Bak-independent mechanism of cytochrome c release. *J Biol Chem* 282: 16623-16630, 2007.

102. Mokdad AH, Marks JS, Stroup DF, and Gerberding JL. Actual causes of death in the United States, 2000. *Jama* 291: 1238-1245, 2004.

103. Montgomery RI, Coleman WB, Eble KS, and Cunningham CC. Ethanol-elicited alterations in the oligomycin sensitivity and structural stability of the mitochondrial F0 . F1 ATPase. *J Biol Chem* 262: 13285-13289, 1987.

104. Nagy LE. Molecular aspects of alcohol metabolism: transcription factors involved in early ethanol-induced liver injury. *Annu Rev Nutr* 24: 55-78, 2004.

105. Nakayama N, Eichhorst ST, Muller M, and Krammer PH. Ethanol-induced apoptosis in hepatoma cells proceeds via intracellular Ca(2+) elevation, activation of TLCK-sensitive proteases, and cytochrome c release. *Exp Cell Res* 269: 202-213, 2001.

106. Narita M, Shimizu S, Ito T, Chittenden T, Lutz RJ, Matsuda H, and Tsujimoto Y. Bax interacts with the permeability transition pore to induce permeability transition and cytochrome c release in isolated mitochondria. *Proc Natl Acad Sci U S A* 95: 14681-14686, 1998.

107. Nechushtan A, Smith CL, Lamensdorf I, Yoon SH, and Youle RJ. Bax and Bak coalesce into novel mitochondria-associated clusters during apoptosis. *J Cell Biol* 153: 1265-1276, 2001.

108. Nicholls DG, and Chalmers S. The integration of mitochondrial calcium transport and storage. *J Bioenerg Biomembr* 36: 277-281, 2004.

109. Obe G, Jonas R, and Schmidt S. Metabolism of ethanol in vitro produces a compound which induces sister-chromatid exchanges in human peripheral lymphocytes in vitro: acetaldehyde not ethanol is mutagenic. *Mutat Res* 174: 47-51, 1986.

110. Pastorino JG, Marcineviciute A, Cahill A, and Hoek JB. Potentiation by chronic ethanol treatment of the mitochondrial permeability transition. *Biochem Biophys Res Commun* 265: 405-409, 1999.

111. Petrosillo G, Casanova G, Matera M, Ruggiero FM, and Paradies G. Interaction of peroxidized cardiolipin with rat-heart mitochondrial membranes: induction of permeability transition and cytochrome c release. *FEBS Lett* 580: 6311-6316, 2006.

112. Petrosillo G, Ruggiero FM, Pistolese M, and Paradies G. Ca2+-induced reactive oxygen species production promotes cytochrome c release from rat liver mitochondria via mitochondrial permeability transition (MPT)-dependent and MPT-independent mechanisms: role of cardiolipin. *J Biol Chem* 279: 53103-53108, 2004.

113. Pfeiffer DR, Gunter TE, Eliseev R, Broekemeier KM, and Gunter KK. Release of Ca2+ from mitochondria via the saturable mechanisms and the permeability transition. *IUBMB Life* 52: 205-212, 2001.

114. Price ER, Zydowsky LD, Jin MJ, Baker CH, McKeon FD, and Walsh CT. Human cyclophilin B: a second cyclophilin gene encodes a peptidyl-prolyl isomerase with a signal sequence. *Proc Natl Acad Sci U S A* 88: 1903-1907, 1991.

115. Purohit V, Russo D, and Coates PM. Role of fatty liver, dietary fatty acid supplements, and obesity in the progression of alcoholic liver disease: introduction and summary of the symposium. *Alcohol* 34: 3-8, 2004.

116. Rasola A, and Bernardi P. The mitochondrial permeability transition pore and its involvement in cell death and in disease pathogenesis. *Apoptosis* 12: 815-833, 2007.

117. Robin MA, Sauvage I, Grandperret T, Descatoire V, Pessayre D, and Fromenty B. Ethanol increases mitochondrial cytochrome P450 2E1 in mouse liver and rat hepatocytes. *FEBS Lett* 579: 6895-6902, 2005.

118. Sampson MJ, Lovell RS, and Craigen WJ. The murine voltage-dependent anion channel gene family. Conserved structure and function. *J Biol Chem* 272: 18966-18973, 1997.

119. Schonbrunner ER, Mayer S, Tropschug M, Fischer G, Takahashi N, and Schmid FX. Catalysis of protein folding by cyclophilins from different species. *J Biol Chem* 266: 3630-3635, 1991.

120. Seitz HK, and Stickel F. Risk factors and mechanisms of hepatocarcinogenesis with special emphasis on alcohol and oxidative stress. *Biol Chem* 387: 349-360, 2006.

121. Shimizu S, Eguchi Y, Kamiike W, Funahashi Y, Mignon A, Lacronique V, Matsuda H, and Tsujimoto Y. Bcl-2 prevents apoptotic mitochondrial dysfunction by regulating proton flux. *Proc Natl Acad Sci U S A* 95: 1455-1459, 1998.

122. Shinohara Y, Kamida M, Yamazaki N, and Terada H. Isolation and characterization of cDNA clones and a genomic clone encoding rat mitochondrial adenine nucleotide translocator. *Biochim Biophys Acta* 1152: 192-196, 1993.

123. Siegmund SV, Dooley S, and Brenner DA. Molecular mechanisms of alcohol-induced hepatic fibrosis. *Dig Dis* 23: 264-274, 2005.

124. Sousa SC, Maciel EN, Vercesi AE, and Castilho RF. Ca2+-induced oxidative stress in brain mitochondria treated with the respiratory chain inhibitor rotenone. *FEBS Lett* 543: 179-183, 2003.

125. Spach PI, Bottenus RE, and Cunningham CC. Control of adenine nucleotide metabolism in hepatic mitochondria from rats with ethanol-induced fatty liver. *Biochem J* 202: 445-452, 1982.

126. Spach PI, and Cunningham CC. Control of state 3 respiration in liver mitochondria from rats subjected to chronic ethanol consumption. *Biochim Biophys Acta* 894: 460-467, 1987.

127. Thayer WS, Ohnishi T, and Rubin E. Characterization of iron-sulfur clusters in rat liver submitochondrial particles by electron paramagnetic resonance spectroscopy. Alterations produced by chronic ethanol consumption. *Biochim Biophys Acta* 591: 22-36, 1980.

128. Thayer WS, and Rubin E. Effects of chronic ethanol intoxication on oxidative phosphorylation in rat liver submitochondrial particles. *J Biol Chem* 254: 7717-7723, 1979.

129. Thurman RG. II. Alcoholic liver injury involves activation of Kupffer cells by endotoxin. *Am J Physiol* 275: G605-611, 1998.

130. Tsukamoto H, Horne W, Kamimura S, Niemela O, Parkkila S, Yla-Herttuala S, and Brittenham GM. Experimental liver cirrhosis induced by alcohol and iron. *J Clin Invest* 96: 620-630, 1995.

131. Tsukamoto H, Reidelberger RD, French SW, and Largman C. Long-term cannulation model for blood sampling and intragastric infusion in the rat. *Am J Physiol* 247: R595-599, 1984.

132. Tsukamoto H, Takei Y, McClain CJ, Joshi-Barve S, Hill D, Schmidt J, Deaciuc I, Barve S, Colell A, Garcia-Ruiz C, Kaplowitz N, Fernandez-Checa JC, Yokoyama H, Okamura Y, Nakamura Y, Ishii H, Chawla RK, Watson W, Nelson W, Lin M, Ohata M, Motomura K, Enomoto N, Ikejima K, Kitamura T, Oide H, Hirose M, Bradford BU, Rivera CA, Kono H, Peter S, Yamashina S, Konno A, Ishikawa M, Shimizu H, Sato N, and Thurman R. How is the liver primed or sensitized for alcoholic liver disease? *Alcohol Clin Exp Res* 25: 171S-181S, 2001.

133. Tuma DJ, and Casey CA. Dangerous byproducts of alcohol breakdown--focus on adducts. *Alcohol Res Health* 27: 285-290, 2003.

134. Venkatraman A, Landar A, Davis AJ, Ulasova E, Page G, Murphy MP, Darley-Usmar V, and Bailey SM. Oxidative modification of hepatic mitochondria protein thiols: effect of chronic alcohol consumption. *Am J Physiol Gastrointest Liver Physiol* 286: G521-527, 2004.

135. Whitfield JB, Zhu G, Heath AC, Powell And LW, and Martin NG. Effects of alcohol consumption on indices of iron stores and of iron stores on alcohol intake markers. *Alcohol Clin Exp Res* 25: 1037-1045, 2001.

136. Wu D, and Cederbaum AI. Alcohol, oxidative stress, and free radical damage. *Alcohol Res Health* 27: 277-284, 2003.

137. Yan M, Zhu P, Liu HM, Zhang HT, and Liu L. Ethanol induced mitochondria injury and permeability transition pore opening: role of mitochondria in alcoholic liver disease. *World J Gastroenterol* 13: 2352-2356, 2007.

138. Zoratti M, and Szabo I. The mitochondrial permeability transition. *Biochim Biophys Acta* 1241: 139-176, 1995.

139. Zoratti M, Szabo I, and De Marchi U. Mitochondrial permeability transitions: how many doors to the house? *Biochim Biophys Acta* 1706: 40-52, 2005.

APPENDIX A

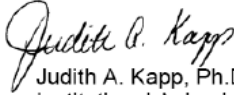**UAB** THE UNIVERSITY OF ALABAMA AT BIRMINGHAM

Institutional Animal Care and Use Committee (IACUC)

NOTICE OF APPROVAL

DATE: January 30, 2008

TO: Shannon M. Bailey, Ph.D.
Ryals-629 0022
FAX: 975-6341

FROM: *Judith A. Kapp*
Judith A. Kapp, Ph.D., Chair
Institutional Animal Care and Use Committee

SUBJECT: Title: Redox Modification of Thiols in Alcohol Hepatotoxicity
Sponsor: NIH
Animal Project Number: 080107077

On January 30, 2008, the University of Alabama at Birmingham Institutional Animal Care and Use Committee (IACUC) reviewed the animal use proposed in the above referenced application. It approved the use of the following species and numbers of animals:

Species	Use Category	Number in Category
Rats	B	70
Rats	A	70

Animal use is scheduled for review one year from January 2008. Approval from the IACUC must be obtained before implementing any changes or modifications in the approved animal use.

Please keep this record for your files, and forward the attached letter to the appropriate granting agency.

Refer to Animal Protocol Number (APN) 080107077 when ordering animals or in any correspondence with the IACUC or Animal Resources Program (ARP) offices regarding this study. If you have concerns or questions regarding this notice, please call the IACUC office at 934-7692.

Institutional Animal Care and Use Committee
B10 Volker Hall
1670 University Boulevard
205.934.7692
FAX 205.934.1188

Mailing Address:
VH B10
1530 3RD AVE S
BIRMINGHAM AL 35294-0019

APPENDIX B

Dear Adrienne,

Thank you for your request. John Wiley & Sons, Inc. has no objections to your proposed reuse of this material.

Permission is hereby granted for the use requested subject to the usual acknowledgements (author, title of material, title of book/journal, ourselves as publisher). Any third party material is expressly excluded from this permission. If any of the material you wish to use appears within our work with credit to another source, authorization from that source must be obtained. This permission does not include the right to grant others permission to photocopy or otherwise reproduce this material except for versions made by non-profit organisations for use by the blind or handicapped persons.

Sincerely,

Paulette Goldweber| Associate Manager, Permissions| Global Rights - John Wiley & Sons, Inc.
Ph: 201-748-8765 | F: 201-748-6008| pgoldweb@wiley.com

Request for Permission to Reproduce
Previously Published Material

(please save this file to your desktop, fill out, save again, and e-mail to permissions@the-aps.org)

Your Name: Adrienne L. King   E-mail: aking@ms.soph.uab.edu

Affiliation: University of Alabama at Birmingham

University Address (for PhD students): 1530 3rd Ave. South Ryals 629
Birmingham AL 35294

Description of APS material to be reproduced (check all that apply):

☑ Figure   ☐ Partial Article   ☐ Abstract
☑ Table   ☑ Full Article   ☐ Book Chapter
   Other (please describe):

Are you an author of the APS material to be reproduced?   ⊙ Yes   ○ No

Please provide all applicable information about the APS material you wish to use:

Author(s): Adrienne L. King, Telisha M. Swain, Dale A. Dickinson, Mathieu J. Lesort, and Shannon M. Bailey

Article or Chapter Title: Chronic ethanol consumption enhances sensitivity to Ca2+-mediated opening of the mi

Journal or Book Title: AJP-Gastrointestinal and Liver Physiology

Volume: _____   Page No(s): _____   Figure No(s): _____   Table No(s): _____

Year: 2010   DOI: 10.1152/ajpgi.00246.2010

(If you are reproducing figures or tables from more than one article, please fill out and send a separate form for each citation.)

Please provide all applicable information about where the APS material will be used:

How will the APS material be used? (please select from drop-down list)   Dissertation
If "other," please describe:

Title of publication or meeting where APS material will be used (if used in an article or book chapter, please
provide the journal name or book title as well as the article/chapter title):
Chronic alcohol consumption promotes opening of the mitochondrial permeability transition pore and increases
mitochondrial injury in liver

Publisher (if journal or book): _____

URL (if website): _____

Date of Meeting or Publication: _____

Will readers be charged for the material: ○ Yes   ⊙ No

Additional Information:

200